THE OPTIMIZATION OF THE CYCLIC OPERATION OF A MOLECULAR SIEVE ADSORBER

by

Daniel Edward Kowler

A dissertation submitted in partial fulfillment
of the requirements for the degree of
Doctor of Philosophy in
The University of Michigan
1969.

Doctoral Committee:

Associate Professor Robert H. Kadlec, Chairman
Associate Professor Brice Carnahan
Professor Rane L. Curl
Professor Elmer G. Gilbert
Assistant Professor Bruce H. Karnopp
Professor G. Brymer Williams

ACKNOWLEDGEMENTS

I would like to express my sincere appreciation to Professor Robert H. Kadlec, chairman of the doctoral committee, for his guidance and encouragement and to the members of the committee for their interest and helpful suggestions.

Financial assistance in the form of a National Defense Education Act Title IV Fellowship is gratefully acknowledged.

Appreciation is extended to my parents for their guidance, support and encouragement throughout my education.

Finally, I wish to thank my wife, Judith, for her patience and encouragement throughout the last years of my graduate study and for her excellent work in the typing of this thesis.

TABLE OF CONTENTS

TABLE OF CONTENTS (Continued)

LIST OF TABLES

LIST OF FIGURES

LIST OF FIGURES (Continued)

LIST OF APPENDICES

NOMENCLATURE

English Alphabet

a_i	group of constants defined by equations (3.10B) and (3.16B)
A	cross sectional area of the adsorption column (cm.^{3})
b_i	grouping of terms defined by equation (3.94)
B	arbitrary factor in the variational equation
c	concentration of gas in flowing gas stream (mg. moles/cm.^{3})
C	weighting factor for exhaust minimization
d_i	grouping of terms defined by equation (3.94)
D_i	grouping of terms defined by equation (3.23B)
f_i	functions for $\mathring{z}_i$ defined by equations (3.74) and (3.75)
F_i	functions defined by equations (3.10A) and (3.23A)
F_{FV}	fraction of period that feed valve is open
g_i	functions for $\mathring{y}_i$ defined by equations (3.83) and (3.84)
G_i	functions defined by equations (3.16A) and (3.28)
h_i	set of constants
H	Hamiltonian function
I	performance index
k	constant in the Freundlich adsorption isotherm
K	permeability of the packed adsorption column (darcy)
l	dimensionless distance variable
L	length of the adsorption column (cm.)
m_i	functions making up the integral performance index
M_o	group of terms defined by equation (3.63)
n	number of stages in the cell model
N	amount of gas adsorbed (mg. moles)

p_i adjoint variable associated with the pressure variables

P pressure (atm.)

q_i adjoint variable associated with the composition variables

Q_p product flowrate (mg. mole/hr.)

r_i state variables in the product line volume

R ideal gas law constant (.082 atm. $cm.^3$/(mg. mole °K))

t time variable (sec.)

t_o initial time (sec.)

T temperature (°K)

u controlled variable

v velocity of gas flow (cm./sec.)

V_R volume of the product line preceding the pressure regulator ($cm.^3$)

w_i state variables in the adsorption column

W weight of adsorbent in column (g.)

x composition of nitrogen in the adsorbed phase

y composition of nitrogen in the gas phase

$\bar{y}_i$ composition of gas flowing between cell i and cell $i-1$

z pressure ^{2} ($atm.^2$)

Z_i dimensionless pressure variable

Greek Alphabet

α relative volatility

β_i arbitrary constant

γ power constant in the Freundlich adsorption isotherm

δ small variation of a state or control variable

Δ	difference between values
ϵ	porosity of adsorption column
η_i	adjoint variables associated with pressure regulator variables
θ	dimensionless time variable
λ	distance variable (cm.)
μ	average viscosity of gas flow stream (cp.)
ν	distributed control
ξ_i	arbitrary constant
Π	matrix of solutions to the homogeneous part of adjoint equations associated with pressure
ρ_i	adjoint variables associated with adsorption column distributed variables
τ	length of operating period (sec.)
ϕ	constant which determines the magnitude of the correction of the control
χ	grouping of the discontinuous feed boundary Hamiltonian terms
ψ	grouping of the continuous feed boundary Hamiltonian terms
Ω	set of solutions to the homogeneous part of adjoint equations associated with composition

Subscripts

F	relating to a property of the feed gas
i	one of a set
j	one of a set
max	upper limit of possible values for variable
min	lower limit of possible values for variable
N_2	relating to nitrogen

o applicable at feed boundary of the column

R relating to the product line between end of adsorption column and pressure regulator

λ first partial derivative with respect to distance

$\lambda\lambda$ second partial derivative with respect to distance

Superscripts

$^{\circ}$ first partial derivative with respect to time

$^{\rightarrow}$ vector quantity

^{P} particular solution

^{T} transpose of a vector

* optimal value

$^{\prime}$ rescaled variable

† starting value

†† corrected value

ABSTRACT

Recent studies have shown that periodic processing can improve certain chemical processes. This research is primarily concerned with the optimal control of an inherently periodic process, the cyclically operated molecular sieve adsorber. This adsorber is operated by alternating the flow of the feed gas mixture with the flow of exhaust gas at one end of the adsorption column while regulating the product end of the column for constant flow. The separation accomplished and the fraction of feed gas recovered as product depend upon the manner in which the pressure is controlled at the feed boundary.

A simplified model for this system, neglecting rate limitations and neglecting variations of the flow and adsorption properties with composition, is presented. Using a variational approach, the necessary conditions for optimality are derived for the resulting system of partial and ordinary differential equations. The maximization of a performance index, which includes a product composition profit term and can include an exhaust rate cost term, is considered. For this performance index the controls of maximum pressure, minimum pressure and zero flow are possible nonsingular optimal control function segments. Because the state and adjoint equations of the control problem are exceedingly complex, a cell model approximation for the adsorber and the associated adjoint variable equations are also presented.

A numerical algorithm, similar to that suggested by Horn and Lin, is used to locate the optimal control function. From the numerical computations for a nitrogen-methane gas mixture with 20-50 mesh Davison 5A Molecular Sieve as the adsorbent, it is found that the cyclic sequence

of maximum pressure followed by minimum pressure maximizes product composition. This is then investigated experimentally for a 5 foot column with a permeability of 101 darcys and a comparison is made between the predicted and actual optimal controls. It is found that the optimal frequency of 0.35 cycles/sec. is independent of product flowrate in the range of 1.16 SCFH - 2.4 SCFH. However, the optimal fraction of period for applying the maximum pressure is affected by product flowrate. Both numerical and experimental results indicate that this optimal fraction increases as product flowrate increases.

The addition of the exhaust minimzation term into the performance index changes the form of the optimal control. In this case, the cyclic sequence of maximum pressure, zero flow, minimum pressure optimizes the performance index. As the importance of the exhaust minimization term increases relative to the product composition maximization term, the optimal frequency decreases, the optimal fraction of the cycle for applying maximum pressure decreases and the optimal fraction of the period for applying the control of zero flow increases. Experimental results verify the fact that short applications of the zero flow control decreases the exhaust rate without significantly reducing the separation accomplished.

A dimensional analysis of the state equations is also presented to determine the influence of the design factors. From this analysis it is concluded that the area affects only the capacity of the system. It is also found that within the region of the validity of the model, shorter lengths for the adsorption column or higher permeability in the packed bed results in higher capacity without affecting the relationship between separation and fraction of feed gas recovered as product. However, as shorter lengths or higher permeabilities are used, the frequencies required to

obtain the optimal operation are increased.

Another design parameter that is studied is the volume between the product end of the column and the pressure regulator. Preliminary numerical results show that increasing this volume both increases product composition and decreases the exhaust flowrate. It thus appears that maintaining constant pressure at the end of the column is most beneficial to the process.

The mathematical model and the numerically computed optimal controls provide a better understanding of the influence of both the above mentioned design factors and the feed boundary pressure control in the cyclic adsorption process. Also, the theoretical and computational procedures that are presented should be useful in the treatment of other optimal control problems involving periodic distributed-parameter systems.

1. INTRODUCTION

For most continuous processes within the chemical industry, it was formerly assumed that using constant operating conditions was the best mode of operation. Recent studies have shown, however, that cyclic or periodic operations in some of these processes can lead to improvements in the process outputs. Since the magnitude and direction of the change in process outputs caused by cycling can vary, it is important to be able to locate the best possible operating conditions. This leads to the application of optimal control theory.

Initial contributions to the theory of optimal control were primarily concerned with discrete systems. Since there are many distributed-parameter systems in chemical processing, recent attention has been directed to optimal control theory in this area. It is the purpose of this thesis to theoretically, computationally and experimentally investigate the optimal control of a periodic distributed-parameter process.

An inherently periodic process and the subject of this research is a cyclically operated molecular sieve adsorber. This gas separation column has practical significance due to the following advantages over some present adsorption methods:

1) No separate adsorbent regeneration process necessary

2) Continuous operation

3) No solids handling needed during operation.

In addition, its fast startup time may make it practical where the start-up delays of conventional continuous mode plants are not acceptable.

This cyclic adsorber is operated at ambient temperature by alternating the flow of a feed gas mixture with the flow of exhaust gas at

one end of the column while regulating the product end of the column for constant flow. It is noted that the manner in which the column is pressurized and depressurized at the feed end, that is, the feed boundary pressure control, can greatly affect the composition of the product stream and the amount of gas exhausted. Therefore, it is necessary to establish the optimal feed boundary pressure control which maximizes certain performance criteria of the adsorber.

The above adsorber is described by two partial differential equations for pressure and composition, and by ordinary differential equations at the product boundary. In this research the necessary conditions for the optimal control problem have been derived both for the distributed-parameter system and for a cell model approximation of it. Computational work using the cell model and experimental studies, investigate the performance index of product composition maximization for a fixed product flowrate and a limited available pressure for the methane-nitrogen feed gas. A comparison is then made between the numerically determined optimal feed boundary pressure cycle and the one determined from actual equipment performance.

Another performance criterion, which includes a term for minimizing exhaust rate as well as a term for maximizing product composition, is also investigated computationally.

2. LITERATURE SURVEY

Since the subject of this research involves the areas of periodic processing, adsorption and optimal control, the literature in each of these areas will be briefly examined.

2.1. Periodic Processing

During the past decade, controlled cycling has been investigated in a number of chemical processes. Initial work was concentrated on the staged operations of distillation and extraction. Cannon reviewed these studies which found that by alternating the liquid (or heavy phase) flow with the vapor (or light phase) flow, the capacity and efficiency of a plate distillation (or extraction) column could be increased (9). Further work in distillation was carried out on a plant scale by Schrodt et al. (35).

Investigation into periodic processes was stimulated when thermal parametric pumping was conceived by Wilhelm. This separation principle depends upon the dynamic coupling of a cyclic relative displacement between two phases and a cyclic interphase solute flux. Unlike the cycled staged operations, the relative motions between the two phases is not unidirectional but alternates. Separations using parametric pumping in an ion exchange column were reported by Wilhelm, Rice and Bendelius (40) and by Wilhelm, Rice, Rolke and Sweed (41). An equilibrium theory for the mathematical modeling of this system was presented by Pigford (30) while Rolke and Wilhelm (33) and Sweed and Wilhelm (38) presented models and computational procedures for their work.

The batch gas adsorption process, which operates in a separation

mode followed by regeneration, can also be thought of as being a cyclic process. Since there are two major means of regeneration, thermal and pressure swings, two types of parametric pumping can be applied to adsorption. McAndrew studied thermal parametric pumping using a gaseous methane-nitrogen system (27). The process known as heatless adsorption was described by Skarstrom in 1959 as a system for drying air over a silica gel bed (37). This process is very similar to parametric pumping using pressure as the varied parameter. Alexis then applied heatless adsorption to upgrade hydrogen by the removal of hydrocarbons (1).

In separating oxygen and nitrogen, the Esso Research Laboratories used a variation of the heatless adsorber which no longer required two alternating adsorbers (18). Rapid pressure swings at the feed boundary of the adsorber were imposed while a limited purified fraction of gas was removed from the product end. This cyclically operated adsorber then fits into the category of pressure parametric pumping. Further research into this process was done by Turnock studying a methane-nitrogen system using molecular sieve as the adsorbent (39). As a result of his work, Turnock found that use of the equilibrium theory in modeling this distributed-parameter system adequately described the process.

Recently, attention has also been directed to the effects of cyclic operations in chemical reactors. Studies by Douglas show that product yields in certain reaction systems could be improved by periodic operations (14). Research into the performance of periodic polymerization reactions has been reported by Ray (32) and by Laurence and Vasudevan (25).

2.2. Adsorption

A basic text concerned with the theory and conventional applications of adsorption has been written by Mantell (28).

Adsorption equilibria for methane-nitrogen mixtures on Linde Molecular Sieve Type 5A were studied extensively at high pressures by Lederman (26). At the pressures studied, the total amount of gas adsorbed appeared to be composition invariant and the data were well represented by the Freundlich isotherm relationship. To relate the relative equilibrium adsorption of the gas components a composition invariant relative volatility was introduced.

Further data on molecular sieve behavior are presented in a text prepared by Hersh (19). However, well defined properties for methane-nitrogen adsorption on Davison Molecular Sieve Type 5A, which is used in this research, are not available in the literature.

2.3. Optimal Control Theory

Initially, the theory used to compute optimal control functions was based on the calculus of variations. Interest in optimal control theory was greatly stimulated when Pontryagin and his co-workers wrote the basic theoretical text on the Maximum Principle (31). This work was then simply presented by Rozonoer (34). An elementary text which presents the basic principles of control, a heuristic proof of the Maximum Principle, and several applications of the theory was written by Athans and Falb (3).

The development of the Maximum Principle enabled workers to investigate the optimal control of systems that are described by ordinary differential equations. In chemical engineering, following the work of

Bilous and Amundson (4), Aris (2) and Jackson (21), Javinsky reviewed and studied the minimization of reactor startup time (22) and Newberger reviewed and studied the maximization of reactor product yields (29). Both included experimental as well as computational work. Horn and Lin presented a method to solve both the system equations and the optimal control of a lumped-parameter periodic process (20).

However, there are many physical systems which are distributed-parameter systems and require formulation by partial differential equations. For example, some systems with heat, mass and momentum transfer must be modeled by partial differential equations. Thus, the need developed to derive a maximum principle for distributed-parameter systems.

The first workers to formulate this problem were Butkovskii and Lerner (5). Butkovskii subsequently considered the optimal control of a class of systems describable by a set of nonlinear integral equations (6, 7). He also suggested discretizing the partial differential equations to create a set of lumped-parameter systems to which the Maximum Principle is applicable (8). He did point out, however, that convergence as the number of spacial grid points is increased is not guaranteed.

Although Butkovskii had derived the necessary conditions for optimality, the results depended upon the solution of nonlinear integral equations involving multiple integrals. This method required an explicit solution of the system equations which restricted the results to linear systems. With the use of functional analysis, Katz eliminated the above problem by formulating a maximum principle which could be applied to parabolic and first-order hyperbolic systems as well as lumped-parameter systems (23). Here, however, the adjoint operator must be constructed for each specific problem, which is an unwieldy procedure, and the

formulation does not include cases where the control enters through the boundary conditions. Similar necessary conditions were presented by Egorov for second order hyperbolic systems and parabolic systems (15-17).

Following the approach he used for lumped-parameter systems, Denn used a variational procedure with a Green's function solution to provide a simplified derivation of the necessary conditions for distributed-parameter systems (12). In addition, boundary controls could be considered as well as distributed controls. Denn, Gray and Ferron then used the conditions of optimality to maximize the conversion in a packed tubular reactor with the wall heat flux as the control variable (13). Other applications of distributed-parameter optimal control theory in chemical engineering have been limited to heat exchangers and chemical reactors. Seinfeld investigated, with reference to heat transfer and reaction systems, the computational methods available for constructing optimal controls as well as presenting the theoretical basis for computing singular controls (36). Koppel and Shih considered the optimal control problem with heat exchangers (24) while Chang and Bankoff studied the optimal control of tubular reactors (11).

None of the problems of optimal control of distributed-parameter systems thus far examined has involved a separation process. In addition, except for Chang and Bankoff's study where a noncontrollable periodic input was imposed (10), a study of the optimal control of a periodic distributed-parameter process has not yet been reported. Therefore, investigating the optimal control of a cyclically operated molecular sieve adsorber will not only increase the understanding of this separation process but will also yield further insight into optimal control problems in periodic distributed-parameter processes.

3. THEORETICAL BACKGROUND

This chapter will deal with the development of a mathematical model of the molecular sieve adsorber and with the formulation of the necessary conditions for optimal control. The resulting set of equations for the state variables of the system and for the adjoint variables of the control problem will be governed by partial differential equations. Because of the complexity of these equations and of the computational procedures involved, the computer cost for a finely spaced finite difference solution of these equations would be excessive. Therefore, after the distributed-parameter system is examined, a lumped-parameter model, i.e. cell model, approximation of it will be studied.

3.1. Bases for Model of Adsorption System

The adsorption system being studied is a molecular sieve bed that is flow controlled at the feed boundary and regulated for constant flow at the product boundary. A simplified diagram of the process is shown in Figure 3.1. It is the feed boundary pressure control that produces the alternating flow of the methane-nitrogen feed mixture with the exhaust gas. For a chosen constant product flowrate the resulting composition of the product and the resulting exhaust rate depend only upon this feed boundary pressure control.

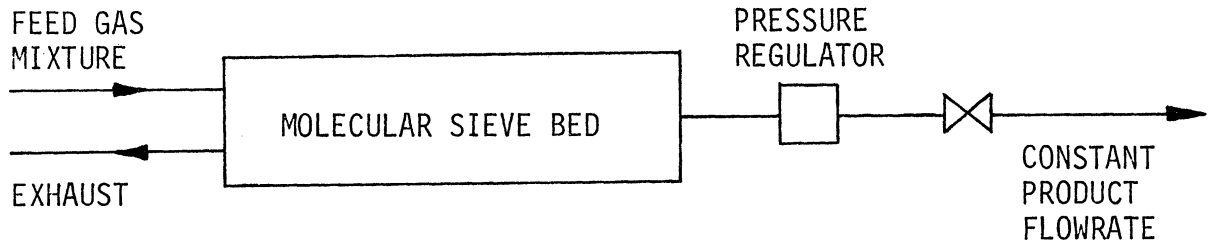

Figure 3.1. Molecular Sieve Adsorber.

In establishing the bases for a model for the molecular sieve bed, Turnock made the following assumptions and approximations (39):

(A) Ideal gas behavior

(B) Darcy's Law representation of the gas flow

(C) Viscosity of the gas phase is composition invariant

(D) Plug flow conditions

(E) At any instant, equilibrium exists between the gas phase and the adsorbed phase.

Based upon Lederman's studies of methane-nitrogen adsorption on Linde Molecular Sieve Type 5A (26) the following observations were made:

(F) The total equilibrium amount adsorbed is independent of composition.

(G) The equilibrium adsorption isotherms are fit well by the Freundlich relationship:

$$N = kWP^{\gamma} \tag{3.1}$$

(H) The relative volatility, α, relates the relative adsorption of the two gas components and does not vary with composition.

$$\alpha = \frac{y/x}{(1-y)/(1-x)} \tag{3.2}$$

With the above assumptions, approximations and observations the behavior of the system is fully described. However, before deriving the state equations for the system, a brief look into the validity and importance of some of the above relations will be made.

Since Davison 5A Molecular Sieve was used in this study, the adsorption equilibria of methane and nitrogen on this sieve were investigated and reported in Appendix I. Shown in Figure 3.2 are the

adsorption isotherms for the pure components and for a mixture of 28.6% nitrogen and the balance methane. Also shown on this figure is the predicted isotherm for 60% nitrogen and 40% methane based upon a linear relationship between adsorption and composition.

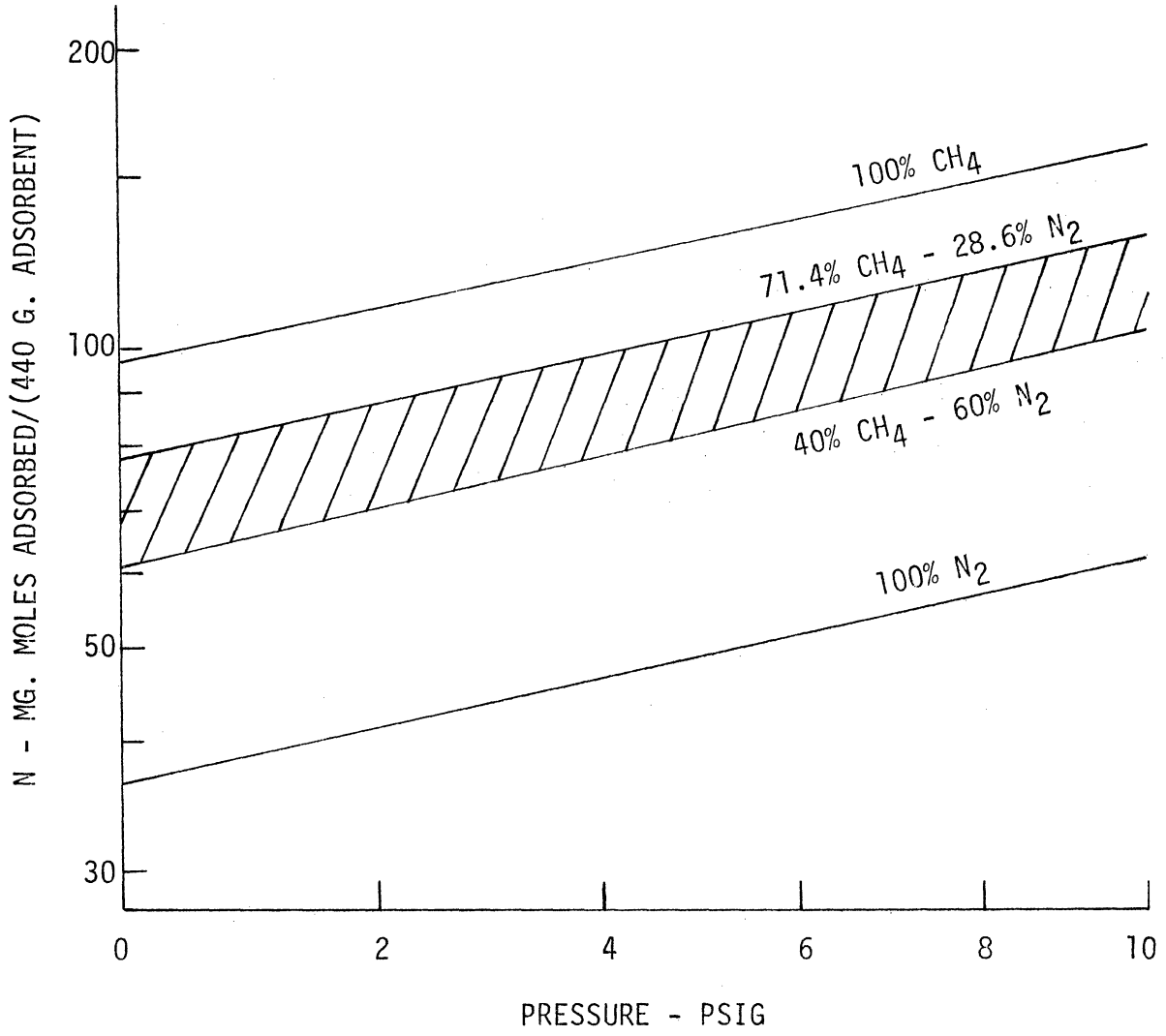

Figure 3.2. Methane-Nitrogen Adsorption Isotherms (295°K).

Looking at the pure component adsorption, it would seem that relation (F) is not valid. However, the composition during the operation of the bed will only vary from a feed composition of about 30% nitrogen to a product composition of about 60% nitrogen. It is therefore a

reasonable approximation to use an average total adsorption independent of composition. This approximation is an important factor in uncoupling the solution of the pressure equation from the solution of the composition equation. This greatly simplifies the numerical solution of the system equations and the optimal control problem.

Relations (C) and (H) are also needed to uncouple the pressure equation. The relative volatility has been found to be constant over the range of operating conditions. However, the gas viscosity will vary with composition. But here again, it is a reasonable approach to use an average for the viscosity.

Since the rate of adsorption is rapid, instantaneous equilibrium is assumed as in relation (E). This then eliminates rate considerations from the model.

3.2. Mathematical Model

With the use of Darcy's Law to describe the gas flow and a Freundlich isotherm to describe the phase equilibria, the equations for pressure and composition are derived from material balances on the differential element shown in Figure 3.3.

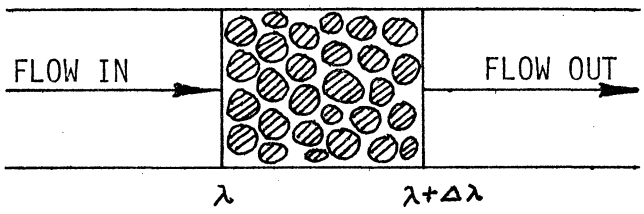

Figure 3.3. Differential Element of Packed Bed.

For all material balances on the element,

$$\text{FLOW (IN-OUT)} = \text{ACCUMULATION (GAS + ADSORBENT)} \qquad (3.3)$$

Total Material Balance:

$$A\left[(vc)_{AT\,\lambda} - (vc)_{AT\,\lambda+\Delta\lambda}\right] = A\epsilon(\Delta\lambda)\frac{\partial\left(\frac{P}{RT}\right)}{\partial t} + \frac{W(\Delta\lambda)}{L}\frac{\partial(kP^{\gamma})}{\partial t} \tag{3.4}$$

Darcy's Law: $$v = -\frac{K}{\mu}\frac{\partial P}{\partial \lambda} \tag{3.5}$$

Ideal Gas Law: $$c = \frac{P}{RT} \tag{3.6}$$

Combining (3.4) - (3.6),

$$\frac{\partial P}{\partial t}\left[\frac{\epsilon A}{RT} + \frac{Wk}{L}\gamma P^{\gamma-1}\right] = \frac{\frac{AK}{\mu RT}\left[\left(P\frac{\partial P}{\partial \lambda}\right)_{AT\,\lambda+\Delta\lambda} - \left(P\frac{\partial P}{\partial \lambda}\right)_{AT\,\lambda}\right]}{\Delta\lambda} \tag{3.7}$$

In the limit as $\Delta\lambda \longrightarrow 0$

$$\frac{\partial P}{\partial t}\left[\frac{\epsilon A}{RT} + \frac{Wk}{L}\gamma P^{\gamma-1}\right] = \frac{AK}{\mu RT}\frac{\partial\left(P\frac{\partial P}{\partial \lambda}\right)}{\partial \lambda} \tag{3.8}$$

Letting $z = P^2$ and rearranging,

$$\frac{\partial z}{\partial t} = \dot{z} = \frac{\frac{AK}{\mu} z^{1/2}\frac{\partial^2 z}{\partial \lambda^2}}{\left[\epsilon A + \frac{WRTk\gamma}{L} z^{((\gamma-1)/2)}\right]} \tag{3.9}$$

Grouping constants and simplifying notation,

$$\dot{z} = \frac{a_2 z^{1/2} z_{\lambda\lambda}}{\left(a_1 + a_3 z^{((\gamma-1)/2)}\right)} = F_1 \tag{3.10A}$$

Where $a_1 = \epsilon A$, $a_2 = \frac{AK}{\mu}$ and $a_3 = \frac{WRTk\gamma}{L}$ (3.10B)

The above parabolic partial differential equation requires one time condition and two boundary conditions. For periodic processes,

$$z(\lambda, t_o) = z(\lambda, t_o + \tau) \tag{3.11}$$

At the feed boundary, $z(0,t)$ is controlled. Since there is negligible

pressure drop in the product line between the product end of the column and the pressure regulator, uniform pressure, $z_R(t)$, will be assumed in this product line volume. Then for the boundary condition at the product end of the column

$$z(L,t) = z_R(t) \tag{3.12}$$

With the pressure regulator providing constant molar flow, Q_P, a material balance on the product line volume, V_R, yields

$$A(vc)_{\lambda=L} - Q_P = V_R \frac{\partial\left(\frac{P_R}{RT}\right)}{\partial t} \tag{3.13}$$

Again using equations (3.5) and (3.6)

$$\underline{\text{At } \lambda=L,} \qquad -\frac{AKP}{\mu RT}\frac{\partial P}{\partial \lambda} = Q_P + \frac{V_R}{RT}\frac{\partial P_R}{\partial t} \tag{3.14}$$

$$\text{or} \qquad -\frac{AK}{\mu}\frac{\partial z}{\partial \lambda} = 2RTQ_P + \frac{V_R}{z_R^{1/2}}\frac{\partial z_R}{\partial t} \tag{3.15}$$

Rearranging, grouping constants and simplifying notation,

$$\dot{z}_R = G_1 = \frac{-z_R^{1/2}}{V_R}(a_2 z_\lambda + a_4 Q_P) \tag{3.16A}$$

$$\text{where } a_4 = 2RT \tag{3.16B}$$

Since (3.16) is an ordinary differential equation, it requires a time condition. For periodic processes,

$$z_R(t_0) = z_R(t_0+\tau) \tag{3.17}$$

With the pressure equations for the adsorption bed and the product line now fully described, attention is turned to the composition equation.

Nitrogen Material Balance:

$$A\left[(vC_{N_2})_{AT\ \lambda} - (vC_{N_2})_{AT\ \lambda+\Delta\lambda}\right] = A\epsilon(\Delta\lambda)\frac{\partial\left(\frac{yP}{RT}\right)}{\partial t} + \frac{W}{L}(\Delta\lambda)\frac{\partial(xkP^{\gamma})}{\partial t} \tag{3.18}$$

Ideal Gas Law: $$C_{N_2} = \frac{yP}{RT} \tag{3.19}$$

Substituting (3.5) and (3.19) into (3.18) and letting $\Delta\lambda \longrightarrow 0$

$$\frac{AK}{\mu RT}\frac{\partial\left(yP\frac{\partial P}{\partial\lambda}\right)}{\partial\lambda} = A\epsilon\frac{\partial(yP)}{\partial t} + \frac{Wk}{L}\frac{\partial(xP^{\gamma})}{\partial t} \tag{3.20}$$

Expanding partial derivatives and using equations (3.2) and (3.8)

$$\frac{AK}{\mu RT}P\frac{\partial P}{\partial\lambda}\frac{\partial y}{\partial\lambda} = \left\{\begin{array}{l} \frac{\partial y}{\partial t}\left[\frac{A\epsilon P}{RT} + \frac{Wk\alpha P^{\gamma}}{L(y+\alpha(1-y))^2}\right] \\ + \frac{\partial P}{\partial t}\left[\frac{Wk\gamma P^{\gamma-1}y(1-y)(1-\alpha)}{L(y+\alpha(1-y))}\right] \end{array}\right\} \tag{3.21}$$

Rearranging and letting $z = P^2$,

$$\frac{\partial y}{\partial t} = \dot{y} = \frac{\frac{AK}{\mu}\frac{\partial z}{\partial\lambda}\frac{\partial y}{\partial\lambda} - \frac{\dot{z}}{z^{1/2}}\left[\frac{WRTk\gamma z^{((\gamma-1)/2)}y(1-y)(1-\alpha)}{L(y+\alpha(1-y))}\right]}{2z^{1/2}\left[\epsilon A + \frac{WRTk\alpha z^{((\gamma-1)/2)}}{L(y+\alpha(1-y))^2}\right]} \tag{3.22}$$

Replacing $\dot{z}$ by equation (3.10) and simplifying notation,

$$\dot{y} = F_2 = \frac{a_2 z_\lambda y_\lambda - \frac{a_2 z_{\lambda\lambda}\left[a_3 z^{((\gamma-1)/2)}y(1-y)(1-\alpha)\right]}{(a_1 + a_3 z^{((\gamma-1)/2)})(y+\alpha(1-y))}}{2z^{1/2}D} \tag{3.23A}$$

where $$D = \left(a_1 + \frac{\alpha a_3 z^{((\gamma-1)/2)}}{\gamma(y+\alpha(1-y))^2}\right) \tag{3.23B}$$

The above is a hyperbolic partial differential equation. Its solution requires one time condition. It also requires a boundary condition when and where flow enters into the adsorber. When flow leaves the system, no boundary condition is required. For periodic processes,

$$y(\lambda, t_o) = y(\lambda, t_o + \tau) \tag{3.24}$$

At the feed boundary, the flow into the system is the feed gas.

$$\text{when} \quad z_\lambda(0,t) < 0 \qquad y(0,t) = y_F \tag{3.25}$$

The flow into the product boundary, if any, would come from the product line.

$$\text{when} \quad z_\lambda(L,t) > 0 \qquad y(L,t) = y_R(t) \tag{3.26}$$

The above two boundary conditions correspond to the beginning of characteristics of the hyperbolic partial differential equation. Boundary conditions are not needed at $\lambda = L$ when $z_\lambda(L,t) \leq 0$ or at $\lambda = 0$ when $z_\lambda(0,t) \geq 0$. The latter lack of a boundary condition will have an important consequence in the optimal control problem.

Equation (3.26) requires knowledge of the composition in the product volume. Use of a nitrogen material balance for this volume assuming uniform composition and of equation (3.15) yields

$$\text{when} \quad z_\lambda(L,t) < 0 \qquad \dot{y}_R = \frac{-AK \frac{\partial z_R}{\partial \lambda}(y - y_R)}{2\mu V_R z_R^{1/2}} \tag{3.27}$$

$$\text{or} \quad \dot{y}_R = G_2 = \frac{-a_2 z_\lambda (y - y_R)}{2 z_R^{1/2} V_R} \tag{3.28A}$$

$$\text{when} \quad z_\lambda(L,t) \geq 0 \qquad \dot{y}_R = 0 \tag{3.28B}$$

$$\text{where} \qquad y_R(t_o) = y_R(t_o + \tau) \tag{3.29}$$

For any given feed boundary pressure control and a set product flowrate, the system is fully described by the differential equations, time conditions and boundary conditions which are compiled in Table 3.1. For a desired product capacity, the performance of the adsorption system is directly related to this feed boundary pressure control. It is then necessary to establish the conditions necessary to find the control that optimizes the performance of the adsorber.

TABLE 3.1

MATHEMATICAL MODEL FOR THE ADSORPTION SYSTEM

State Equations:

Adsorption Bed:

$$\dot{z} = F_1 = \frac{a_2 z^{1/2} z_{\lambda\lambda}}{(a_1 + a_3 z^{((\gamma-1)/2)})} \tag{3.10A}$$

$$\dot{y} = F_2 = \frac{a_2 z_\lambda y_\lambda - \dfrac{a_2 z_{\lambda\lambda}[a_3 z^{((\gamma-1)/2)} y(1-y)(1-\alpha)]}{(a_1 + a_3 z^{((\gamma-1)/2)})(y + \alpha(1-y))}}{2 z^{1/2} D} \tag{3.23A}$$

Product line at $\lambda = L$:

$$\dot{z}_R = G_1 = -\frac{z_R^{1/2}}{V_R}(a_2 z_\lambda + a_4 Q_p) \tag{3.16A}$$

when $z_\lambda(L,t) < 0$, $\qquad \dot{y}_R = G_2 = \dfrac{-a_2 z_\lambda (y - y_R)}{2 z^{1/2} V_R}$ (3.28A)

when $z_\lambda(L,t) \geq 0$, $\qquad \dot{y}_R = 0$ (3.28B)

TABLE 3.1 (continued)

Time Conditions:

$$z(\lambda,t_o) = z(\lambda,t_o+\tau) \tag{3.11}$$

$$y(\lambda,t_o) = y(\lambda,t_o+\tau) \tag{3.24}$$

$$z_R(t_o) = z_R(t_o+\tau) \tag{3.17}$$

$$y_R(t_o) = y_R(t_o+\tau) \tag{3.29}$$

$\lambda = 0$

when $z_\lambda(0,t) < 0$, $\quad y(0,t) = y_F$ (3.25)

$z(0,t)$ controlled

$\lambda = L$

when $z_\lambda(L,t) > 0$, $\quad y(L,t) = y_R(t)$ (3.26)

$$z(L,t) = z_R(t) \tag{3.12}$$

For the above equations,

$$a_1 = \epsilon A, \quad a_2 = \frac{AK}{\mu} \text{ and } a_3 = \frac{WRT\kappa\gamma}{L} \tag{3.10B}$$

$$a_4 = 2RT \tag{3.16B}$$

$$D = \left(a_1 + \frac{\alpha a_3 z^{((\gamma-1)/2)}}{\gamma(y+\alpha(1-y))^2}\right) \tag{3.23B}$$

3.3. General Optimal Control Problem

With ordinary differential equations entering the boundary conditions at $\lambda = L$ and the control entering at the $\lambda = 0$ boundary, the method for setting up the necessary conditions as proposed by Katz (23) or the conditions presented by Egorov (15-17) are inadequate. Following the

variational approach used by Denn (12), however, the necessary conditions for optimality in the adsorption system can be formulated.

To simplify the development, the state vectors $\vec{w}$ and $\vec{r}$ will be defined.

$$\vec{w}(\lambda,t) = \begin{bmatrix} z(\lambda,t) \\ y(\lambda,t) \end{bmatrix} = \begin{bmatrix} w_1(\lambda,t) \\ w_2(\lambda,t) \end{bmatrix}$$
$$\vec{r}(t) = \begin{bmatrix} z_R(t) \\ y_R(t) \end{bmatrix} = \begin{bmatrix} r_1(t) \\ r_2(t) \end{bmatrix} \tag{3.30}$$

Noting from Table 3.1 that

$$\begin{aligned} \dot{z} &= F_1(z, z_{\lambda\lambda}) \\ \dot{y} &= F_2(z, y, z_\lambda, y_\lambda, z_{\lambda\lambda}) \end{aligned} \tag{3.31}$$

and

$$\dot{z}_R = G_1(z_R, [z_\lambda]_{\lambda=L})$$

when $z_\lambda(L,t) < 0$, $\dot{y}_R = G_2(z_R, y_R, [y, z_\lambda]_{\lambda=L})$ (3.32)

when $z_\lambda(L,t) \geq 0$, $\dot{y}_R = 0$

Thus, the state equations take the form

$$\begin{aligned} \dot{\vec{w}} &= \vec{F}(\vec{w}, \vec{w}_\lambda, \vec{w}_{\lambda\lambda}) && 0 < \lambda < L \\ \dot{\vec{r}} &= \vec{G}(\vec{r}, \vec{w}, \vec{w}_\lambda) && \lambda = L \end{aligned} \tag{3.33}$$

The general distributed system, containing a distributed control, v, as well as a boundary control, u, is optimized by maximizing the value of the performance index, I. This index is an average over a steady state cycle of functions of the state and control variables.

$$I = \frac{1}{\tau}\int_{t_0}^{t_0+\tau} \left\{ \left[m_1(\vec{w}, \vec{w}_\lambda) \right]_{\lambda=0} + \left[m_2(\vec{w}) \right]_{\lambda=L} + m_3(\vec{r}) + \int_0^L m_4(\vec{w}, v)\, d\lambda \right\} dt \tag{3.34}$$

In the above, depending upon the forms of the functions m_1, m_2, m_3 and m_4, the criteria for optimum performance of the distributed system can vary.

For this adsorption system, there is no distributed control, ν , nor do the values taken by the state variables within the bed have any direct significance. The only terms of interest in the performance index for this research will depend upon the product composition and the exhaust from the system. For further work, therefore, only the following performance index will be considered:

$$I = \frac{1}{\tau}\int_{t_0}^{t_0+\tau} \left[m_1(\omega_{1_\lambda})_{\lambda=0} + m_3(r_2) \right] dt \qquad (3.35)$$

where $m_2(\vec{\omega}) = m_4(\vec{\omega}, \nu) = 0$

$$\begin{aligned} m_1(\vec{\omega}, \vec{\omega}_\lambda)_{\lambda=0} &= m_1(\omega_{1_\lambda})_{\lambda=0} \\ m_3(\vec{r}) &= m_3(r_2) \end{aligned} \qquad (3.36)$$

The value that the above index can achieve is constrained by equations (3.33). The control, u , applied at the $\lambda = 0$ boundary is constrained by the maximum available feed gas pressure and atmospheric pressure so that

$$\text{At } \lambda = 0 , \qquad 1 \leq z \leq z_{max} \qquad (3.37)$$

In addition, the control is required to be periodic, piecewise continuous with discontinuities only at a finite number of points.

The differential equation constraints (3.33) are introduced into the performance index with the use of the adjoint variables; that is, the set of Lagrange Multipliers. In the following development, the existence of these adjoint variables, although not guaranteed, will be assumed and they will be denoted by

$$\vec{\rho}(\lambda,t) = \begin{bmatrix} \rho_1(\lambda,t) \\ \rho_2(\lambda,t) \end{bmatrix} \text{ and } \vec{\eta}(t) = \begin{bmatrix} \eta_1(t) \\ \eta_2(t) \end{bmatrix} \qquad (3.38)$$

Entering the differential equation constraints into the performance index for an arbitrary value of $\mathcal{B}$,

$$I = \frac{1}{\tau}\int_{t_0}^{t_0+\tau}\left\{\begin{array}{l}\left[m_1(\omega_{1_\lambda})\right]_{\lambda=0} - \vec{\eta}^T(\dot{\vec{r}} - \vec{G}(\vec{r}, [\omega, \omega_\lambda]_{\lambda=L})) \\ + m_3(r_2) - \mathcal{B}\int_0^L \vec{\rho}^T(\dot{\vec{\omega}} - \vec{F}(\vec{\omega}, \vec{\omega}_\lambda, \vec{\omega}_{\lambda\lambda}))d\lambda\end{array}\right\} dt \tag{3.39}$$

The value of I has not been altered as

$$\begin{aligned}\dot{\vec{r}} - \vec{G}(\vec{r}, [\omega, \omega_\lambda]_{\lambda=L}) &= 0 \\ \dot{\vec{\omega}} - \vec{F}(\vec{\omega}, \vec{\omega}_\lambda, \vec{\omega}_{\lambda\lambda}) &= 0\end{aligned} \tag{3.40}$$

As stated previously, using a given product flowrate, for a particular control function, u, the system is fully specified. That is, a unique solution $\vec{\omega}$ and $\vec{r}$ is defined. Thus, if a small variation δu is made, a new solution is defined, $\vec{\omega} + \delta\vec{\omega}$ and $\vec{r} + \delta\vec{r}$. $\delta\vec{\omega}$ and $\delta\vec{r}$ may be made as small as desired by choosing a sufficiently small δu. If the functions $\vec{F}$ and $\vec{G}$ have bounded derivatives at all but a finite number of points, then the following variational equation, for constant τ, can be written. Whenever repeating indices arise, summation will be assumed.

$$\delta I = \frac{1}{\tau}\int_{t_0}^{t_0+\tau}\left\{\begin{array}{l}\left[\frac{\partial m_1}{\partial \omega_{1_\lambda}}\delta\omega_{1_\lambda}\right]_{\lambda=0} - \left[\eta_i\delta\dot{r}_i - \eta_j\left(\frac{\partial G_j}{\partial r_i}\delta r_i + \frac{\partial G_j}{\partial \omega_i}\delta\omega_i + \frac{\partial G_j}{\partial \omega_{i_\lambda}}\delta\omega_{i_\lambda}\right)\right]_{\lambda=L} \\ + \frac{\partial m_3}{\partial r_i}\delta r_i - \mathcal{B}\int_0^L\left[\rho_i\delta\dot{\omega}_i - \rho_j\left(\frac{\partial F_j}{\partial \omega_i}\delta\omega_i + \frac{\partial F_j}{\partial \omega_{i_\lambda}}\delta\omega_{i_\lambda} + \frac{\partial F_j}{\partial \omega_{i_{\lambda\lambda}}}\delta\omega_{i_{\lambda\lambda}}\right)\right]d\lambda\end{array}\right\} dt \tag{3.41}$$

Integration by parts operating on $\eta_i \delta \dot{r}_i$, $\rho_i \delta \dot{\omega}_i$, $\rho_j \frac{\partial F_j}{\partial \omega_{i_\lambda}} \delta \omega_{i_\lambda}$ and $\rho_j \frac{\partial F_j}{\partial \omega_{i_{\lambda\lambda}}} \delta \omega_{i_{\lambda\lambda}}$,

$$\delta I = \frac{1}{\tau} \left\{ \begin{aligned} & -\left[\eta_i \delta r_i\right]_{t_0}^{t_0+\tau} - B \int_0^L \left[\rho_i \delta \omega_i\right]_{t_0}^{t_0+\tau} d\lambda + \int_{t_0}^{t_0+\tau} \left(\dot{\eta}_i + \left[\eta_j \frac{\partial G_j}{\partial r_i}\right]_{\lambda=L} + \frac{\partial m_3}{\partial r_i}\right) \delta r_i \, dt \\ & + \int_{t_0}^{t_0+\tau} \left(B\left(\left[\rho_j \frac{\partial F_j}{\partial \omega_{i_\lambda}}\right] - \left[\rho_j \frac{\partial F_j}{\partial \omega_{i_{\lambda\lambda}}}\right]_\lambda\right)_0^L + \left[\eta_j \frac{\partial G_j}{\partial \omega_i}\right]_{\lambda=L} \right) \delta \omega_i \, dt \\ & + \int_{t_0}^{t_0+\tau} \left(\left(\left[B \rho_j \frac{\partial F_j}{\partial \omega_{i_{\lambda\lambda}}}\right]_0^L + \left[\eta_j \frac{\partial G_j}{\partial \omega_{i_\lambda}}\right]_{\lambda=L} \right) \delta \omega_{i_\lambda} + \left[\frac{\partial m_1}{\partial \omega_{1_\lambda}} \delta \omega_{1_\lambda}\right]_{\lambda=0} \right) dt \\ & + B \int_{t_0}^{t_0+\tau} \int_0^L \left(\dot{\rho}_i + \rho_j \frac{\partial F_j}{\partial \omega_i} - \left(\rho_j \frac{\partial F_j}{\partial \omega_{i_\lambda}}\right)_\lambda + \left(\rho_j \frac{\partial F_j}{\partial \omega_{i_{\lambda\lambda}}}\right)_{\lambda\lambda} \right) \delta \omega_i \, d\lambda \, dt \end{aligned} \right\} \tag{3.42}$$

The purpose of this variational approach is to relate the change of performance, δI, with a change in control, δu. In order to eliminate all the terms in the above equation that do not relate to δu, the form of the control must first be decided upon. The inequality constraint (3.37) directly limits $z(0,t)$. Although $z(0,t)$ is the actual controlled variable, and will be treated as such in the numerical computations, a simpler analysis of the variational equation results if $z_\lambda(0,t)$ is treated as the controlled variable. Then at $\lambda = 0$,

$$\begin{aligned} u &= \omega_{i_\lambda} \\ \delta u &= \delta \omega_{1_\lambda} \end{aligned} \tag{3.43}$$

Then all terms remaining that involve $\delta \omega_i$, $\delta \omega_{i_\lambda}$, and δr_i must be made to vanish. The relations that result fully define the behavior of the adjoint variables. These equations are compiled in Table 3.2 as functions of z, y, z_R and y_R. A complete derivation of these and the remaining terms of the variational equation is provided in Appendix II.

TABLE 3.2

MATHEMATICAL DESCRIPTION OF THE ADJOINT VARIABLES

Partial Differential Equations

$$\dot{\rho}_1 = \left\{\left(\frac{-\rho_1 \dot{z}}{2z} + \frac{\rho_2 \dot{y}}{2z}\right) + \left(\frac{\rho_2 a_2 y_\lambda}{2z^{1/2} D}\right)_\lambda + \left(\frac{-\rho_1 a_2 z^{1/2}}{(a_1+a_3)} + \frac{\rho_2 a_2 a_3 y(1-y)(1-\alpha)}{2z^{1/2} D(a_1+a_3)(y+\alpha(1-y))}\right)_{\lambda\lambda}\right\}$$

(3.44)

$$\dot{\rho}_2 = \left\{\frac{\rho_2 a_3 (1-\alpha)\left(\frac{\dot{z}}{z}\left[a_1(\alpha[y-1]^2 - y^2) - \frac{\alpha a_3 (y[3y(1-\alpha) - 2(2\alpha-1)] - \alpha)}{(y+\alpha(1-y))^2}\right] - \frac{\alpha a_2 z^{1/2} y_\lambda z_\lambda}{(y+\alpha(1-y))}\right)}{2z D^2 (y+\alpha(1-y))^2} + \left(\frac{\rho_2 a_2 z_\lambda}{2z^{1/2} D}\right)_\lambda\right\}$$

Boundary Conditions and Ordinary Differential Equations

At $\lambda = 0$

$$-\frac{\rho_2 a_2 y_\lambda}{2z^{1/2} D} + \left(\frac{\rho_1 a_2 z^{1/2}}{(a_1+a_3)} - \frac{\rho_2 a_2 a_3 y(1-y)(1-\alpha)}{2z^{1/2} D(a_1+a_3)(y+\alpha(1-y))}\right)_\lambda = 0$$

(3.45)

when $u = z_\lambda(0,t) > 0$ $\qquad \rho_2 = 0$

At $\lambda = L$

$$\dot{\eta}_1 = -\frac{\eta_1 \dot{z}_R}{2 z_R} + \frac{\eta_2 \dot{y}_R}{2 z_R} + B\left(\frac{-\rho_2 a_2 y_\lambda}{2z^{1/2} D} + \left(\frac{\rho_1 a_2 z^{1/2}}{(a_1+a_3)} - \frac{\rho_2 a_2 a_3 y(1-y)(1-\alpha)}{2z^{1/2} D(a_1+a_3)(y+\alpha(1-y))}\right)_\lambda\right)$$

when $z_\lambda(L,t) < 0$

$$B\left(\frac{\rho_1 a_2 z^{1/2}}{(a_1+a_3)} - \frac{\rho_2 a_2 a_3 y(1-y)(1-\alpha)}{2z^{1/2} D(a_1+a_3)(y+\alpha(1-y))}\right) - \frac{\eta_1 a_2 z_R^{1/2}}{V_R} - \frac{\eta_2 a_2 (y-y_R)}{2z^{1/2} V_R} = 0 \tag{3.47}$$

$$\frac{B\rho_2 a_2 z_\lambda}{2z^{1/2} D} - \frac{\eta_2 a_2 z_\lambda}{2z^{1/2} V_R} = 0$$

$$\dot{\eta}_2 = \frac{-\eta_2 a_2 z_\lambda}{2z^{1/2} V_R} - \frac{\partial m_3}{\partial y_R} \tag{3.48}$$

when $z_\lambda(L,t) > 0$

$$B\left(\frac{\rho_1 a_2 z^{1/2}}{(a_1+a_3)} - \frac{\rho_2 a_2 a_3 y(1-y)(1-\alpha)}{2z^{1/2} D(a_1+a_3)(y+\alpha(1-y))}\right) - \frac{\eta_1 a_2 z_R^{1/2}}{V_R} = 0 \tag{3.49}$$

$$\dot{\eta}_2 = \frac{B\rho_2 a_2 z_\lambda}{2z^{1/2} D} - \frac{\partial m_3}{\partial y_R} \tag{3.50}$$

Time Conditions

$$\vec{\rho}(t_o) = \vec{\rho}(t_o + \tau) \quad \text{and} \quad \vec{\eta}(t_o) = \vec{\eta}(t_o + \tau) \tag{3.51}$$

With small modifications, the necessary conditions could also have been derived for $u' = z(0,t)$. Major simplification of these complex equations was possible by letting $\gamma = 1.0$. Since a narrow pressure range is used in this work and the experimental value for γ is 0.87, the approximation using $\gamma = 1.0$ is reasonable.

It should be noted that the uncoupling of the pressure and composition equations led to a partial differential equation for ρ_2 independent of ρ_1 . Thus, a complete solution for ρ_2 may be made before ρ_1 need be considered. The significance of this uncoupling will become clear when the problems involved in the numerical computations are discussed.

When the adjoint variables are described as in Table 3.2 then

$$\delta I = \frac{1}{\tau}\int_{t_0}^{t_0+\tau} \left(\frac{\partial m_1}{\partial u} - B\rho_j \frac{\partial F_j}{\partial w_{i_{\lambda\lambda}}}\right)_{\lambda=0} \delta u \, dt \qquad (3.52)$$

For convenience the function H_0 is defined such that

$$H_0 = m_1(u) - \left(B\rho_j \frac{\partial F_j}{\partial w_{i_{\lambda\lambda}}}\right)_{\lambda=0} u \qquad (3.53)$$

Then

$$\delta I = \frac{1}{\tau}\int_{t_0}^{t_0+\tau} \left[\frac{\partial H_0}{\partial u}\, \delta u\right]_{\lambda=0} dt \qquad (3.54)$$

For the optimal choice of $u(t)$, which is denoted by u^* and is composed of subarcs which will hereafter be referred to as the optimal control components, δI must be nonpositive for all allowable variations. Therefore, for an optimal system where the adjoint variables are described as in Table 3.2, the following maximum principle must be satisfied:

Except at a finite number of points, the function H_o, the feed boundary Hamiltonian, is made stationary with respect to the components of u^* which lie in the interior of its admissible region. The Hamiltonian is made a maximum with respect to the components of u^* which lie at the boundary of the admissible region.

Note that the optimal control satisfying the above maximum principle is not necessarily a unique extremal nor is the existence of such an optimal control assured.

The preceding development for the necessary conditions were based on a constant period, τ. A necessary condition for the optimal period is now needed. Following the approach used by Horn and Lin (20) for ordinary differential equations, consider a variation of the length of operating period.

$$\text{Let } I' = \tau I$$

$$\text{Then } I' = \int_{t_o}^{t_o+\tau} [m_1(\omega_{1_\lambda}) + m_3(r_2)]dt \tag{3.55}$$

Once an optimal control has been found at a constant τ, consider a variation in period length, $\delta\tau$. Then

$$\begin{aligned} \delta\vec{\omega}(t_o) &= \delta\vec{\omega}(t_o+\tau) + \vec{F}(t_o+\tau)\,\delta\tau \\ \delta\vec{r}(t_o) &= \delta\vec{r}(t_o+\tau) + \vec{G}(t_o+\tau)\,\delta\tau \end{aligned} \tag{3.56}$$

Horn and Lin have shown that retaining the definition for the adjoint system (for $\vec{\rho}$ and $\vec{\eta}$ as given in Table 3.2) yields the following relation if the variation of the optimal control, δu, is independent of the

variation of the period length $\delta\tau$:

$$\delta I' = -\left\{\eta_i \delta r_i + B\int_0^L \rho_i \delta\omega_i \, d\lambda\right\}_{t_0}^{t_0+\tau} + \left\{m_1(\omega_{1_\lambda}) + m_3(r_2)\right\}_{t_0+\tau} \delta\tau \qquad (3.57)$$

Using relations (3.56),

$$\delta I' = \left\{\vec{\eta}^T\vec{G} + B\int_0^L \vec{\rho}^T\vec{F}\, d\lambda + m_1(\omega_{1_\lambda}) + m_3(r_2)\right\}_{t_0+\tau} \delta\tau \qquad (3.58)$$

Since

$$\frac{dI}{d\tau} = -\frac{1}{\tau^2} I' + \frac{1}{\tau}\frac{dI'}{d\tau} \qquad (3.59)$$

then

$$\frac{dI}{d\tau} = \frac{1}{\tau}\left\{\vec{\eta}^T\vec{G} + B\int_0^L \vec{\rho}^T\vec{F}\, d\lambda + m_1(\omega_{1_\lambda}) + m_3(r_2)\right\}_{t_0+\tau} - \frac{1}{\tau} I \qquad (3.60)$$

The above relation is only valid when $u' = z(0,t)$ is treated as the control. If $u = z_\lambda(0,t)$ is treated as the control, the change in the period length would result in a change of the region of permissible pressure gradients. Thus, the above necessary condition for optimal τ could not be used.

3.4. Applications of the Maximum Principle

Before the maximum principle can be used to predict possible forms of the optimal control, the behavior of the Hamiltonian should be examined. Written in terms of ρ_1, ρ_2, z and y,

$$H_0 = m_1(u) - u\left[\frac{Ba_2}{(a_1+a_3)}\left(\rho_1 z^{1/2} - \rho_2 \frac{a_3 y(1-y)(1-\alpha)}{2z^{1/2} D(y+\alpha(1-y))}\right)\right]_{\lambda=0} \qquad (3.61)$$

For gas entering the system, $u < 0$, the behavior of ρ_2 is described by the hyperbolic partial differential equation (3.44). When flow direction changes and leaves the system at $\lambda = 0$, $u > 0$, there is

no boundary condition for composition so that ρ_2 is immediately constrained by the boundary condition $\rho_2 = 0$. This could lead to a discontinuous behavior for $\frac{\partial H_0}{\partial u}$ and would occur only in switching from $u < 0$ to $u > 0$.

In switching from $u > 0$ to $u < 0$, initially $\rho_2 = 0$. This adjoint variable must then change value continuously as described by equation (3.44) and thus no discontinuity in ρ_2 would result from a switch in this direction. For the case where exhaust flow is to be minimized, $\frac{\partial m_1}{\partial u}$ has a value only when flow leaves the system, $u > 0$. This could increase still further any discontinuous behavior of $\frac{\partial H_0}{\partial u}$ in switching from $u < 0$ to $u > 0$ and would create a discontinuity in switching from $u > 0$ to $u < 0$.

3.4.1. Maximization of Product Composition

The simplest performance criterion is that of maximization of product composition. For this performance index

$$I = \frac{1}{\tau} \int_{t_0}^{t_0+\tau} y_R \, dt \tag{3.62}$$

In order to understand the behavior of u^* for the above index, the Hamiltonian is examined.

$$\text{Letting } M_0 = -\left(\frac{a_3 y(1-y)(1-\alpha)}{2z D(y+\alpha(1-y))} \right)_{\lambda=0} > 0$$

$$H_0 = -u \left(\frac{B a_2 z^{1/2}}{a_1 + a_3} \right) \left[\rho_1 + \begin{cases} M_0 \rho_2, & u \le 0 \\ 0, & u > 0 \end{cases} \right]_{\lambda=0} \tag{3.63}$$

From the maximum principle, for components of u^* that lie at the boundary of the admissible region, the Hamiltonian is maximized. From this principle, possible optimal control components can be derived for values of

$\vec{\rho}$ such that $\frac{\partial H_0}{\partial u} \neq 0$.

Where u_{min} and u_{max} are the extreme values of the control of $(\text{pressure})^2$ gradient obtained by applying the maximum available feed pressure and the minimum (atmospheric) pressure respectively and remembering that $\rho_2(0,t) = 0$ for $u > 0$,

$$\begin{aligned} &\text{At } \lambda = 0 \text{ for } \rho_1 + M_0 \rho_2 > 0 \\ &\qquad \text{and} \quad -\rho_1 u_{max} < -(\rho_1 + M_0 \rho_2) u_{min} \\ &\qquad \text{then} \quad u^* = u_{min} \\ &\qquad \text{or if} \quad -\rho_1 u_{max} > -(\rho_1 + M_0 \rho_2) u_{min} \\ &\qquad \text{then} \quad u^* = u_{max} \end{aligned} \tag{3.64}$$

If $\rho_1 + M_0 \rho_2 < 0$ but $\rho_1 > 0$, application of either u_{max} or u_{min} would give a negative Hamiltonian. In this case, restricting flow into or out of the system, $u = 0$, maximizes the Hamiltonian.

$$\begin{aligned} &\text{Thus, for } \rho_1 + M_0 \rho_2 < 0 \\ &\qquad \text{and} \quad \rho_1 < 0 \\ &\qquad \text{then} \quad u^* = u_{max} \\ &\qquad \text{or if} \quad \rho_1 > 0 \\ &\qquad \text{then} \quad u^* = 0 \end{aligned} \tag{3.65}$$

Thus, where a switch from $u < 0$ to $u > 0$ might have created a discontinuous change in H_0 , a control of $u = 0$ is applied and H_0 retains a continuous behavior.

For any situation where $\frac{\partial H_0}{\partial u} = 0$, it is possible that a control from the interior of the admissible region maximizes the Hamiltonian. This will arise if, for an interior control,

$$\rho_1 = -M_0 \rho_2 \tag{3.66}$$

occurs at more than a finite number of points. The optimal control is then referred to as a singular control. A graphical representation of all the optimal control components for values of $\vec{\rho}(0,t)$ is presented in Figure 3.4.

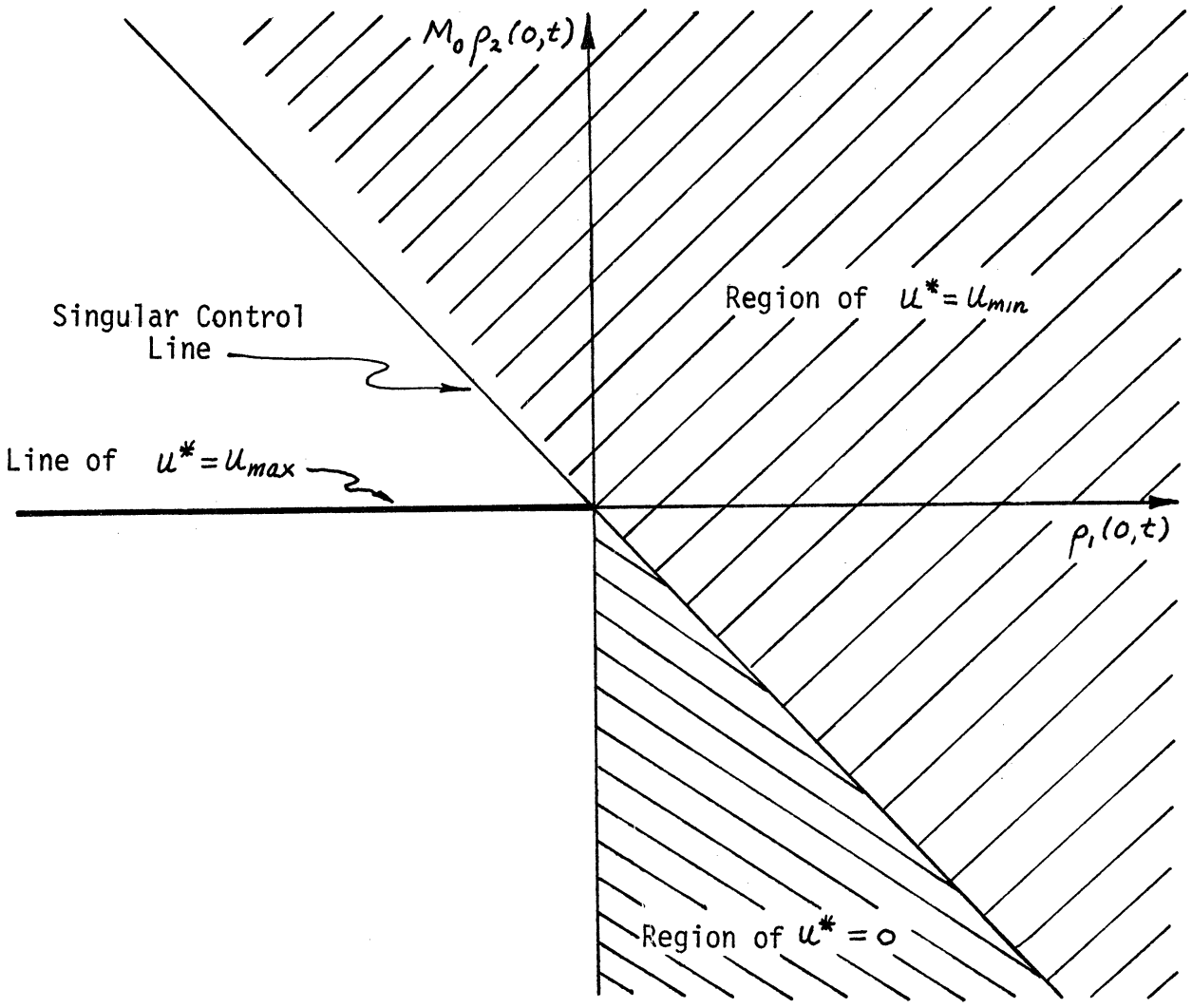

Figure 3.4. Relation of Optimal Control Components and Adjoint Variables at the Control Boundary for Product Composition Maximization.

At some time in the operation of this adsorption system the situation must exist when $u>0$. Otherwise, with no exhaust flow, there could be no separation in steady state operation. From Figure 3.4 it can be seen that $u^* = u_{max}$ is the only possible optimal control component for

$u > 0$ unless $\rho_1(0,t) = 0$ for a singular control component. It is also noted that since H_0 would exhibit the discontinuous behavior only in the switch from $u < 0$ to $u > 0$, the component $u^* = 0$ can only occur, if at all, after $u^* < 0$ has been applied.

To find the actual optimal control switching sequence, it is necessary to know the optimal trajectory of $\vec{\rho}(0,t)$. Although it is established that this trajectory must complete a closed loop (since $\vec{\rho}(\lambda,t_0) = \vec{\rho}(\lambda,t_0+\tau)$), other loops within the larger loop may exist. Thus, actual numerical computation is needed to determine the optimal trajectory which establishes the optimal control switching sequence.

Although at this point in the mathematical development the uniqueness of such an optimal control is not assured, knowledge of the behavior of the adsorption system leads to the conclusion that the existence of at least one such practical extremal is guaranteed. Specifically, if no control switching is made, there is no steady state separation. If infinitely fast switching is made between u_{max} and u_{min}, the feed gas would almost completely bypass the bed and exhaust except for a small unseparated product flowrate. Since it is known that steady state cyclic separations are possible, there must exist some maximum in product composition for a control switching sequence between no switching and infinite switching.

3.4.2. Minimization of Exhaust Rate with Maximization of Product Composition

In the operation of the adsorption system, it is noted that the highest product compositions are accompanied by large exhaust rates. Since the large exhaust rates are undesirable in the performance of the adsorption system, an exhaust minimzation term is introduced into the

performance index.

$$I = \frac{1}{\tau}\int_{t_0}^{t_0+\tau} (y_R - Cu)\, dt \tag{3.67}$$

where $C = 0$ for $u < 0$

With the exhaust rate proportional to u when $u > 0$, the magnitude of C determines the relative importance to be placed on exhaust minimization versus product composition maximization. This leads to

$$H_0 = -u\left[\frac{B a_2 z^{1/2}}{(a_1+a_3)}\right]\left[\rho_1 + \begin{cases} M_0\rho_2, & u \le 0 \\ C', & u > 0 \end{cases}\right]$$

$$C' = \left(\frac{C(a_1+a_3)}{B a_2 z^{1/2}}\right)_{\lambda=0} \tag{3.68}$$

Examination of the above Hamiltonian leads to the possible optimal control components. A graphical representation of the regions for applying these optimal components for values of $\vec{\rho}(0,t)$ is presented in Figure 3.5. Since C' enters or leaves the Hamiltonian for the switch from $u<0$ to $u>0$ or from $u>0$ to $u<0$, the optimal control component $u^*=0$ can occur after $u^* = u_{min}$ or after $u^* = u_{max}$.

Thus, in order to find this optimal control sequence, it is necessary to find the optimal trajectory in adjoint variable space. Again, because this will determine whether or not singular control components exist and the sequence and number of switches between the control u_{max}, 0 and u_{min}, it is necessary to follow the trajectory via numerical computation.

The model for the adsorption system previously derived leads to a very complex adjoint system. Therefore, in turning to the numerical solution of the problem, a simplified cell model approximation of the system will be derived.

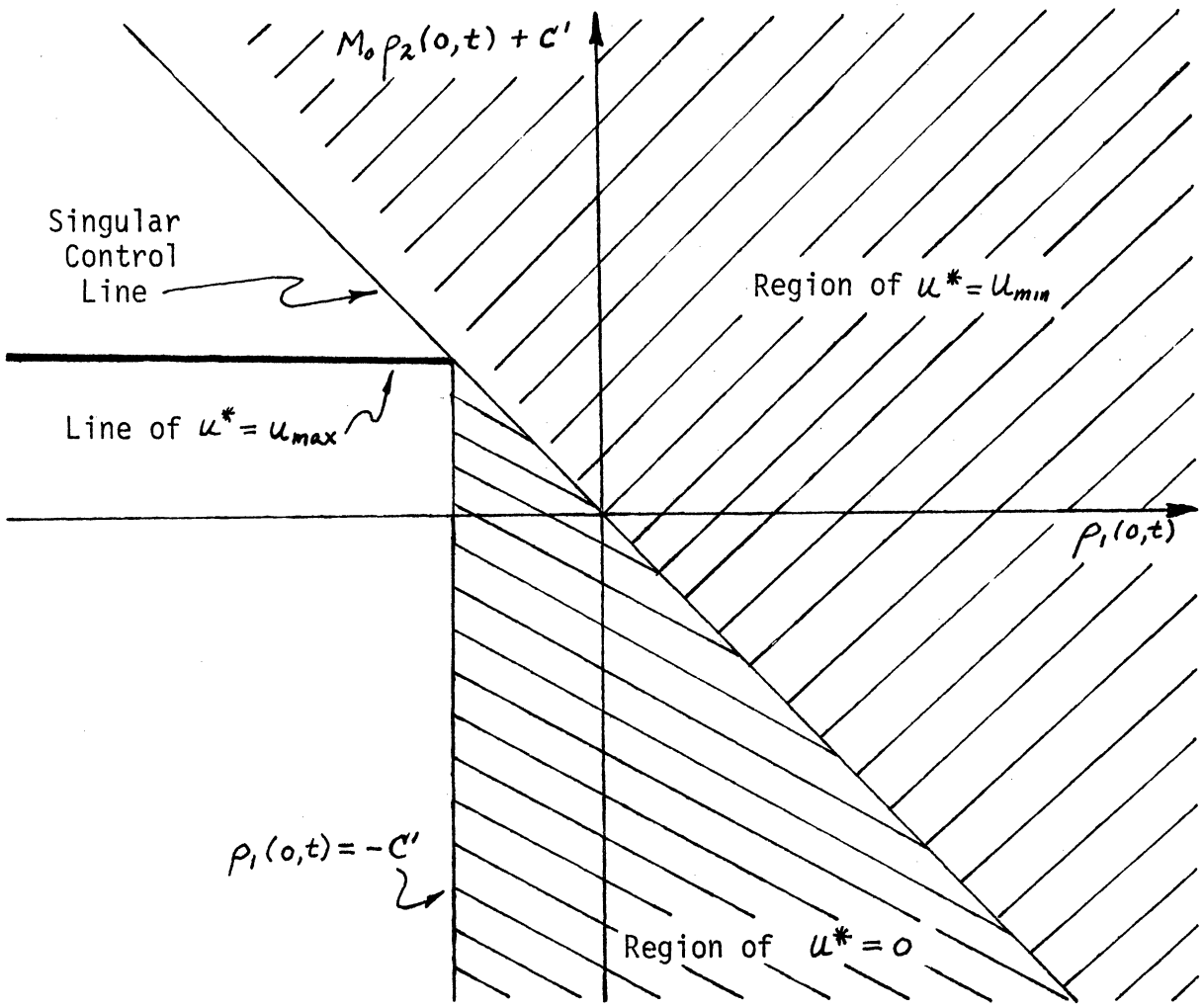

Figure 3.5. Relation of Optimal Control Components and Adjoint Variables at the Control Boundary for Product Composition Maximization and Exhaust Minimization.

3.5. Cell Model Approximation of Adsorption System

In the formulation of the cell model the column is equally divided into n segments, each one of which behaves like an ideally mixed stage. To fully describe this cell system shown in Figure 3.6 the following assumptions are made:

(A) Within each ideally mixed state the gas and adsorbed phases are in equilibrium.

(B) The pressure drop between cells is caused by a Darcy's Law pressure drop across the adsorbent.

(C) The pressure of the gas flowing between cells is taken as the average of the cell pressures.

(D) The last cell includes the volume of the product line.

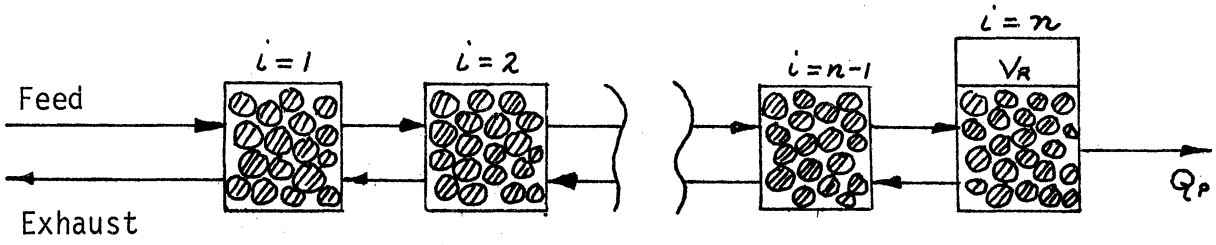

Figure 3.6. Model for the Cell System.

Total Material Balance:

$$A\left([vc]_i - [vc]_{i+1}\right) = A\epsilon\left(\frac{L}{n}\right)\frac{\partial\left(\frac{P_i}{RT}\right)}{\partial t} + \frac{W}{n}\frac{\partial(kP_i^{\gamma})}{\partial t} \qquad (3.69)$$

Darcy's Law: $$v = -\frac{K}{\mu}\frac{(P_i - P_{i-1})}{(L/n)} \qquad (3.70)$$

Average Pressure in Ideal Gas Law: $$c_i = \frac{(P_{i-1} + P_i)}{2RT} \qquad (3.71)$$

For simplifying the complexity of the control problem, as in the case of the distributed system, let $\gamma = 1.0$. Then the equation for the pressure of the i^{th} stage becomes

$$\dot{P}_i = \frac{a_2\left(\frac{1}{L/n}\right)^2}{2(a_1 + a_3)}\left(P_{i-1}^2 - 2P_i^2 + P_{i+1}^2\right) \qquad (3.72)$$

A similar balance on the n^{th} cell yields

$$\dot{P}_n = \frac{a_2\left(\frac{1}{L/n}\right)(P_{n-1}^2 - P_n^2) - a_4 Q_p}{2\left[(a_1 + a_3)(L/n) + V_R\right]} \qquad (3.73)$$

Letting $z_i = P_i^2$

$$\dot{z}_i = \frac{a_2 z_i^{1/2}(z_{i-1} - 2z_i + z_{i+1})}{(a_1 + a_3)(L/n)^2} \tag{3.74}$$

and $$\dot{z}_n = \frac{z_n^{1/2}\left(a_2\left(\frac{1}{L/n}\right)(z_{n-1} - z_n) - a_4 Q_P\right)}{[(a_1 + a_3)(L/n) + V_R]} \tag{3.75}$$

Noting that equations (3.74) and (3.75) contain the finite difference approximations for $\frac{\partial^2 z}{\partial \lambda^2}$ and $\frac{\partial z}{\partial \lambda}$ respectively, these equations will converge to equations (3.10A) and (3.16A) of the distributed model, for $\gamma = 1.0$, in the limit as $n \to \infty$. z_n then becomes equivalent to z_R.

The boundary control enters into equation (3.70) for $i = 1$. If the control at the feed boundary is to be (pressure)^2

$$u' = z_0 \tag{3.76}$$

If the (pressure)^2 gradient at the feed boundary is to be the control,

$$u = \frac{(z_1 - z_0)}{(L/n)} \tag{3.77}$$

In either case the pressure at the feed boundary is limited by the inequality (3.37). Since in each of these cells the pressure is periodic, the time conditions are

$$z_i(t_0) = z_i(t_0 + \tau) \tag{3.78}$$

Nitrogen Material Balance:

$$A\left[(VC_{N_2})_i - (VC_{N_2})_{i+1}\right] = A\epsilon\left(\frac{L}{n}\right)\frac{\partial\left(\frac{y_i P_i}{RT}\right)}{\partial t} + \frac{W}{n}\frac{\partial(x_i k P_i^{\gamma})}{\partial t} \tag{3.79}$$

Average Pressure in Ideal Gas Law:

$$C_{N_2 i} = \frac{y_i(P_{i-1} + P_i)}{2RT} \tag{3.80}$$

Using equations (3.69), (3.70) and (3.80) in equation (3.79)

for $\gamma = 1.0$ and simplifying,

$$\dot{y}_i = \frac{\frac{a_2}{(L/n)}\left[(P_{i-1}^2 - P_i^2)(\bar{y}_i - y_i) - (P_i^2 - P_{i+1}^2)(\bar{y}_{i+1} - y_i)\right] - \frac{2a_3 \dot{P}_i y_i (1-y_i)(1-\alpha)(L/n)}{(y_i + \alpha(1-y_i))}}{2P_i\left[a_1 + \frac{\alpha a_3}{(y_i + \alpha(1-y_i))^2}\right](L/n)} \tag{3.81}$$

where $\bar{y}_i = y_i$ when $P_i > P_{i-1}$

and $\bar{y}_i = y_{i-1}$ when $P_i < P_{i-1}$

A similar balance on the n^{th} cell yields

$$\dot{y}_n = \frac{\frac{a_2}{(L/n)}\left[(P_{n-1}^2 - P_n^2)(\bar{y}_n - y_n)\right] - \frac{2a_3 \dot{P}_n y_n (1-y_n)(1-\alpha)(L/n)}{(y_n + \alpha(1-y_n))}}{2P_n\left[\left(a_1 + \frac{\alpha a_3}{(y_n + \alpha(1-y_n))^2}\right)(L/n) + V_R\right]} \tag{3.82}$$

Letting $z_i = P_i^2$ and $D_i = \left(a_1 + \frac{\alpha a_3}{(y_i + \alpha(1-y_i))^2}\right)$,

$$\dot{y}_i = \frac{\frac{a_2}{(L/n)}\left[(z_{i-1} - z_i)(\bar{y}_i - y_i) - (z_i - z_{i+1})(\bar{y}_{i+1} - y_i)\right] - \frac{a_3 \dot{z}_i y_i (1-y_i)(1-\alpha)(L/n)}{z_i^{1/2}(y_i + \alpha(1-y_i))}}{2z_i^{1/2} D_i (L/n)} \tag{3.83}$$

and

$$\dot{y}_n = \frac{\frac{a_2}{(L/n)}\left[(z_{n-1} - z_n)(\bar{y}_n - y_n)\right] - \frac{a_3 \dot{z}_n y_n (1-y_n)(1-\alpha)(L/n)}{z_n^{1/2}(y_n + \alpha(1-y_n))}}{2z_n^{1/2}\left[D_n(L/n) + V_R\right]} \tag{3.84}$$

Since equations (3.83) and (3.84) contain the finite difference approximations for $\frac{\partial z}{\partial \lambda}$ and $\frac{\partial y}{\partial \lambda}$, these equations will converge to equations (3.23) and (3.28), for $\gamma = 1.0$, in the limit as $n \longrightarrow \infty$. y_n then becomes equivalent to y_R.

For the periodic process it is also required that

$$y_i(t_0) = y_i(t_0 + \tau) \tag{3.85}$$

At the feed boundary,

$$y_0 = y_F \tag{3.86}$$

which enters into equation (3.83) for $i = 1$ and $z_1 < z_0$. At the product

boundary, the convergence of equation (3.83) for $i = n-1$ is examined. Because $(y_n - y_{n-1})$ for $z_n > z_{n-1}$ does not become a differential quantity as $n \to \infty$, $\dot{y}_{n-1}$ would then become unbounded unless

$$\text{for } z_n > z_{n-1}, \qquad y_n = y_{n-1} \tag{3.87}$$

This relation is equivalent to equation (3.26) as y_{n-1} becomes equivalent to $y(L,t)$ as $n \to \infty$.

Thus, this system of equations for the cell model compiled in Table 3.3 in the limit as $n \to \infty$, will converge to the mathematical description of the distributed model. Therefore, if the cell model is examined numerically for increasing values of n, the limits of its converging behavior will define the behavior of the distributed model.

Before the cell model is examined numerically, the necessary conditions for optimality associated with this approximate system must be derived.

3.6. Optimal Control Problem for the Cell Model

Butkovskii (8) has suggested the discretization of the distributed-parameter model so that Pontryagin's Maximum Principle can be used to derive the necessary conditions for optimal control (31). These necessary conditions are well presented and applied in the text by Athans and Falb (3). The following formulation will concern itself only with the system of interest.

For the cell model, the behavior of the system is described by

$$\begin{aligned} \dot{z}_i &= f_i(\vec{z}, u) \\ \dot{y}_i &= g_i(\vec{z}, \vec{y}, u) \end{aligned} \tag{3.88}$$

where f_i and g_i are the right hand sides of equations (3.74), (3.75),

TABLE 3.3

EQUATIONS FOR THE CELL MODEL APPROXIMATION TO THE ADSORPTION SYSTEM

Pressure Equations

$$\dot{z}_i = \frac{a_2 z_i^{1/2}(z_{i-1} - 2z_i + z_{i+1})}{(a_1+a_3)(L/n)^2} \tag{3.74}$$

$$\dot{z}_n = \frac{z_n^{1/2}\left(a_2\left(\frac{1}{L/n}\right)(z_{n-1}-z_n) - a_4 Q_P\right)}{\left[(a_1+a_3)(L/n) + V_R\right]} \tag{3.75}$$

$$z_i(t_0) = z_i(t_0+\tau) \tag{3.78}$$

$$u' = z_0 \quad \text{or} \quad u = \frac{(z_1 - z_0)}{(L/n)} \tag{3.76) or (3.77}$$

Composition Equations

$$\dot{y}_i = \frac{\frac{a_2}{(L/n)}\left[(z_{i-1}-z_i)(\bar{y}_i - y_i) - (z_i - z_{i+1})(\bar{y}_{i+1} - y_i)\right] - \frac{a_3 \dot{z}_i y_i(1-y_i)(1-\alpha)(L/n)}{z_i^{1/2}(y_i + \alpha(1-y_i))}}{2z_i^{1/2}\left[a_1 + \frac{\alpha a_3}{(y_i+\alpha(1-y_i))^2}\right](L/n)}$$

when $z_i > z_{i-1}$, $\bar{y}_i = y_i$ (3.83)

when $z_i < z_{i-1}$, $\bar{y}_i = y_{i-1}$

$$\dot{y}_n = \frac{\frac{a_2}{(L/n)}\left[(z_{n-1}-z_n)(\bar{y}_n - y_n)\right] - \frac{a_3 \dot{z}_n y_n(1-y_n)(1-\alpha)(L/n)}{z_n^{1/2}(y_n + \alpha(1-y_n))}}{2z_n\left[\left(a_1 + \frac{\alpha a_3}{(y_n+\alpha(1-y_n))^2}\right)(L/n) + V_R\right]} \tag{3.84}$$

$$y_i(t_0) = y_i(t_0+\tau) \tag{3.85}$$

$$y_0 = y_F \text{ for } z_1 < z_0 \tag{3.86}$$

(3.83) and (3.84). These state equations are the dynamical constraints on the performance index

$$I = \frac{1}{\tau}\int_{t_o}^{t_o+\tau} m_5(z_1, y_n, u)\,dt \qquad (3.89)$$

As in the variational approach, adjoint variables must be used to introduce these dynamical constraints into the performance index. Thus, similar to equation (3.38), $p_i(t)$ will be the adjoint variables associated with z_i and $q_i(t)$ will be the adjoint variables associated with y_i.

The Hamiltonian function is defined as

$$H = (p_i f_i + q_i g_i) + m_5(z_1, y_n, u) \qquad (3.90)$$

The maximum principle states that for an optimal control trajectory, the above Hamiltonian is maximized with respect to the control at all times provided that the adjoint variables are defined by

$$\dot{p}_i = -\frac{\partial H}{\partial z_i} \quad \text{and} \quad q_i = -\frac{\partial H}{\partial y_i} \qquad (3.91)$$

$$\text{or} \quad \dot{p}_i = -\left(p_j \frac{\partial f_j}{\partial z_i} + q_j \frac{\partial g_j}{\partial z_i}\right) - \frac{\partial m_5}{\partial z_i}$$

$$\text{and} \quad \dot{q}_i = -\left(q_j \frac{\partial g_j}{\partial y_i}\right) - \frac{\partial m_5}{\partial y_i} \qquad (3.92)$$

The adjoint variables are also constrained by the time condition for periodic processes.

$$p_i(t_o) = p_i(t_o+\tau) \quad \text{and} \quad q_i(t_o) = q_i(t_o+\tau) \qquad (3.93)$$

The maximized Hamiltonian, for the optimal system using the above definitions for the adjoint system, will be constant over the time period when the directly constrained variable, z_o, is treated as the control.

Replacing f_i and g_i in equations (3.88) by expressions given in Table 3.3 and expanding the partial derivatives, these equations can be

written in terms of z_i and y_i. This development is presented in Appendix III and the resulting equations are compiled in Table 3.4. As was shown in the development, as the number of cells in the model increases, these equations will approach the mathematical description of the adjoint variables for the distributed-parameter model.

However, the equivalence of these two sets of equations was established for $B = 1/(L/n)$. As the number of cells increases, B will increase and in the limit as $n \to \infty$, $B \to \infty$. It then seems as though convergence of the solution of these equations is not guaranteed. This problem is resolved by noting that the adjoint equations are linear in the adjoint variables. Thus, any particular adjoint variable can be redefined such that

$$p_i' = \beta_i p_i$$
$$q_i' = \xi_i q_i \qquad (3.102)$$

Then the Hamiltonian would be redefined by

$$H = (\beta_i p_i f_i + \xi_i q_i g_i) + m_5(z_1, y_n, u) \qquad (3.103)$$

For example, the values of the arbitrary constants could have been picked such that

$$\beta_i = \xi_i = L/n \quad \text{for} \quad i = 1, n-1$$
$$\text{and} \quad \beta_n = \xi_n = 1 \qquad (3.104)$$

For these values $B = 1$ would equalize the two systems of adjoint variables. This then suggests that, in numerical computation, if any of the adjoint variable profiles begins to diverge as $n \to \infty$, these variables could be scaled down by the proper selection of the constants β_i and ξ_i to maintain convergence of the complete set of profiles.

TABLE 3.4

ADJOINT EQUATIONS FOR THE CELL MODEL APPROXIMATION

For the following equations,

$$\left.\begin{aligned} b_i &= (a_1+a_3)(L/n) \\ d_i &= \left(a_1+\frac{\alpha a_3}{(y_i+\alpha(1-y_i))^2}\right)(L/n) \end{aligned}\right\} \text{ for } i=1,n-1 \qquad \begin{aligned} b_n &= (a_1+a_3)(L/n)+V_R \\ d_n &= \left(a_1+\frac{\alpha a_3}{(y_n+\alpha(1-y_n))^2}\right)(L/n)+V_R \end{aligned} \tag{3.94}$$

At $i=1$

$$\dot{q}_1 = \left\{ \begin{aligned} &\frac{a_2(z_1-z_0)q_1\left(\frac{\partial \bar{y}_1}{\partial y_1}-1\right)}{(L/n)\,2z_1^{1/2}d_1} - \frac{a_3 q_1 \dot{z}_1 (L/n)^2(1-\alpha)\left[\frac{\alpha a_3 y_1(3y_1(1-\alpha)+2(2\alpha-1))-\alpha)}{(y_1+\alpha(1-y_1))^2} - a_1(\alpha(y_1-1)^2-y_1^2)\right]}{2z_1 d_1^2 (y_1+\alpha(1-y_1))^2} \\ &+\frac{a_2(z_2-z_1)}{2(L/n)}\left(\frac{q_2\left(\frac{\partial \bar{y}_2}{\partial y_1}\right)}{z_2^{1/2}d_2} - \frac{q_1\left(\frac{\partial \bar{y}_2}{\partial y_1}-1\right)}{z_1^{1/2}d_1}\right) - \frac{a_2 q_1 \alpha a_3(1-\alpha)[(\bar{y}_2-y_1)(z_2-z_1)-(\bar{y}_1-y_1)(z_1-z_0)]}{z^{1/2}d_1^2(y_1+\alpha(1-y_1))^3} \end{aligned} \right\} \tag{3.95}$$

for $u=\frac{(z_1-z_0)}{(L/n)}$, $\quad m_5 = y_n - Cu$ where $C=0$ for $u<0$

$$\dot{p}_1 = \left\{ \begin{aligned} &-\frac{p_1\dot{z}_1}{2z_1} + \frac{a_2(p_1 z_1^{1/2}-p_2 z_2^{1/2})}{b_1(L/n)} + \frac{q_1 a_2}{2z_1^{1/2}d_1(L/n)}\left[(\bar{y}_2-y_1) - \frac{a_3 y_1(1-y_1)(1-\alpha)(L/n)}{b_1(y_1+\alpha(1-y_1))}\right] \\ &+\frac{q_1\dot{y}_1}{2z_1} - \frac{q_2 a_2}{2z_2^{1/2}d_2(L/n)}\left[(\bar{y}_2-y_2) - \frac{a_3 y_2(1-y_2)(1-\alpha)(L/n)}{b_2(y_2+\alpha(1-y_2))}\right] \end{aligned} \right\} \tag{3.96A}$$

for $u' = z_0$ $\qquad m_5 = y_n - C\dfrac{(z_1 - u')}{(L/n)}$ where $C = 0$ for $u > z_1$

$$\dot{p}_1 = \left\{ \begin{array}{l} \dfrac{-p_1 \dot{z}_1}{2 z_1} + \dfrac{a_2 (2 p_1 z_1^{1/2} - p_2 z_2^{1/2})}{b_1 (L/n)} + \dfrac{q_1 a_2}{2 z_1^{1/2} d_1 (L/n)} \left[(\bar{y}_2 - y_1) + (\bar{y}_1 - y_1) - \dfrac{2 a_3 y_1 (1-y_1)(1-\alpha)(L/n)}{b_1 (y_1 + \alpha(1-y_1))} \right] \\ + \dfrac{q_1 \dot{y}_1}{2 z_1} - \dfrac{q_2 a_2}{2 z_2^{1/2} d_2 (L/n)} \left[(\bar{y}_2 - y_2) - \dfrac{a_3 y_2 (1-y_2)(1-\alpha)(L/n)}{b_2 (y_2 + \alpha(1-y_2))} \right] + \dfrac{C}{L/n} \end{array} \right\} \qquad (3.96B)$$

At $i = 2, n-1$

$$\dot{q}_i = \left\{ \begin{array}{l} \dfrac{a_2 (z_i - z_{i-1})}{2(L/n)} \left(\dfrac{q_i \left(\dfrac{\partial \bar{y}_i}{\partial y_i} - 1 \right)}{z_i^{1/2} d_i} - \dfrac{q_{i-1} \left(\dfrac{\partial \bar{y}_i}{\partial y_i} \right)}{z_{i-1}^{1/2} d_{i-1}} \right) - a_3 q_i z_i (L/n)^2 (1-\alpha) \left[\dfrac{\alpha a_3 (y_i (3 y_i (1-\alpha) + 2(2\alpha - 1)) - \alpha)}{(y_i + \alpha(1-y_i))^2} - a_1 (\alpha (y_i - 1)^2 - y_i^2) \right] \\ \qquad \dfrac{}{2 z_i d_i^2 (y_i + \alpha(1-y_i))^2} \\ + \dfrac{a_2 (z_{i+1} - z_i)}{2(L/n)} \left(\dfrac{q_{i+1} \left(\dfrac{\partial \bar{y}_{i+1}}{\partial y_i} \right)}{z_{i+1}^{1/2} d_{i+1}} - \dfrac{q_i \left(\dfrac{\partial \bar{y}_{i+1}}{\partial y_i} - 1 \right)}{z_i^{1/2} d_i} \right) - \dfrac{a_2 q_i \alpha a_3 (1-\alpha) \left[(\bar{y}_{i+1} - y_i)(z_{i+1} - z_i) - (\bar{y}_i - y_i)(z_i - z_{i-1}) \right]}{z_i^{1/2} d_i^2 (y_i + \alpha(1-y_i))^3} \end{array} \right\} \qquad (3.97)$$

$$\dot{p}_i = \left\{ \begin{array}{l} \dfrac{-p_i \dot{z}_i}{2 z_i} - \dfrac{a_2 (p_{i-1} z_{i-1}^{1/2} - 2 p_i z_i^{1/2} + p_{i+1} z_{i+1}^{1/2})}{b_i (L/n)} + \dfrac{q_i a_2}{2 z_i^{1/2} d_i (L/n)} \left[(\bar{y}_{i+1} - y_i) + (\bar{y}_i - y_i) - \dfrac{2 a_3 y_i (1-y_i)(1-\alpha)(L/n)}{b_i (y_i + \alpha(1-y_i))} \right] \\ + \dfrac{q_i \dot{y}_i}{2 z_i} - \dfrac{q_{i-1} a_2 \left[(\bar{y}_i - y_{i-1}) - \dfrac{a_3 y_{i-1} (1-y_{i-1})(1-\alpha)(L/n)}{b_{i-1} (y_{i-1} + \alpha(1-y_{i-1}))} \right]}{2 z_{i-1}^{1/2} d_{i-1} (L/n)} - \dfrac{q_{i+1} a_2 \left[(\bar{y}_{i+1} - y_i) - \dfrac{a_3 y_{i+1} (1-y_{i+1})(1-\alpha)(L/n)}{b_{i+1} (y_{i+1} + \alpha(1-y_{i+1}))} \right]}{2 z_{i+1}^{1/2} d_{i+1} (L/n)} \end{array} \right\} \qquad (3.98)$$

TABLE 3.4 (continued)

At $i=n$

$$\dot{q}_n = \left\{ \begin{array}{l} \dfrac{a_2(z_n - z_{n-1})}{2(L/n)}\left[\left(\dfrac{q_n\left(\dfrac{\partial \bar{y}_n}{\partial y_n} - 1\right)}{z_n^{1/2} d_n} - \dfrac{q_{n-1}\left(\dfrac{\partial \bar{y}_n}{\partial y_n}\right)}{z_{n-1}^{1/2} d_{n-1}}\right) + \dfrac{2 q_n \alpha a_3 (1-\alpha)(\bar{y}_n - y_n)(L/n)}{z_n^{1/2} d_n^2 (y_n + \alpha(1-y_n))^3}\right] - 1 \\ \\ - \dfrac{a_3 q_n \dot{z}_n (L/n)^2 (1-\alpha)}{2 z_n d_n^2 (y_n + \alpha(1-y_n))^2}\left[\dfrac{\alpha a_3 (y_n(3y_n(1-\alpha) + 2(2\alpha-1)) - \alpha)}{(y_n + \alpha(1-y_n))^2} - (a_1(L/n) + V_R)(\alpha(y_n-1)^2 - y_n^2)\right] \end{array} \right\} \quad (3.99)$$

$$\dot{p}_n = \left\{ \begin{array}{l} \dfrac{q_n a_2 \left[(\bar{y}_n - y_n) - \dfrac{a_3 y_n (1-y_n)(1-\alpha)(L/n)}{b_n (y_n + \alpha(1-y_n))}\right]}{2 z_n^{1/2} d_n (L/n)} - \dfrac{p_n \dot{z}_n}{2 z_n} + \dfrac{q_n \dot{y}_n}{2 z_n} \\ \\ - \dfrac{q_{n-1} a_2 \left[(\bar{y}_n - y_{n-1}) - \dfrac{a_3 y_{n-1}(1-y_{n-1})(1-\alpha)(L/n)}{b_{n-1}(y_{n-1} + \alpha(1-y_{n-1}))}\right]}{2 z_{n-1}^{1/2} d_{n-1}(L/n)} - \dfrac{p_{n-1} a_2 z_{n-1}^{1/2}}{b_{n-1}(L/n)} + \dfrac{p_n a_2 z_n^{1/2}}{b_n (L/n)} \end{array} \right\} \quad (3.100)$$

Time Conditions

$$p_i(t_o) = p_i(t_o + \tau) \quad \text{and} \quad q_i(t_o) = q_i(t_o + \tau) \quad (3.101)$$

Also derived in Appendix III is the form of the Hamiltonian for the cell system. Since the Hamiltonian must be maximized with respect to the control, just that part of the Hamiltonian that directly depends upon the control is presented.

for $u = \frac{(z_1 - z_0)}{(L/n)}$, $\quad m_5 = y_n - Cu$

(3.105A)

$$H_0 = -Cu - \frac{a_2 u}{(a_1+a_3)(L/n)}\left[p_1 z_1^{1/2} + \frac{q_1\left((a_1+a_3)(\bar{y}_1 - y_1) - \frac{a_3 y_1(1-y_1)(1-\alpha)}{(y_1+\alpha(1-y_1))}\right)}{2 z_1^{1/2} D_1}\right]$$

for $u' = z_0$, $\quad m_5 = y_n - \frac{C(z_1 - u')}{(L/n)}$

(3.105B)

$$H_0' = \frac{C(u'-z_1)}{(L/n)} + \frac{a_2(u'-z_1)}{(a_1+a_3)(L/n)^2}\left[p_1 z_1^{1/2} + \frac{q_1\left((a_1+a_3)(\bar{y}_1 - y_1) - \frac{a_3 y_1(1-y_1)(1-\alpha)}{(y_1+\alpha(1-y_1))}\right)}{2 z_1^{1/2} D_1}\right]$$

Thus, where $C' = \frac{C(a_1+a_3)(L/n)}{a_2 z_1^{1/2}}$

$$(L/n)\frac{\partial H_0'}{\partial u'} = -\frac{\partial H_0}{\partial u} = \frac{a_2 z_1^{1/2}}{(a_1+a_3)(L/n)}\left\{\begin{array}{l}\left[p_1 - \frac{q_1 a_3 y_1(1-y_1)(1-\alpha)}{2 z_1 D_1 (y_1+\alpha(1-y_1))}\right] \\ +\left[C' + \frac{q_1(a_1+a_3)(\bar{y}_1 - y_1)}{2 z_1 D_1}\right]\end{array}\right\} \quad (3.106)$$

Analysis of the Hamiltonian components above, as with the distributed-parameter model, shows a discontinuity could exist when a switch in either direction is made between $u<0\,(u'>z_1)$ and $u>0\,(u'<z_1)$. The continuous and discontinuous terms have been separately grouped in equation (3.106). Although this analysis leads to the possible optimal control components $u^* = u_{max}$, 0 and u_{min} $(u'^* = u'_{min}$, z_1 and $u'_{max})$, the sequence in which $u^* = 0$ may be applied is not clear as was the case with the distributed-parameter model. Since the optimal control components for u or u' are both limited by the inequality constraint (3.37), the

optimal pressure forms for the two sets of optimal components would be equivalent.

Once the necessary conditions for optimality have been satisfied for constant τ, an equation similar to (3.60) is needed for the cell model. Using the same procedure as before, the necessary condition for the optimum τ can be written for a time invariant Hamiltonian.

$$\frac{dI}{d\tau} = \frac{1}{\tau}\left[m_5(z_1, y_n, u) + p_i f_i + q_i g_i\right]_{t_0+\tau} - \frac{1}{\tau} I \qquad (3.107)$$

With the use of the necessary conditions developed for optimality of the cell model, numerical computations for the optimal control can be made.

4. COMPUTATION OF OPTIMAL CONTROLS

In order to compute the optimal controls, a method suitable for use on the IBM 360 digital computer must be developed to find the solution to the necessary conditions for optimality. This method must not only provide a means for converging to the optimal control function from an initial assumed control function but must also provide solutions to the state and adjoint equations.

4.1. Solution of State and Adjoint Equations

Because the state and adjoint variable time conditions require matching, a technique with minimum computation is needed to find the necessary set of conditions. As the mathematical properties of the equations describing these two systems of variables are different, separate techniques are used for the two systems. Horn and Lin suggested the techniques to handle both (20).

4.1.1. State Equations

Using an assumed initial state of the system for an arbitrary control function, the state differential equations, when integrated, will follow the behavior of the system during a startup period. After integration over a number of cycles, the periodic steady state profiles will develop. This is equivalent to following the startup of the actual physical system when the assumed initial conditions and control function are used.

Since the startup of the pressure profile is rapid (less than 5 cycles for most assumed initial states), the integration following this startup would be an acceptable procedure to find the steady state profile.

However, because it may take 40-100 cycles for the complete startup of the composition profile, another technique must be devised to quickly locate this steady state profile. The following technique can be useful in locating both state variable profiles.

Where the sets of state equations are governed by ordinary differential equations (3.74), (3.75), (3.83) and (3.84), the following identities hold:

$$\int_0^\tau p_i(t)\left[\dot{z}_i - f_i(z_i, u)\right] dt = 0$$
$$\int_0^\tau q_i(t)\left[\dot{y}_i - g_i(z_i, y_i, u)\right] dt = 0 \qquad (4.1)$$

which are valid for any set of $p_i(t)$ or $\vec{p}(t)$ and $q_i(t)$ or $\vec{q}(t)$. Since the relative placement of the initial time t_o will have no effect on the results, t_o has been set equal to 0. Because the pressure equation is uncoupled from the composition equation, these two relations can be treated separately. Then first treating the pressure equation, making a variation in the pressure variables z_i,

$$\int_0^\tau p_i(t)\left[\delta \dot{z}_i - \frac{\partial f_i}{\partial z_j}\delta z_j\right] dt = 0 \qquad (4.2)$$

No variation in control is considered because the solution of the state equations needed are for an assumed control function. Integration by parts then yields:

$$p_i(0)\,\delta z_i(0) = p_i(\tau)\,\delta z_i(\tau)$$
$$\text{where} \quad \dot{p}_i = -p_j \frac{\partial f_j}{\partial z_i} \qquad (4.3)$$

The above is a set of linear differential equations that have n independent solutions. It is noted that these equations are the homogeneous parts of the corresponding adjoint differential equations given in Table 3.4.

From experience it has been learned that the integration of the adjoint equations in the direction of decreasing t is numerically more stable than that for increasing t. Using a backwards integration in time, the n independent solutions of equation (4.3) arise from n independent choices of $\vec{p}(\tau)$. These independent solutions then form the rows of the matrix $\Pi(t)$ and equation (4.3) becomes

$$\Pi(0)\,\delta\vec{z}(0) = \Pi(\tau)\,\delta\vec{z}(\tau) \tag{4.4}$$

This equation relates the change in the set $\vec{z}(\tau)$ caused by a small variation in the set of initial values, $\vec{z}(0)$. This relation then is used to find the conditions so that the periodic conditions can be obeyed.

$$z_i(0) = z_i(\tau) \tag{3.78}$$

Specifically, a set of $\vec{z}^{\,+}(0)$ is chosen and integration of the state equations yields $\vec{z}^{+}(\tau)$. Initially, these sets will not obey equation (3.78).

$$\vec{z}^{+}(\tau) - \vec{z}^{+}(0) = \Delta\vec{z}^{+} \tag{4.5}$$

It is then necessary to determine the changes needed for the set of $\vec{z}^{+}(0)$ to meet the periodic requirements of (3.78).

From equation (4.4), the change in the set $\vec{z}(\tau)$ resulting from changes in the set $\vec{z}(0)$ is established.

$$\delta\vec{z}(\tau) = \Pi^{-1}(\tau)\,\Pi(0)\,\delta\vec{z}(0) \tag{4.6}$$

Because the aim here is to make $\Delta\vec{z}$ vanish, the change in the set $\vec{z}(0)$ is made such that

$$\vec{z}^{++}(0) = \vec{z}^{+}(0) + \delta\vec{z}(0) = \vec{z}^{+}(\tau) + \delta\vec{z}(\tau) \tag{4.7}$$

Substituting equation (4.6) into (4.7) and solving for the corrected set $\vec{z}^{++}(0)$,

$$\vec{z}^{++}(0) = \vec{z}^{+}(0) - \left[\Pi(0) - \Pi(\tau)\right]^{-1}\Pi(\tau)\,\Delta\vec{z}^{+} \tag{4.8}$$

The above relation for the corrected initial conditions for the set $z_i(t)$ is based upon a variational technique which considered only small changes of the state variables. With second order and higher terms neglected, equation (4.8) does not give an exact solution for the matching time conditions. Thus, application of the above equation may be required more than once.

When the set of pressure equations has been solved, the composition time conditions can be attacked in the same manner. Thus,

$$\vec{y}^{++}(0) = \vec{y}^{+}(0) - \left[\Omega(0) - \Omega(\tau)\right]^{-1}\Omega(\tau)\,\Delta\vec{y}^{+} \qquad (4.9)$$

where the matrix $\Omega(t)$ is made up of n independent solutions of $q_i(t)$ such that

$$\dot{q}_i = -q_j \frac{\partial g_j}{\partial y_i} \qquad (4.10)$$

Again it is noted that these equations are the homogeneous parts of the corresponding adjoint differential equations given in Table 3.4.

The above technique for speeding up the procedure to locate the periodic time conditions is a Newton-Raphson iteration. For either state variable, pressure or composition, each cycle integrated requires a solution to the n cell state equations and n solutions of the n adjoint equations. For the rapidly evolving pressure profile this technique is not rewarding. However, it does reduce the number of cycles needed for computing the composition profile (using the startup procedure) to but 2-3 cycles.

4.1.2. Adjoint Equations

The uncoupling of the pressure equation from the composition equation allowed the adjoint variables associated with composition, q_i, to be determined before considering the pressure adjoint variables, p_i.

The complete solution of this linear differential equation

$$\dot{q}_i^{\circ} = -q_j \frac{\partial g_j}{\partial y_i} - \frac{\partial m_5}{\partial y_i} \tag{3.92}$$

can be made up of two parts: a set of homogeneous solutions and a particular solution. The set of homogeneous solutions is no more than the set $\Omega(t)$ from equation (4.10). The particular solution, $q_i^p(t)$, is determined for an arbitrary initial or end condition, $q_i^p(0)$ or $q_i^p(\tau)$. Here again, backwards integration is used so that equation (3.92), for an arbitrary set $q_i^p(\tau)$, establishes the set $q_i^p(t)$. Then the complete or general solution of (3.92) is given in matrix form by

$$\vec{q}^T(t) = \vec{q}_p^T(t) + \vec{h}^T \Omega(t) \tag{4.11}$$

where $\vec{h}$ is the set of n integration constants. Since there is a periodic time requirement for $q_i(t)$, the vector $\vec{h}$ is chosen so that

$$\vec{q}_i(0) = \vec{q}_i(\tau) \tag{3.101}$$

Then using equation (4.11) at $t=0$ and $t=\tau$, and equating,

$$\vec{h}^T = \left[\vec{q}^p(0) - \vec{q}^p(\tau)\right]^T \left[\Omega(\tau) - \Omega(0)\right]^{-1} \tag{4.12}$$

And thus,

$$\vec{q}^T(t) = \vec{q}_p^T(t) + \left[\vec{q}^p(0) - \vec{q}^p(\tau)\right]^T \left[\Omega(\tau) - \Omega(0)\right]^{-1} \Omega(t) \tag{4.13}$$

Using the above general solution for $\vec{p}(t)$, the adjoint equations associated with pressure can be solved in a similar manner. The general solution is made up of a set of homogeneous solutions to equation (4.3) and a particular solution of the linear differential equation

$$\dot{p}_i^{\circ} = -p_j \frac{\partial f_j}{\partial z_i} - q_j \frac{\partial g_j}{\partial z_i} - \frac{\partial m_5}{\partial z_i} \tag{3.92}$$

Then the general solution becomes

$$\vec{p}^{\,T}(t) = \vec{p}^{\,T}_{P}(t) + \left[\vec{p}^{\,P}(0) - \vec{p}^{\,P}(\tau)\right]^{T}\left[\Pi(\tau) - \Pi(0)\right]^{-1}\Pi(t) \quad (4.14)$$

The significance of uncoupling the pressure equations from the composition equations now becomes clear. Had these equations been coupled, the search for these steady state profiles would have had to have been treated together. The homogeneous part of the pressure adjoint equations would then have contained not only the terms involving $\vec{p}$ but also the terms involving $\vec{q}$. In addition, the homogeneous and particular parts of composition adjoint equations would have contained terms involving $\vec{p}$.

This increased interdependency of adjoint equations has three effects. First, use of the Newton-Raphson iteration would have required, for each cycle integrated, a solution to the $2n$ state equations and $2n$ solutions of the $2n$ homogeneous adjoint equations, now of a more complex form. Thus, $4n^2$ adjoint solutions per cycle would be needed to find the steady state profiles compared to n^2 solutions for the uncoupled system. Second, the general solution of the adjoint equations would require $4n^2+2n$ adjoint solutions versus the $2n^2+2n$ solutions needed when the state equations are uncoupled. Lastly, for large n, where digital computer storage is limited, the entire $4n^2+2n$ solutions must be stored for each time increment. Presently, storage is needed for but n^2+n solutions because by treating these solutions separately, the same storage space may be used for both sets of homogeneous and particular solutions.

4.2. Algorithm for Location of Optimal Controls

The equation relating a change in performance index with a change

in the control function is given by

$$\delta I = \frac{1}{\tau} \int_0^{\tau} \frac{\partial H_o}{\partial u} \delta u \, dt \qquad (3.54)$$

This equation can be used to converge from an initial arbitrary control to the optimal control by improving the performance index until no further improvement is possible. Then where $u^{+}(t)$ is used as the initial control and $u^{++}(t)$ is the improved control

$$u^{++}(t) = u^{+}(t) + \phi \frac{\partial H_o}{\partial u} \; ; \qquad \phi > 0 \qquad (4.15)$$

unless this violates the inequality constaint (3.37). In this case, $u^{++}(t)$ takes the value of the corresponding boundary of the admissible set of controls. Since second order and higher terms were not considered in deriving equation (3.54), ϕ should be chosen small enough so that these neglected higher order terms will not be significant. With such a value of ϕ the integrand in equation (3.54) becomes $\phi \left(\frac{\partial H_o}{\partial u}\right)^2$ which is always positive and thus improves the performance index I. If ϕ is chosen too large, then a worsening of the performance index may result.

Using this technique for changing the control function, the entire method for computing the optimal control is diagrammed in Figure 4.1.

4.3. Computation of Optimal Controls to Maximize Product Composition

The number of equations to be integrated, per cycle of computation, is approximately four times the square of the number of cells used in the model using the preceding algorithm. This rapid increase in computation and computer storage requirements was an important factor that led to the formulation of the cell model rather than directly discretizing the necessary conditions for the distributed-parameter model. Thus, the aim was to use the IBM 360 digital computer to compute the optimal controls for a

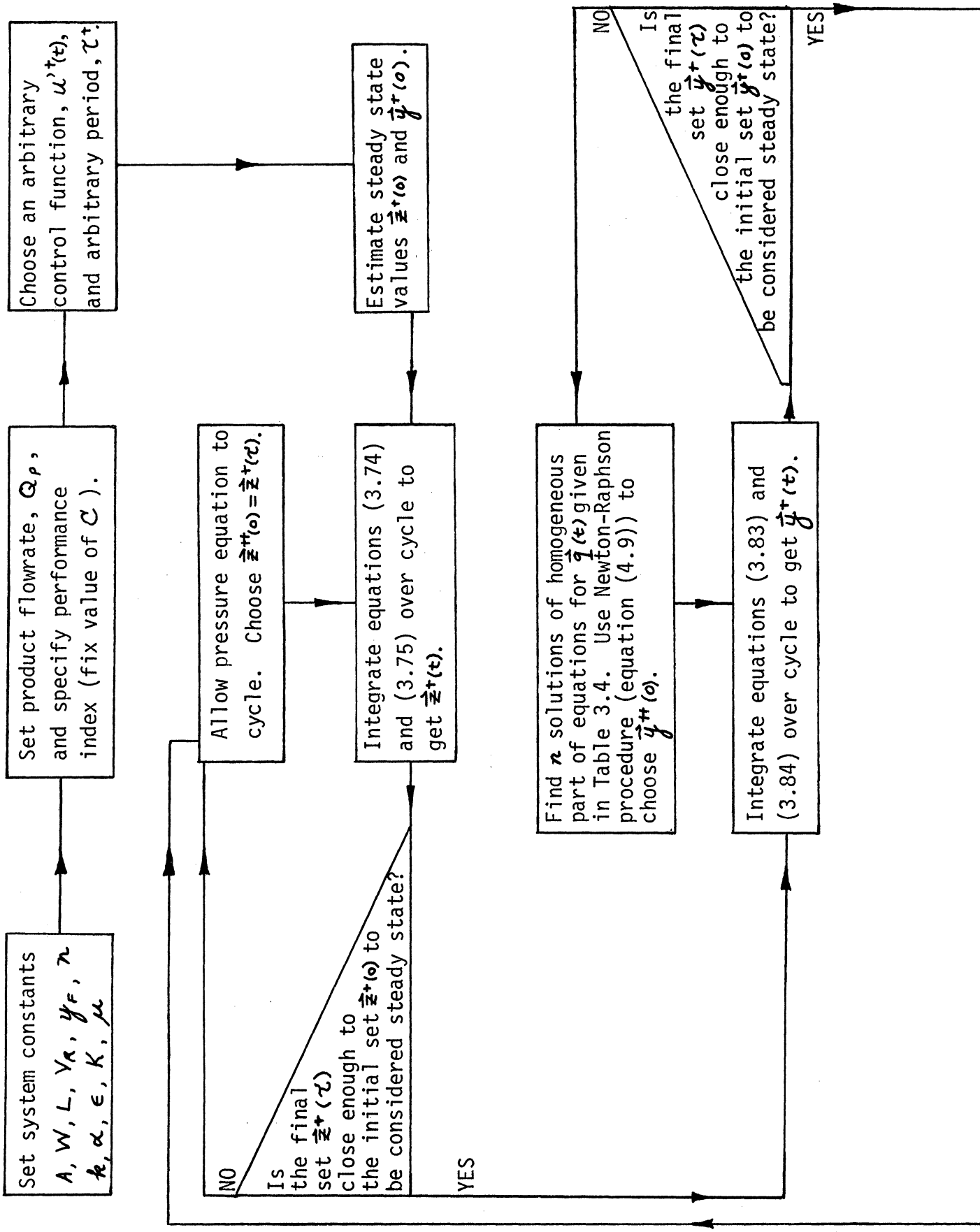
Set system constants
A, W, L, Y_R, y_F, n
k, α, ε, K, μ
Set product flowrate, Q_p, and specify performance index (fix value of C).
Choose an arbitrary control function, $u'^t(t)$, and arbitrary period, τ^t.
Estimate steady state values $\vec{z}^t(0)$ and $\vec{y}^t(0)$.
Allow pressure equation to cycle. Choose $\vec{z}^{tt}(0) = \vec{z}^t(\tau)$.
Integrate equations (3.74) and (3.75) over cycle to get $\vec{z}^t(t)$.
Is the final set $\vec{z}^t(\tau)$ close enough to the initial set $\vec{z}^t(0)$ to be considered steady state?
NO
YES
Find n solutions of homogeneous part of equations for $\vec{q}(t)$ given in Table 3.4. Use Newton-Raphson procedure (equation (4.9)) to choose $\vec{y}^{tt}(0)$.
Integrate equations (3.83) and (3.84) over cycle to get $\vec{y}^t(t)$.
Is the final set $\vec{y}^t(\tau)$ close enough to the initial set $\vec{y}^t(0)$ to be considered steady state?
NO
YES

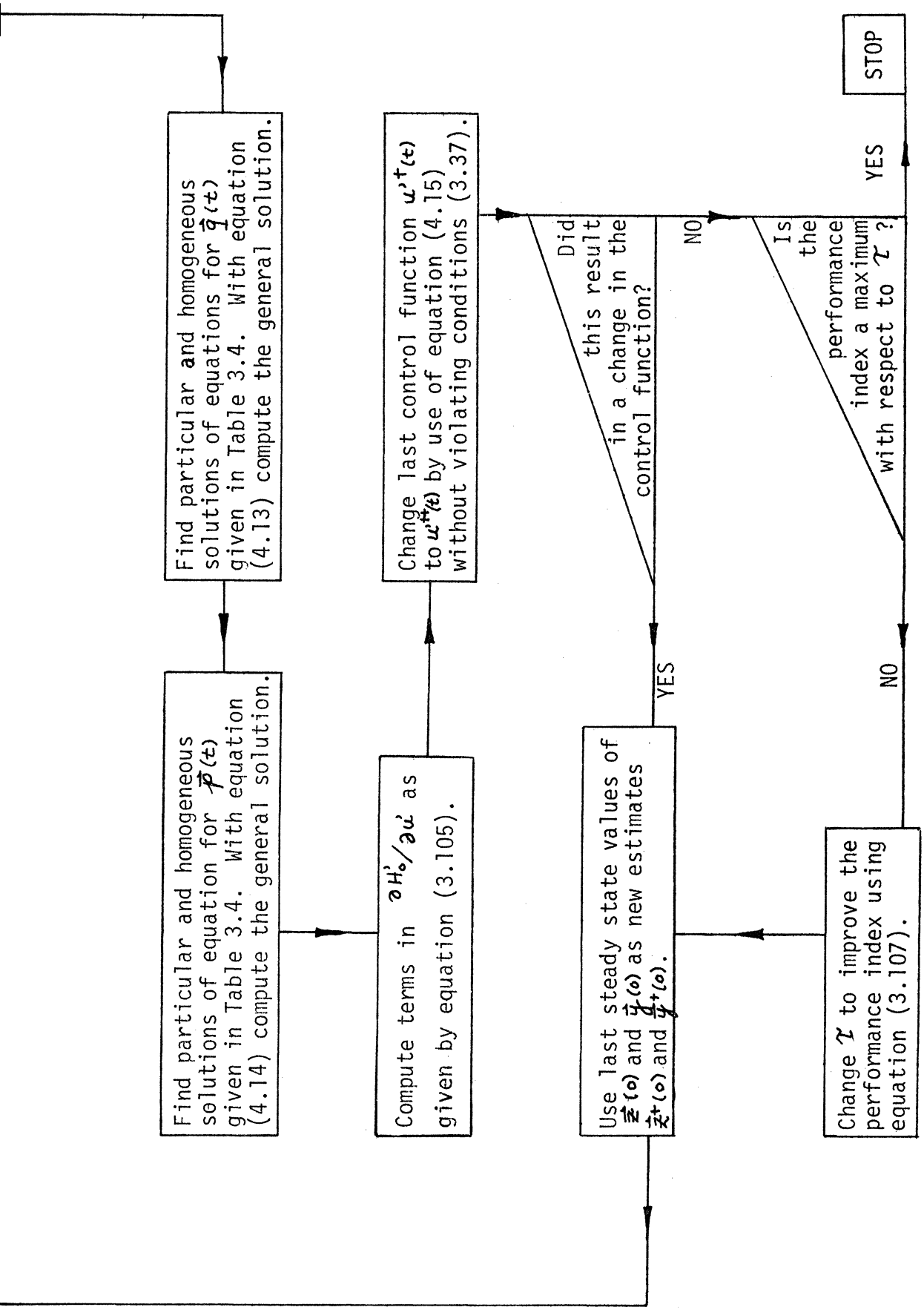

Figure 4.1. Procedure Used to Compute Optimal Controls.

small number of cells. Then the effect of n on these controls was to be examined.

With each of the variables ($z_i(t)$, $y_i(t)$, $q_i(t)$ and $p_i(t)$) being described by a number of interrelated ordinary differential equations, a fourth order Runge-Kutta solution was used for integration. With small n, this procedure was adequate. However, as larger values of n were used, smaller time grid spacings were needed to maintain numerical stability of the solution. This stability problem is similar to the one encountered with some explicit solutions of parabolic partial differential equations. Therefore, had a large value of n been contemplated for much of the work, an implicit method of integration would have been used. The optimal control function for a feed pressure limited to 10.0 PSIG and 1.16 SCFH was computed for the system constants listed in Table 4.1.

Using the algorithm based upon $u' = z_0$ to make corrections in the control function, the resulting improvement in the performance index of product maximization for the 4 cell model is presented in Figure 4.2. The corresponding development of the control function is shown in Figure 4.3. The cyclic control sequence of $[u'_{max}, z_1, u'_{min}]$ maximizes product composition.

TABLE 4.1

SYSTEM CONSTANTS USED IN NUMERICAL COMPUTATIONS

A = 3.45 cm.^{3}	k = 0.155 $\frac{\text{mg. moles adsorbed gas}}{\text{g. adsorbent}}$
W = 440. g.	α = 2.3
L = 152. cm.	ϵ = 0.623
V_R = 40.0 cm.^{3}	K = 101. darcys
y_F = 28.6 %	μ = 0.0175 cp.

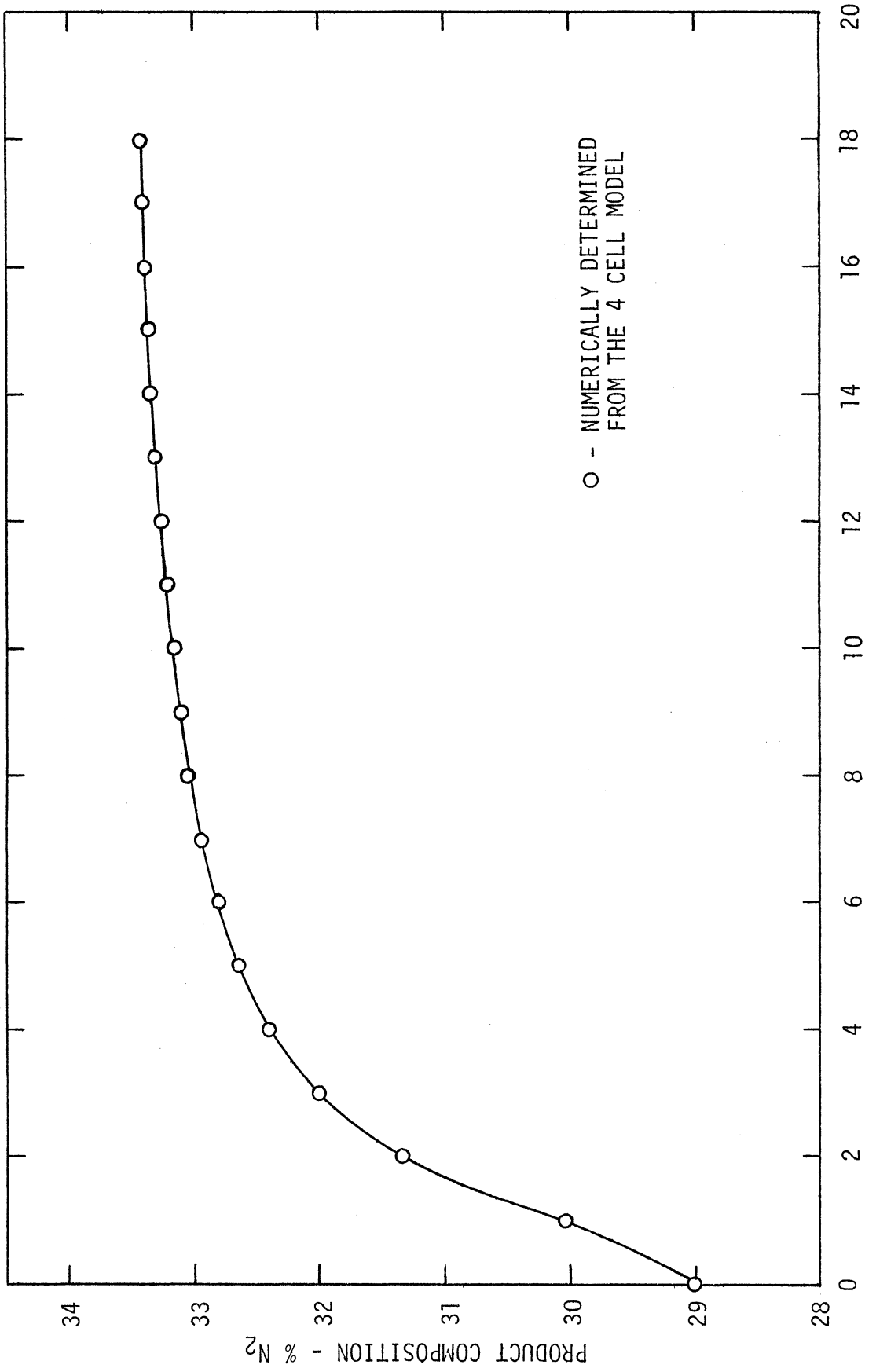

Figure 4.2. Approach of Product Composition of 4 Cell Model to the Optimal Value as Algorithm Changes the Control Function.

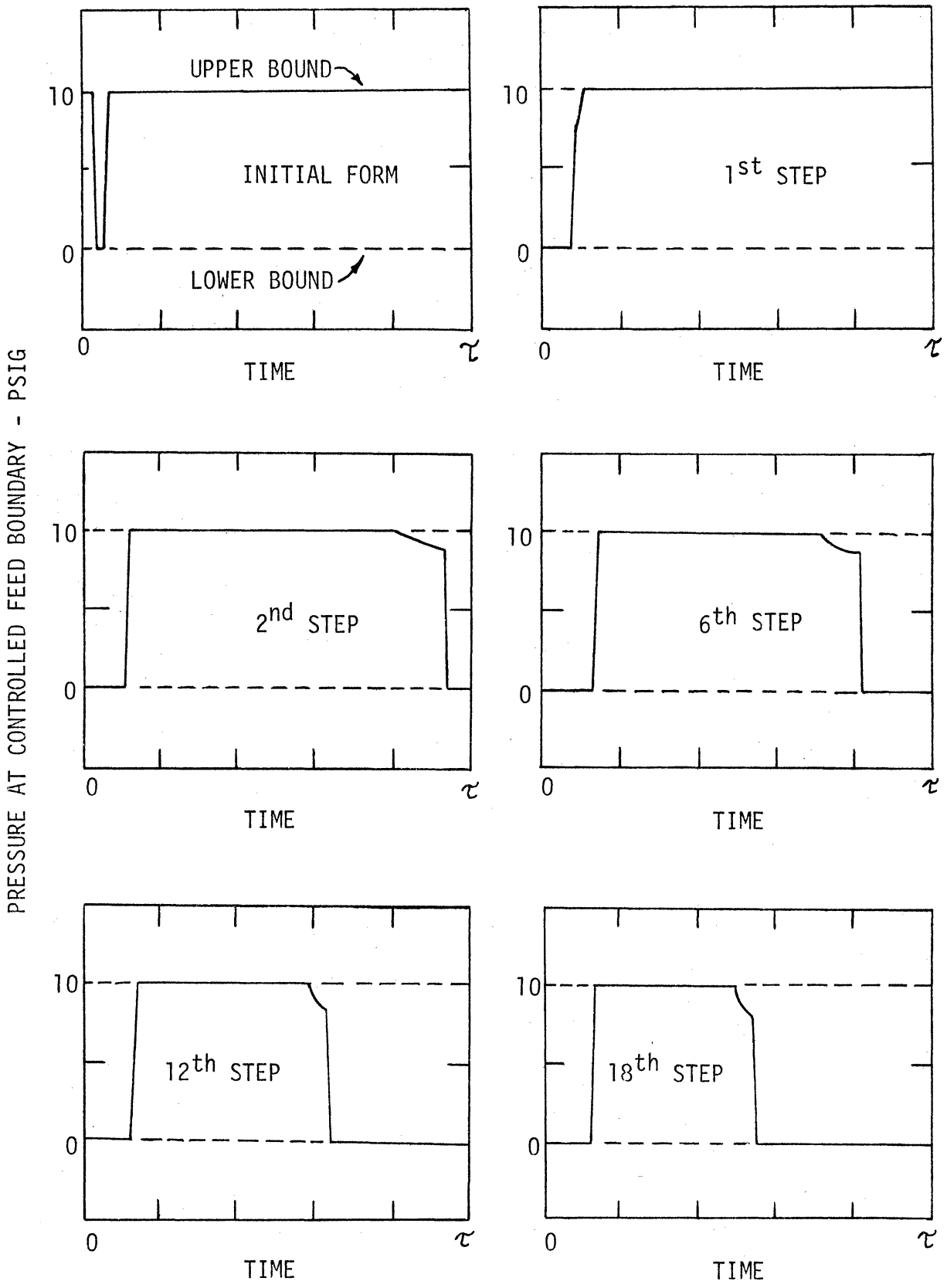

Figure 4.3. Evolution of Optimal Control Function for τ = 10.0 sec.

If a constant pressure had been used as the initial control in the improvement procedure, the state variables would all be time invariant and thus,

$$f_i(t) = 0 \qquad g_i(t) = 0 \qquad \text{and} \quad \frac{\partial f_i}{\partial z_j} = \frac{\partial g_i}{\partial z_j} = \frac{\partial g_i}{\partial y_j} = \text{Time invariant} \tag{4.16}$$

This would then lead to an adjoint system the solution of which is given by

$$-p_j \frac{\partial f_j}{\partial z_i} = q_j \frac{\partial g_j}{\partial z_i} + \frac{\partial m_5}{\partial z_i}$$

$$\text{and} \quad -q_j \frac{\partial g_j}{\partial y_i} = \frac{\partial m_5}{\partial y_i} \tag{4.17}$$

Since this system would automatically satisfy the necessary conditions for optimality, no improvement in the control function could be made even though it is known that a constant pressure control will not result in a steady state gas separation. Therefore, to initiate the improvements, a short interval of the minimum allowable feed boundary pressure is added to a control function of maximum allowable pressure as shown in Figure 4.3. Other possible initial controls that were studied are shown in Figure 4.4.

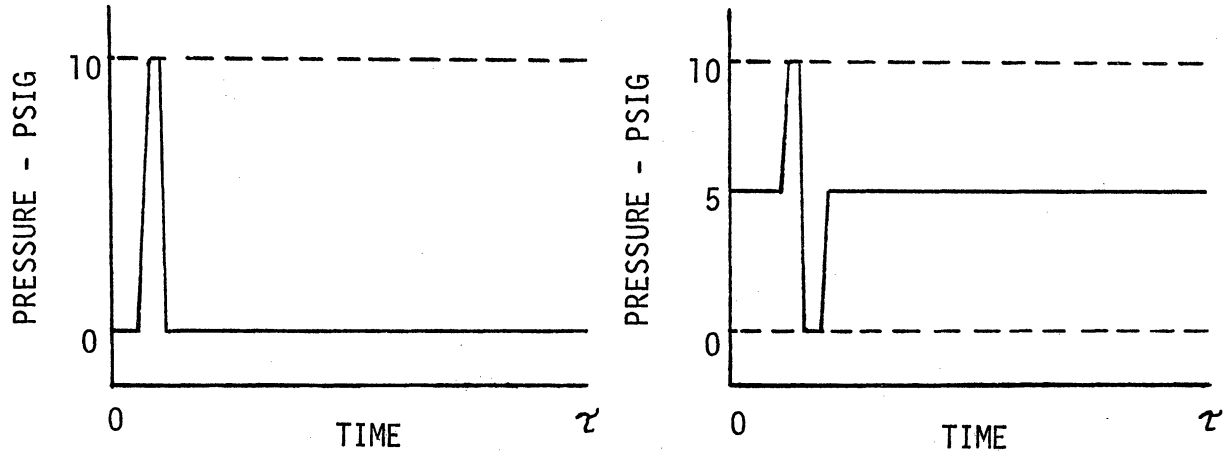

Figure 4.4. Alternate Control Functions Used to Initiate Performance Index Improvement Procedure

It was found that for each of these initial controls, the same optimal control of the 4 cell system was evolved. To allow a slow enough convergence to locate any possible singular control regions or any other optimal control forms, a value of $\phi = 0.4$ was used. When the value of the Hamiltonian components are such that $u'^{*} = z_1$ is the optimal control form, as is $u^{*} = 0$ in equation (3.65), the numerical procedure immediately corrects the control so that the resulting pressure gradient is zero or $u'^{++} = z_1$. Physically, this is equivalent to closing both the feed and exhaust valves so that the resulting correction in pressure is a small continuous change as presented in Figure 4.3. Because use of this overall technique leads to a unique control for all three initial controls, a very large value of ϕ was tried to obtain as rapid a convergence to the optimal form as possible. The evolution of the optimal system shown in Figures 4.2 and 4.3 was achieved using $\phi = 100$. As was expected from the analysis in section 3.4, the control $u^{*} = 0 \; (u'^{*} = z_1)$ is applied directly after the component $u^{*} = u_{min} \; (u'^{*} = u'_{max})$ has been applied.

The optimal control form was evolved for the 3, 4, 5 and 6 cell models for the same set of operating conditions listed in Table 4.1. In order to present a trajectory of the feed boundary Hamiltonian terms through optimal component regions similar to those shown in Figure 3.4, the continuous and discontinuous terms of this Hamiltonian are separately grouped. The continuous and discontinuous groups, ψ and χ respectively, are defined by

$$\psi = p_1 + \frac{q_1 y_1 (1-y_1)(1-\alpha)}{2 z_1 D_1 (y_1 + \alpha(1-y_1))}$$

$$\chi = \frac{q_1 (\bar{y}_1 - y_1)}{2 z_1 D_1} \qquad (4.18)$$

These groups are plotted for $n = 3, 4$ and 6 in Figure 4.5. The ψ axis has been expanded in the region $\psi < 0$ so that the part of the trajectory lying on this line can be followed. Time marks at each 2% of the period have been placed on the trajectory for $n = 3$ to indicate the rate of travel through the various regions. The fractions of the period spent in the regions of $u'^* = z_1$ and $u'^* = u'_{max}$ are presented in Figure 4.6. It is evident from this figure that although the application of $u'^* = z_1$ decreases to a short interval, the fraction of the period for $u'^* = u'_{max}$, F_{FV}, does not change much for increasing n.

The number of cells used in the model has a great effect on the optimal period length, τ^*. Figure 4.7 shows the change of τ^* with increasing n. In addition to the values for the 3-6 cell models, τ^* was computed for the 10 and 12 cell models assuming that the shape of the optimal control form was no longer changing. Although the core storage of the IBM 360 system is large enough to evolve the optimal control for a model containing as many as 20 cells, the extreme increase in computing cost as n increased made the use of the optimal-control-seeking algorithm impractical for the 10 and 12 cell models. Specifically, the computer time required to find the state and adjoint variable profiles for an assumed control function was only about 5 seconds for the 4 cell model. This computation time increased to 35 seconds for the 10 cell model and to 65 seconds for the 12 cell model. Since over twenty-five such computations were required to fully evolve the optimal control, the algorithm was not used for the higher values of n. By plotting τ^* versus $1/n$, as in Figure 4.7, the τ^* for $n = \infty$ can be predicted by extrapolation.

For purposes of comparison with experimental studies, the

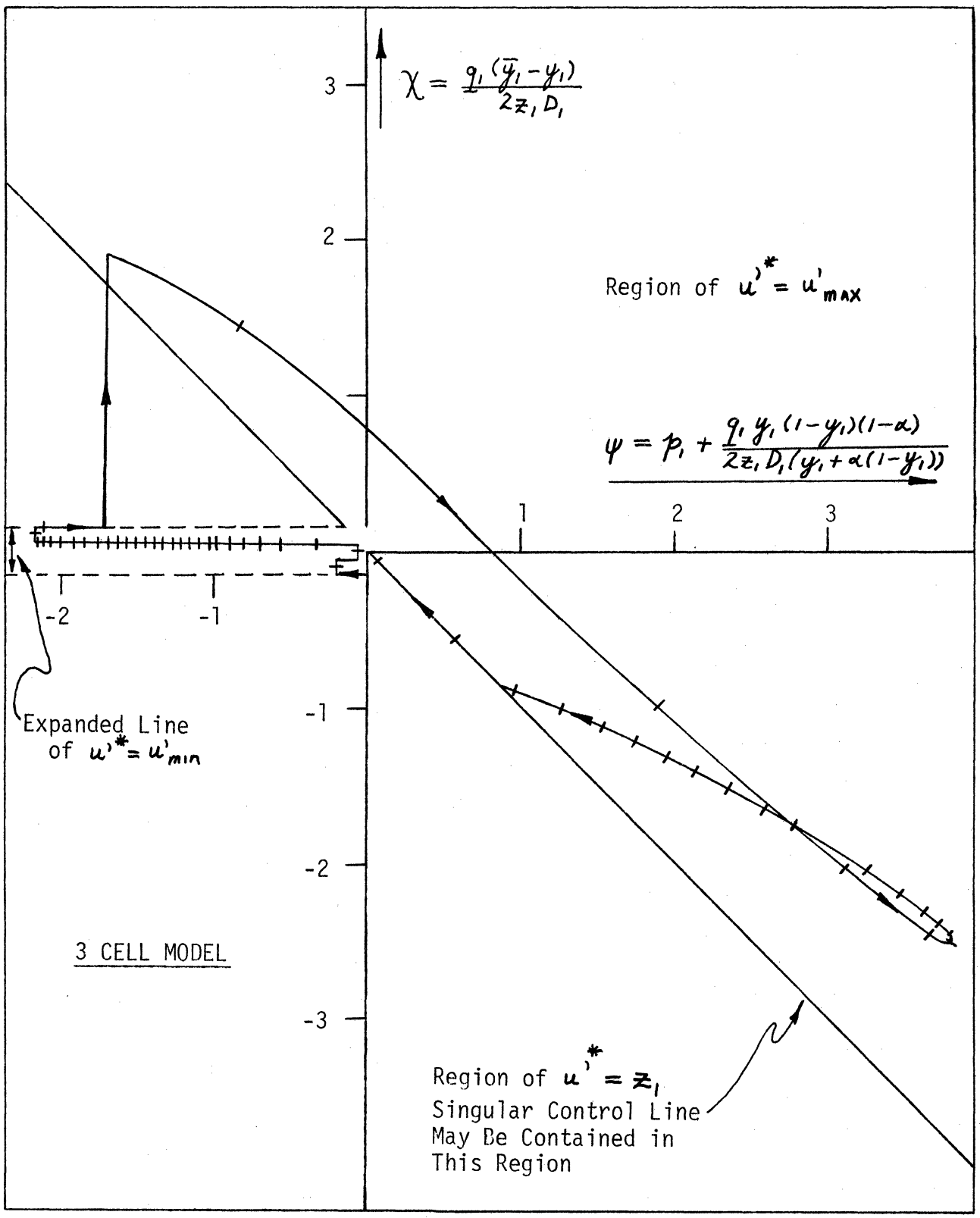

Figure 4.5. Trajectories for Control Boundary Hamiltonian Terms for 3, 4 and 6 Cell Models.

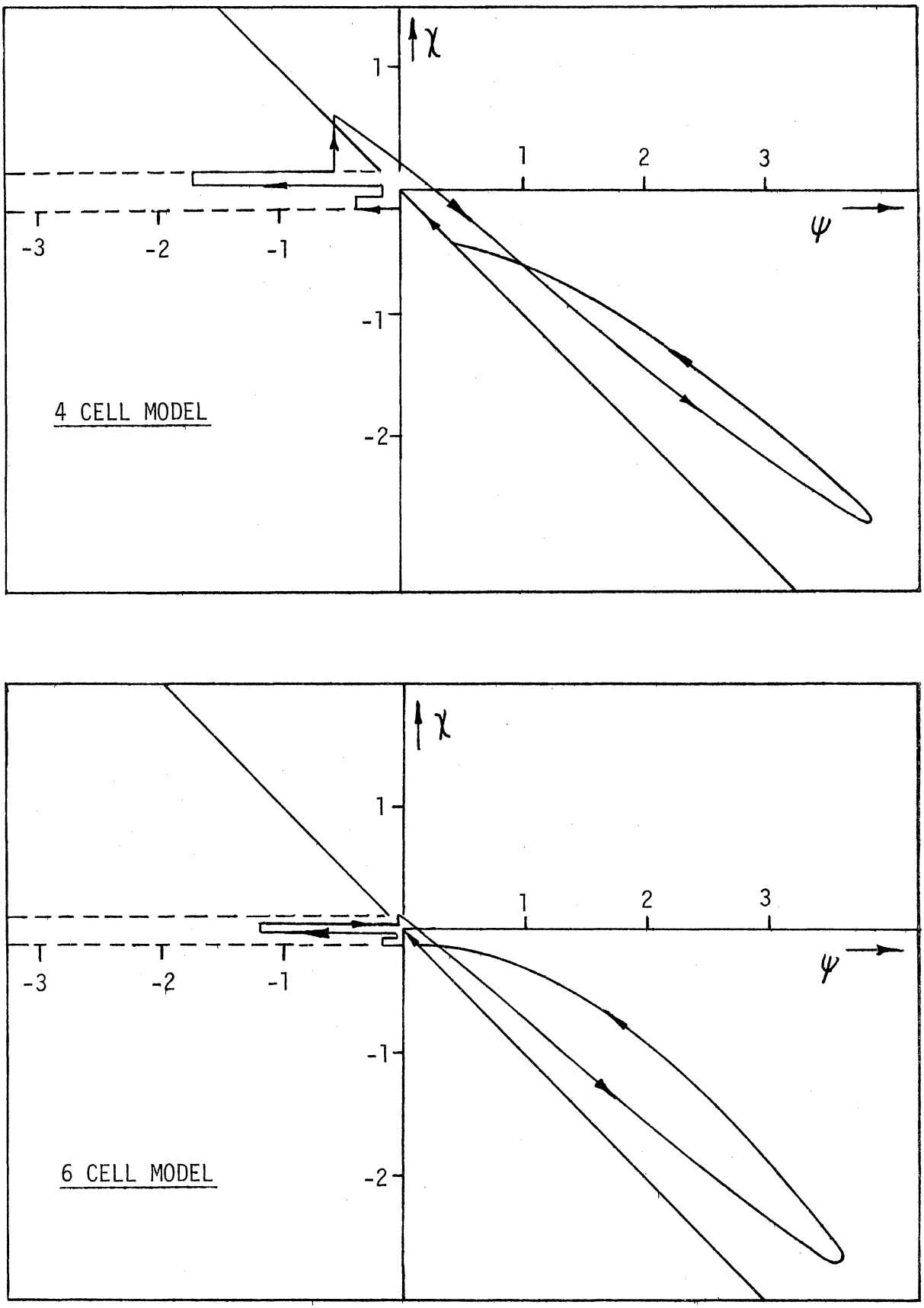

Figure 4.5. (Continued)

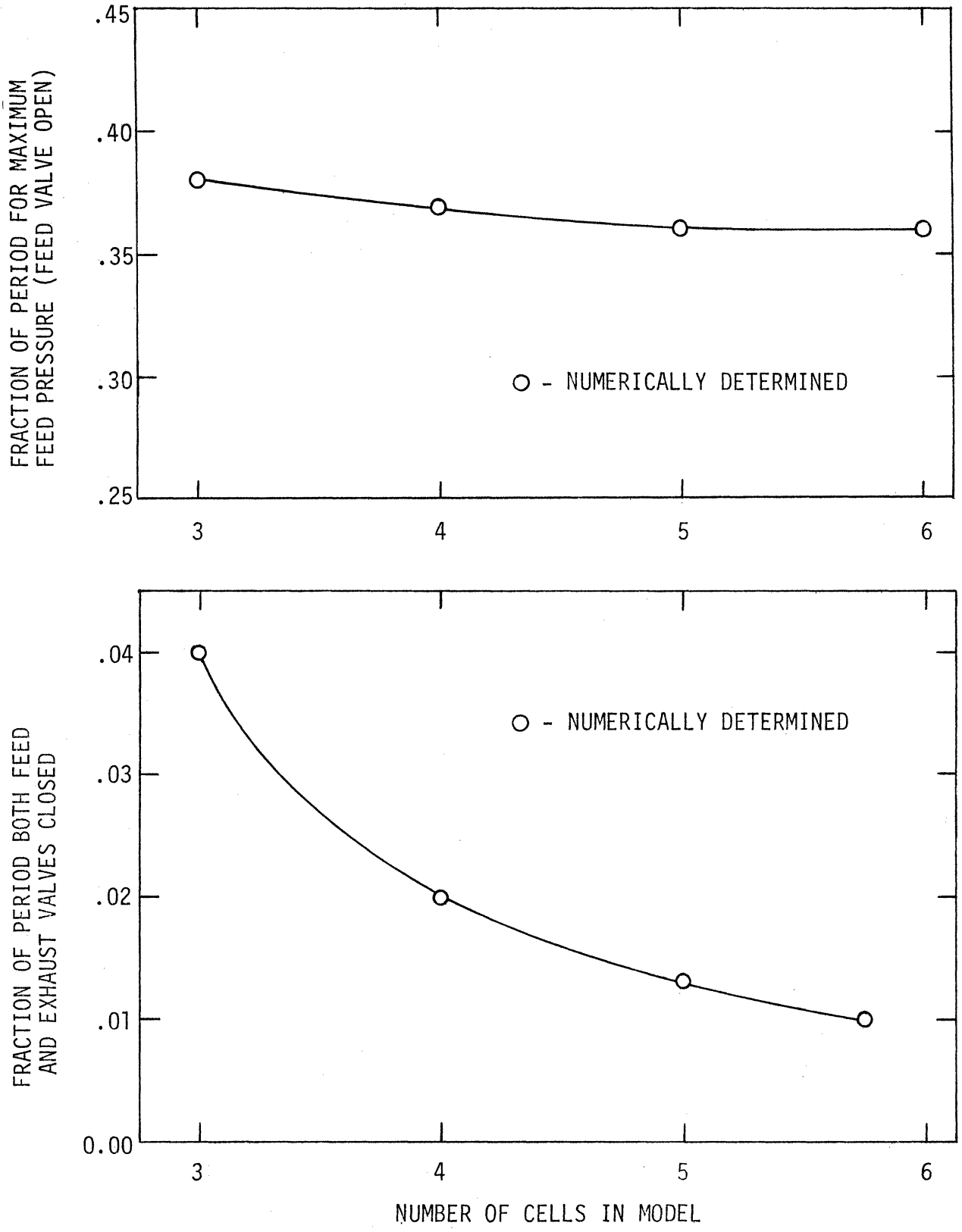

Figure 4.6. Change of Computed Optimal Control Timing as Number of Cells in Model Increases.

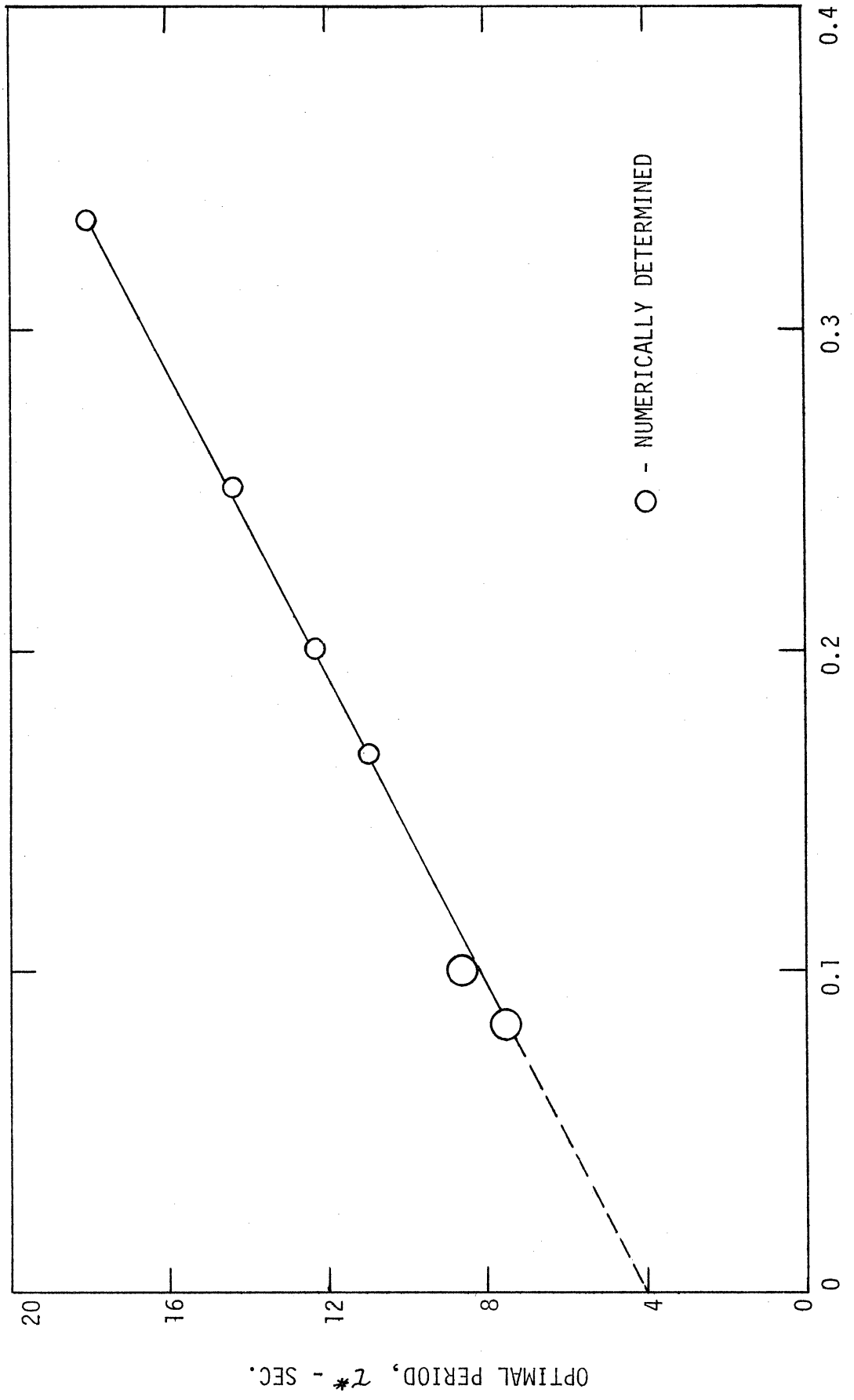

Figure 4.7. Convergence of Optimal Period, τ^*, As Number of Cells in Model Increases.

convergence of the calculated optimal composition and exhaust rate is presented in Figure 4.8. An additional computation was made for $n = 20$ assuming $\tau^* = 6$ seconds.

The method used for calculating the optimal control functions was based on $u' = z_0$. Although the control $u = z_\lambda(0,t)$ is most convenient for the analysis of the distributed-parameter Hamiltonian behavior, u' is more suitable for actual computation. This arises from the fact that the inequality constraint (3.37) directly limits u' whereas it only indirectly limits $u = (z_1 - z_0)/(L/n)$. Thus, where u'_{min} and u'_{max} are constant controls, u_{min} and u_{max} are variable controls.

4.4. Sensitivity of the Optimal Control Function to System Parameters and Operating Variables

The system parameters presented in Table 4.1 and the operating variables of product flowrate and maximum available feed pressure, all affect the operation of the adsorption system. It is noted that the values of these parameters could differ from those used in the previous computations; there is uncertainty involved in determining the adsorbent properties, the equipment specifications were arbitrarily chosen, and operating conditions can vary.

So that the reliability of the computational work can be adequately assessed and extended to new sets of operating conditions, the influence on the optimal control form of the system constants and operating variables was investigated. These computations were carried out for the 4 cell model and the performance index of maximization of product composition. The results of the studies are presented in Table 4.2. Unless otherwise noted, the system constants shown in Table 4.1 were used with a product flowrate of 1.16 SCFH and a maximum feed pressure of 10.0 PSIG.

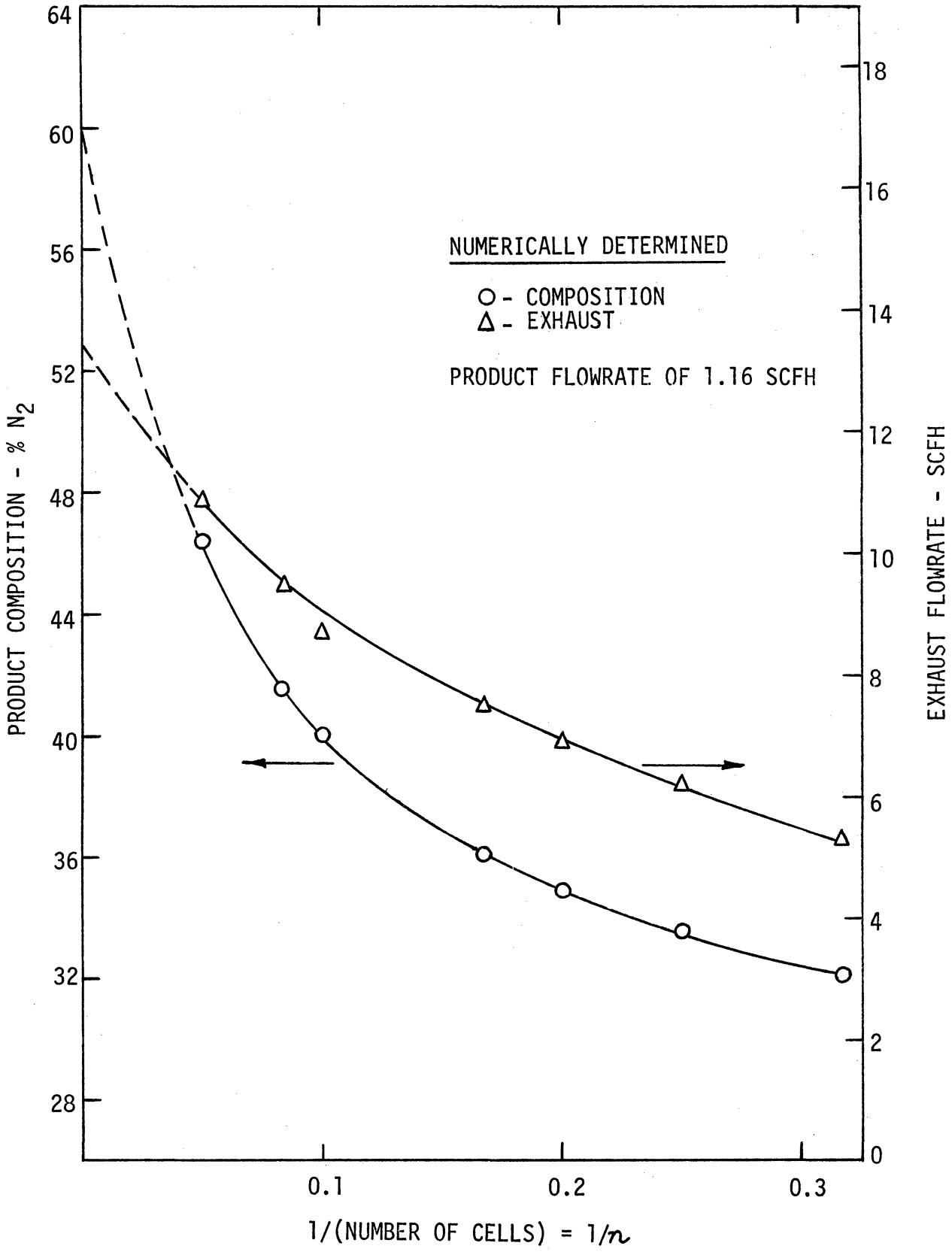

Figure 4.8. Convergence of Product Composition and Exhaust Rate as Number of Cells in Model Increases.

TABLE 4.2

CHANGES IN THE COMPUTED OPTIMAL CONTROL TIMING WITH VARIATIONS IN THE SYSTEM PARAMETERS FOR $n = 4$

Parameter Varied	New Value	Optimal Control: % of Period to be applied: Feed Valve Open	Optimal Control: % of Period to be applied: Both Valves Closed	Optimal Control: Period τ^* sec.	Computed System Outputs: Product Composition % N_2	Computed System Outputs: Exhaust Rate SCFH
Unless otherwise noted, the parameters shown in Table 4.1 were used.						
None	-	37.0	2.	14.3	33.57	6.19
α	1.65	36.5	2.	14.5	31.33	5.16
α	2.95	37.5	2.	14.3	35.37	6.22
k	0.169	37.0	2.	15.2	33.66	6.10
ϵ	0.700	37.0	2.	14.6	33.43	6.13
K	75.0	41.0	2.	19.0	33.13	4.58
μ	0.127	34.0	2.	10.4	33.98	8.49
y_F	0.200	37.5	2.	14.3	24.00	6.22
V_R	70.0	37.0	2.	14.5	33.61	6.17
V_R	500.0	41.0	2.	>20.0	34.23	5.71
V_R **	5000.0	46.0	2.	25.0	35.53	5.09
Q_P	0.60 SCFH	29.0	2.	14.8	34.28	5.81
Q_P	1.80 SCFH	43.0	2.	14.3	32.85	6.10
Q_P	2.40 SCFH	47.0	2.	14.3	32.39	5.89
P_{max}	20.0 PSIG	21.0	1.	15.0 ***	37.74	12.03

** nonoptimal computation made to determine system outputs

*** nonoptimal τ

4.5. Computation of Optimal Controls to Minimize Exhaust Rates while Maximizing Product Composition

In order to consider a performance index which includes two factors, the relative importance of these factors must be established. For exhaust rate minimization and product composition maximization

$$I = \frac{1}{\tau}\int_0^{\tau}\left(y_n - \frac{C(z_1 - u')}{(L/n)}\right)dt \tag{4.19}$$

where $C = 0$ for $u' > z_1$

Thus, the value of C will establish the relative importance of the two performance factors. If exhaust rate minimization is relatively unimportant, $C=0$ and the optimal controls will be the same as computed in the last two sections. If too large a value of C were used, the optimal operation would be either not to operate at all or to operate with a steady flow through the bed. In either case a purified gas product would not be obtained. The value of C thus strongly influences the criterion for optimal control.

In the following computations, the relative importance between the above performance factors was not investigated. Instead, the optimal control has been computed for a few values of C. The effect on the optimal pressure control form of increased importance of the exhaust rate term is then clear. These computed optimal controls for $n=4$ and product flowrate of 1.16 SCFH are shown in Figure 4.9 along with the corresponding system outputs. From Figure 4.8 it is noted that for this small value of n, the degree of gas separation is a much smaller fraction of the extrapolated value for $n=\infty$ than is the computed exhaust rate. Thus, Figure 4.9 illustrates only the relative changes in optimal control form for changing C rather than the actual changes that would be computed for

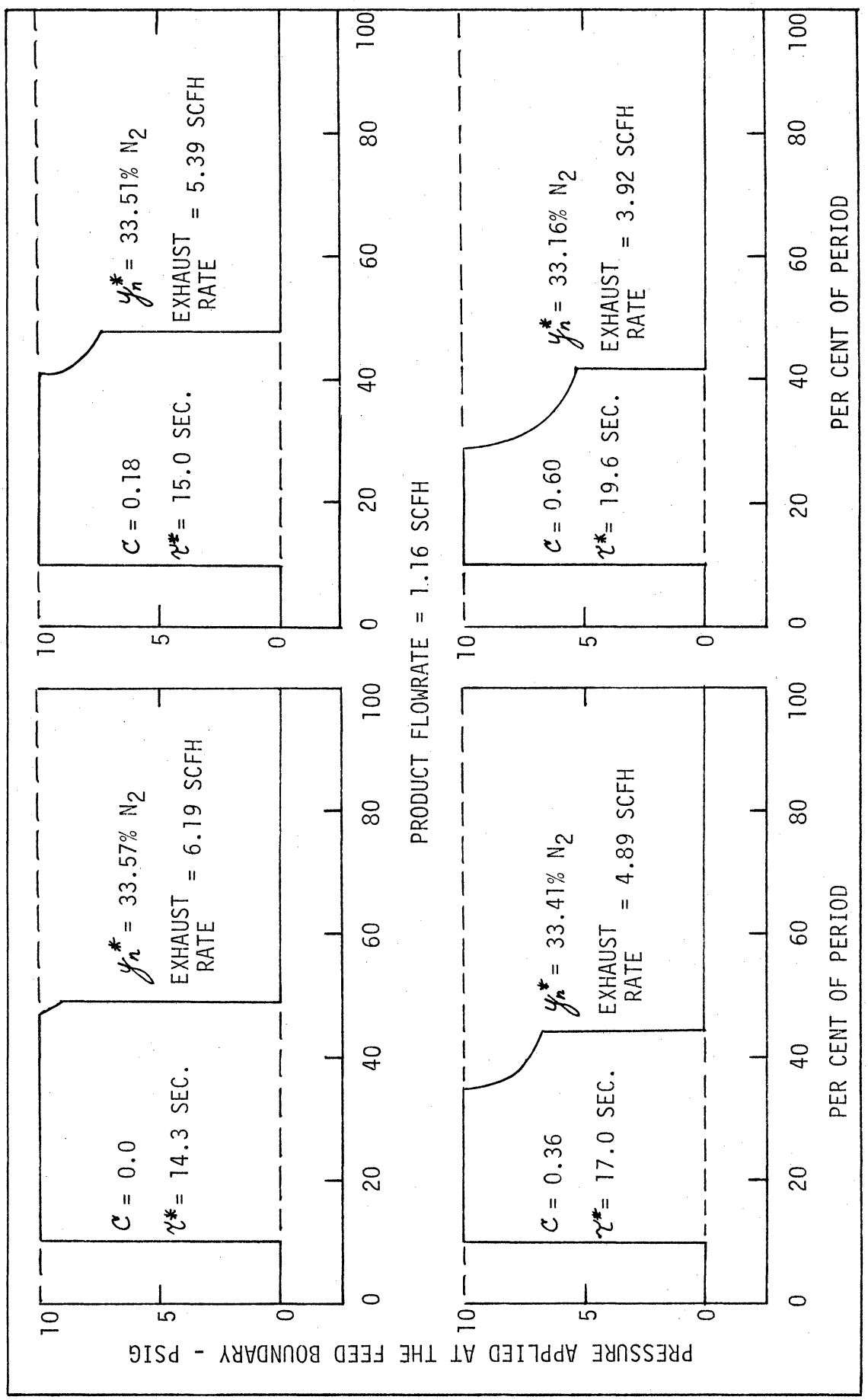

Figure 4.9. Effect on 4 Cell Model Optimal Control Form of Minimizing Exhaust Rate as well as Maximizing Product Composition.

the distributed-parameter model.

The optimal pressure wave forms here again are made up of the optimal control sequence $[u'_{max} \quad z_1 \quad u'_{min}]$. Time marks on an optimal trajectory shown in Figure 4.10 show the rate at which the trajectory passes through the optimal control component regions.

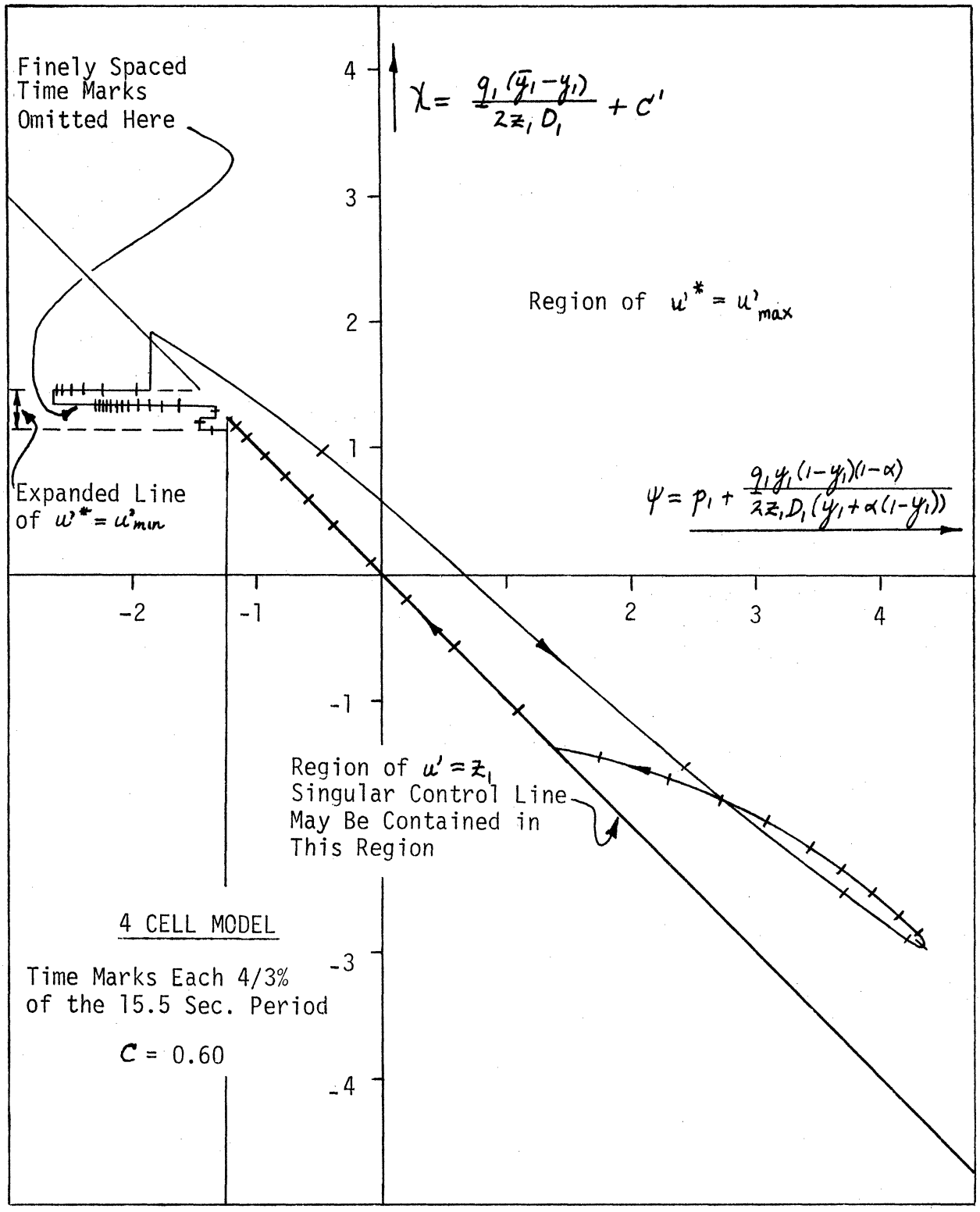

Figure 4.10. Optimal Trajectory for 4 Cell Model when Exhaust Minimzation is included in the Performance Index.

5. THE EXPERIMENTAL ADSORPTION SYSTEM

With unlimited possible control policies, an exhaustive experimental exploration of the adsorption system would be unrealistically complex. Thus, the actual adsorber performance will be investigated only for variations in the general optimal pressure control form that has just been established.

5.1. Equipment

The basic experimental adsorption system used in this research was based upon the work done by Turnock (39). A schematic of this experimental system is shown in Figure 5.1.

The computed cyclic pressure control forms can be physically constructed with two 2-way solenoid valves using the following cycling sequence:

1. Feed valve open, exhaust valve closed
2. Both valves closed
3. Feed valve closed, exhaust valve open

These valves are electrically controlled by direct current relays which are activated by the square wave outputs of an Applied Dynamics AD2-24PB analog computer. The analog circuit used is presented in Figure 5.2 and requires the sine wave output of a Hewlett-Packard function generator. If step 2 of the above sequence is not included in the control, only one single pole, double throw relay is used to control both valves.

To fully implement the control policy of maximal flow in either direction at the feed boundary, surge vessels are used for both the inlet and outlet flow. The nitrogen-methane mixture, pressure regulated at the

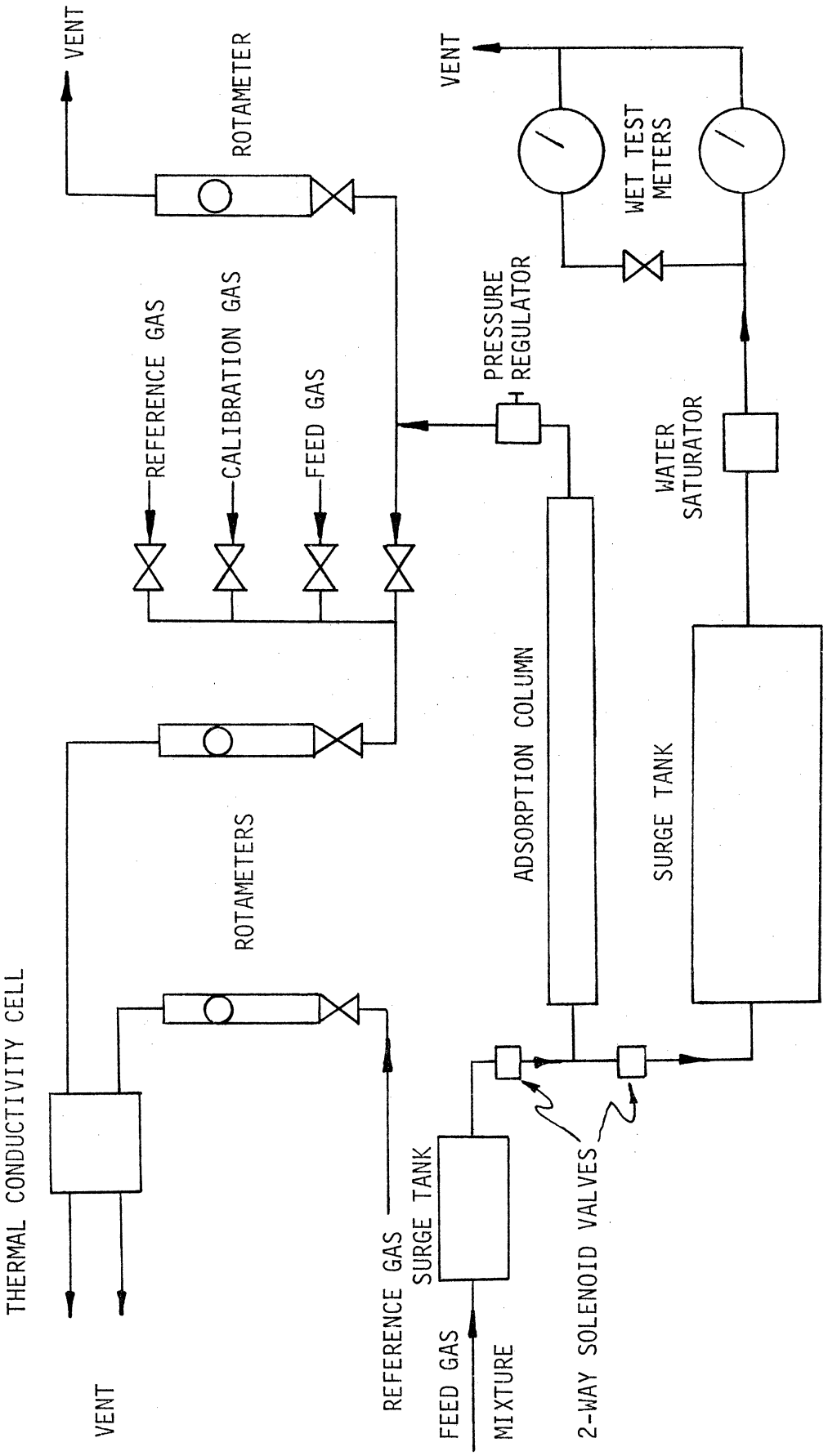

Figure 5.1. Schematic Diagram of the Experimental Adsorption System.

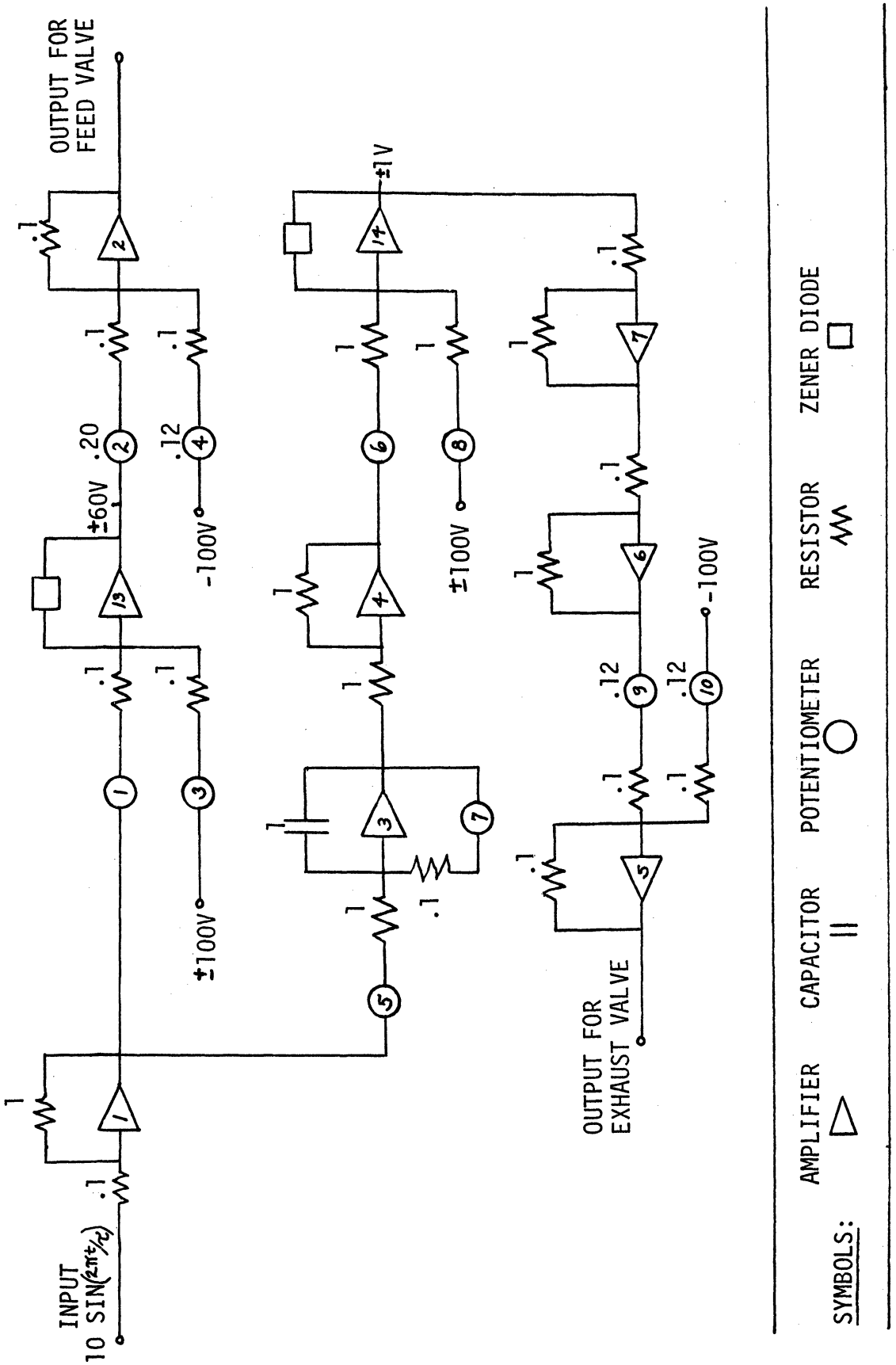

Figure 5.2. Analog Computer Circuit to Control Feed and Exhaust Valves.

feed gas cylinder, passes through a 500 cubic inch surge vessel while the exhaust flows through a 2100 cubic inch surge vessel before its flow is measured. Any other flow resistances are kept to a minimum by using short sections of three-eighth inch diameter polyethylene tubing between the solenoid valves and the surge tanks. The 2-way Valcor solenoid valves were chosen for the one-quarter inch internal orifice which presents very little resistance to flow. The only other obstacle to flow between the surge vessel and the adsorption column is one thickness of 80 mesh screen used to support the adsorbent.

In his research, Turnock found that the use of crushed Linde molecular sieve pellets led to variable flow resistance caused by attrition of the adsorbent particles. Use of 20-50 mesh round particles of Davison 5A molecular sieve as the adsorbent eliminated that problem. Adsorbent is packed into a three-fourth inch diameter, five feet long, steam jacketed, schedule 40 pipe. This packed bed has been mounted on a 35° angle to eliminate the possibility of forming a void channel along the bed. The column and jacket are connected to stainless steel flanges at each end. Matching flanges, with one-fourth inch nominal pipe diameter openings, bolt to the column flanges. A pipe tee connects the solenoid valves to the inlet flange. Quick-disconnect couplings here and at several locations on the column allow measurement of the pressure pulses.

At the end of the column, the product stream passes through a pressure regulator which regulates the pressure of the downstream flow. Thus, the product flow to the product flowmeters is nearly constant whereas the flow at the end of the column varies significantly. This product stream is then metered by two rotameters: one metering and controlling the flow to the Gow-Mac thermal conductivity cell with the

other measuring and controlling the remainder of the product flow.

The composition of this product stream is measured by the calibrated thermal conductivity cell. A 100% N_2 stream, also serving as the reference flow, a 50% N_2 - 50% CH_4 mixture, and the feed gas mixture are used as the calibration gases. The output signal from this thermal conductivity cell is displayed by a 0-20 millivolt Digitec digital volt meter.

A material balance of the operating system is complete when the exhaust flow is measured. The flow pulses from the column are damped by the large surge volume so that the flow is easily measured by two wet test meters. A water saturator precedes these meters to insure the saturation of the gas measured.

5.2. General Operating Procedure

Prior to the operation of the adsorption system, the molecular sieve bed must be prepared. Because the molecular sieve will easily adsorb moisture, regeneration is required after the column has been packed. While maintaining the column at a temperature of 300°F, alternating nitrogen purges with system evacuations accomplishes the regeneration.

To achieve the desired cyclic pressure control, the signals activating the relays which control the feed and exhaust valves must be properly set. The frequency of the cycle is easily fixed by setting the frequency of the output of the Hewlett-Packard function generator. The fraction of the period that the feed valve is to be open is adjusted by the relative settings of potentiometers #1 and #3 in the analog computer circuit shown in Figure 5.2. If the exhaust valve

is to be open for the remainder of the period, just one square wave signal controlling the single pole, double throw relay is required. However, to achieve the delay in opening the exhaust valve, two adjustments must be made. The setting on potentiometer #7 varies the initiation of the signal to open the exhaust valve while the relative settings of potentiometers #6 and #8 will determine the fraction of the period that this valve is to remain open. Care must be taken to make certain that the closing of the exhaust valve exactly coincides with the opening of the feed valve. If there is any time that both valves are simultaneously open, gas will bypass the column and flow directly from the feed to the exhaust.

Once the valve control has been constructed, the operation of the system is straightforward. The feed pressure is limited with the pressure regulator on the feed gas cylinder while the product flow is adjusted with the product rotameters. Because the pressure profile within the column is established rapidly, very little change in these settings is required as the run progresses.

During the startup period, the composition is continuously metered with the output of the thermal conductivity cell. By rechecking the output of this thermal conductivity cell for the calibration gases before and after each run, the uncertainty of a composition based upon the calibration curve is within 0.2% composition. Thus, although the accuracy of a calibration curve determined with the three known gas samples is only within 2%, the precision of the results allows the difference between the compositions of different runs to be known much more accurately.

After the initial startup, the exhaust flow is measured with the wet test meters over a few cycles. This flow, together with the steady state composition output, fully defines the performance of the system

for a given control. These steady state outputs are achieved after periods of five to twenty minutes depending upon the product flowrate.

5.3. Experimental Results

The experimental work was undertaken both to optimize the system to provide a measure by which the computational studies can be compared and to gain a better understanding of the effects of various operating parameters on the performance of the system. Thus, for different product flowrates the outputs of the system were examined as variations were made in the frequency and timing of the cyclic control sequence. So that the amount of gas required for an experimental run is kept to a reasonable level, the limitation of 10.0 PSIG was imposed on the available feed pressure. Although this was a somewhat arbitrary choice, an investigation of the effect of maximum feed pressure is beyond the scope of this work.

As was shown in section 4.2, the computed optimal control form for product maximization requires the closing of the feed and exhaust valves simultaneously for only a small fraction of the period, if at all. Therefore, the initial experimental studies were run with the cyclic sequence $[u'_{max}\ u'_{min}]$, that is, the feed and exhaust valves alternately opening. The first study, shown in Figure 5.3, presents the effect of frequency on product composition. It is noted that neither a different product flowrate, a variation in the per cent of the period that the feed valve remains open, nor a small change in feed gas composition from 28.6% N_2 to 32.2% N_2 will change the frequency at which the maximum in product composition occurs. Thus, the next level of studies, the variation in the timing of the valve switches was carried out at only one frequency

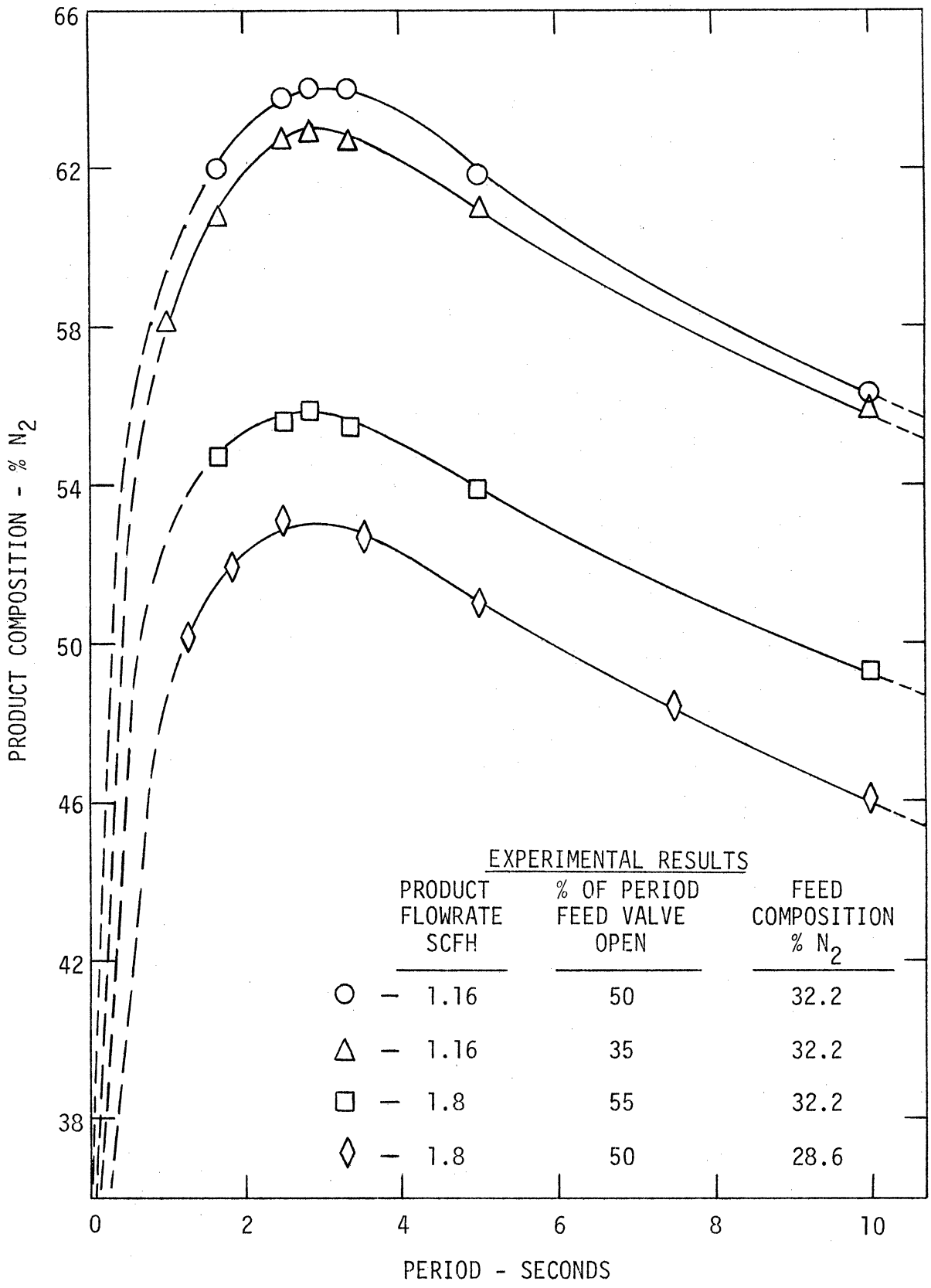

Figure 5.3. Effect of Frequency on Product Composition.

for all product flowrates studied.

Before turning to the next series of studies, the exhaust flowrate is examined as a function of the frequency of the applied control. As expected, Figure 5.4 shows that the faster the control is cycled, the more gas is exhausted. It is this behavior that led to the computational study that included exhaust rate minimization in the performance index. Although not shown here, the exhaust rates were only slightly sensitive to the changes in product flowrate: the exhaust rate decreases slightly as the product flowrate is increased.

At the constant frequency of 0.35 cycles/sec., the effect of the length of time that the feed valve is open, on the product composition is shown in Figure 5.5. As anticipated, a clear maximum in this composition is exhibited. It is clear that if the valve were either not open at all or if it were open 100% of the time, no steady state separation would be possible. Runs were performed in the vicinity of the maxima to more exactly fix their locations. The exhaust rates that accompany these product compositions are shown in Figure 5.6. Here, there are also clear maxima for the exhaust rates.

For simple on-off operation of the feed and exhaust valves, the controls to maximize product composition for different product flowrates have now been specified. Now the effect of delaying the opening of the exhaust valve after the feed valve has been closed can be examined.

By using the three part control sequence previously outlined, a pressure wave form, such as the one shown in Figure 5.7, is imposed at the feed boundary of the column. It is apparent from this profile, obtained with a Statham pressure transducer and a Beckman Dynograph, that the maximum and minimum boundary pressure are not immediately imposed

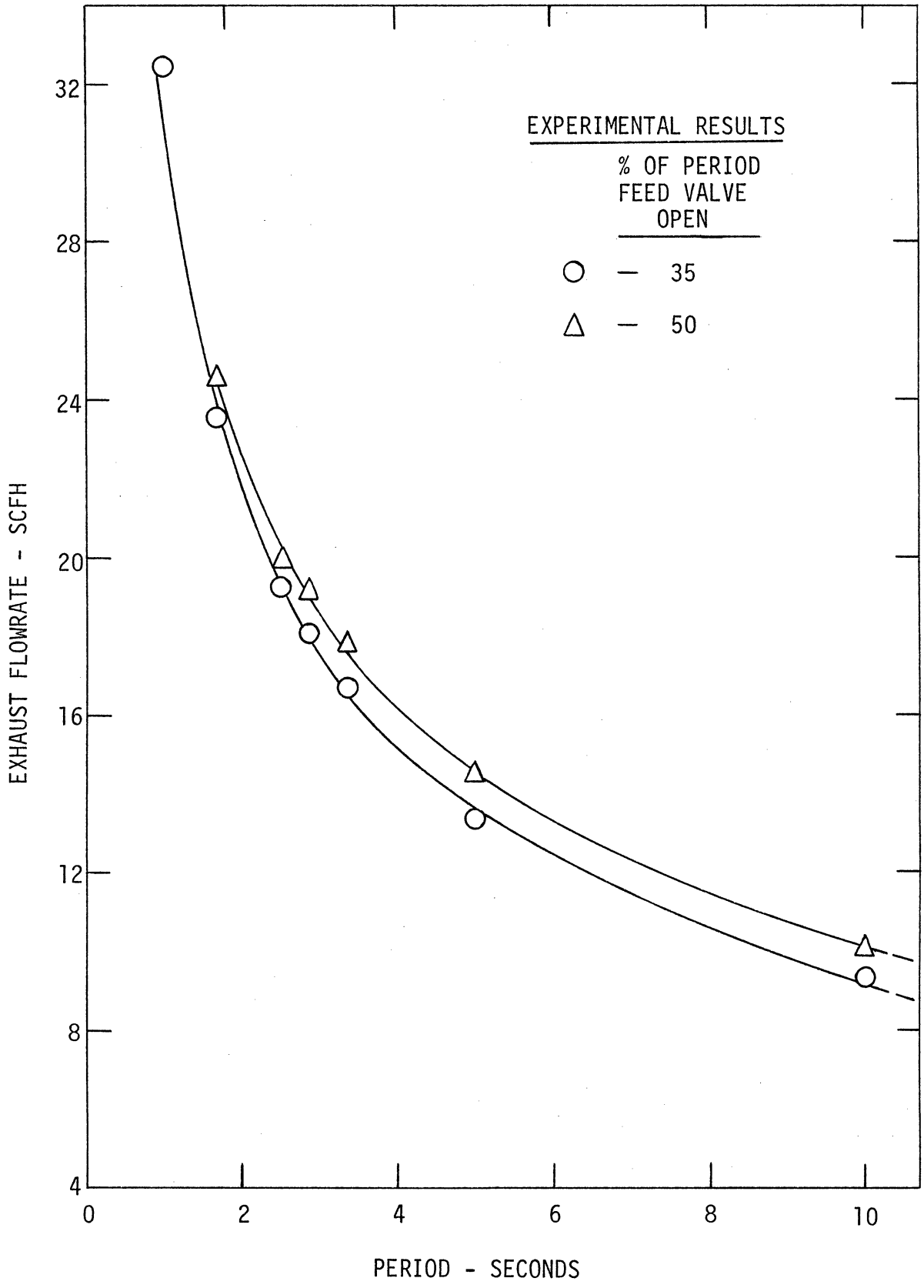

Figure 5.4. Effect of Frequency on Exhaust Flowrate for a Product Flowrate of 1.16 SCFH.

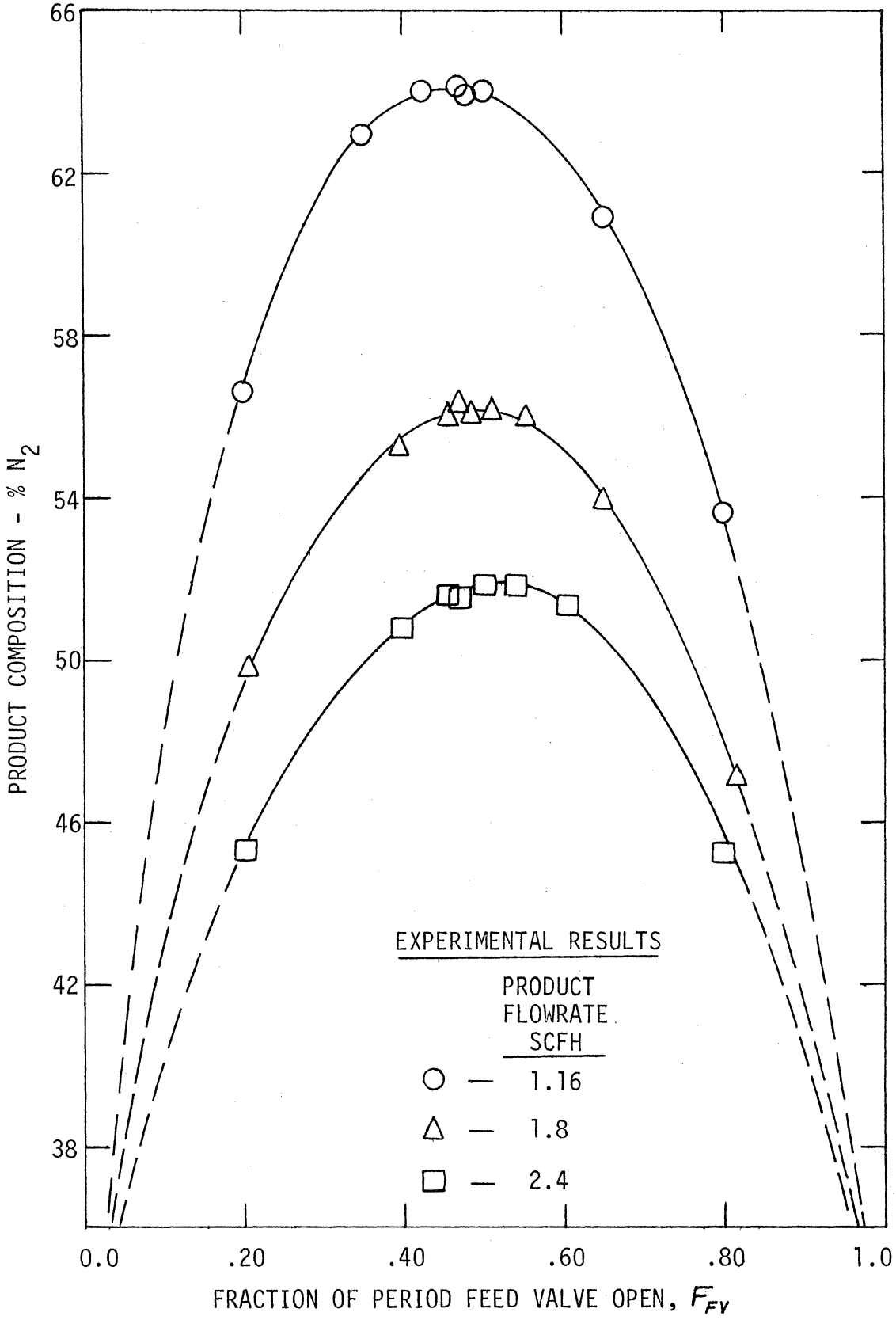

Figure 5.5. Effect of Fraction of Period Feed Valve Open on Product Composition for 0.35 cycles/sec. and a Feed Gas Composition of 32.2% N_2 - 67.8% CH_4.

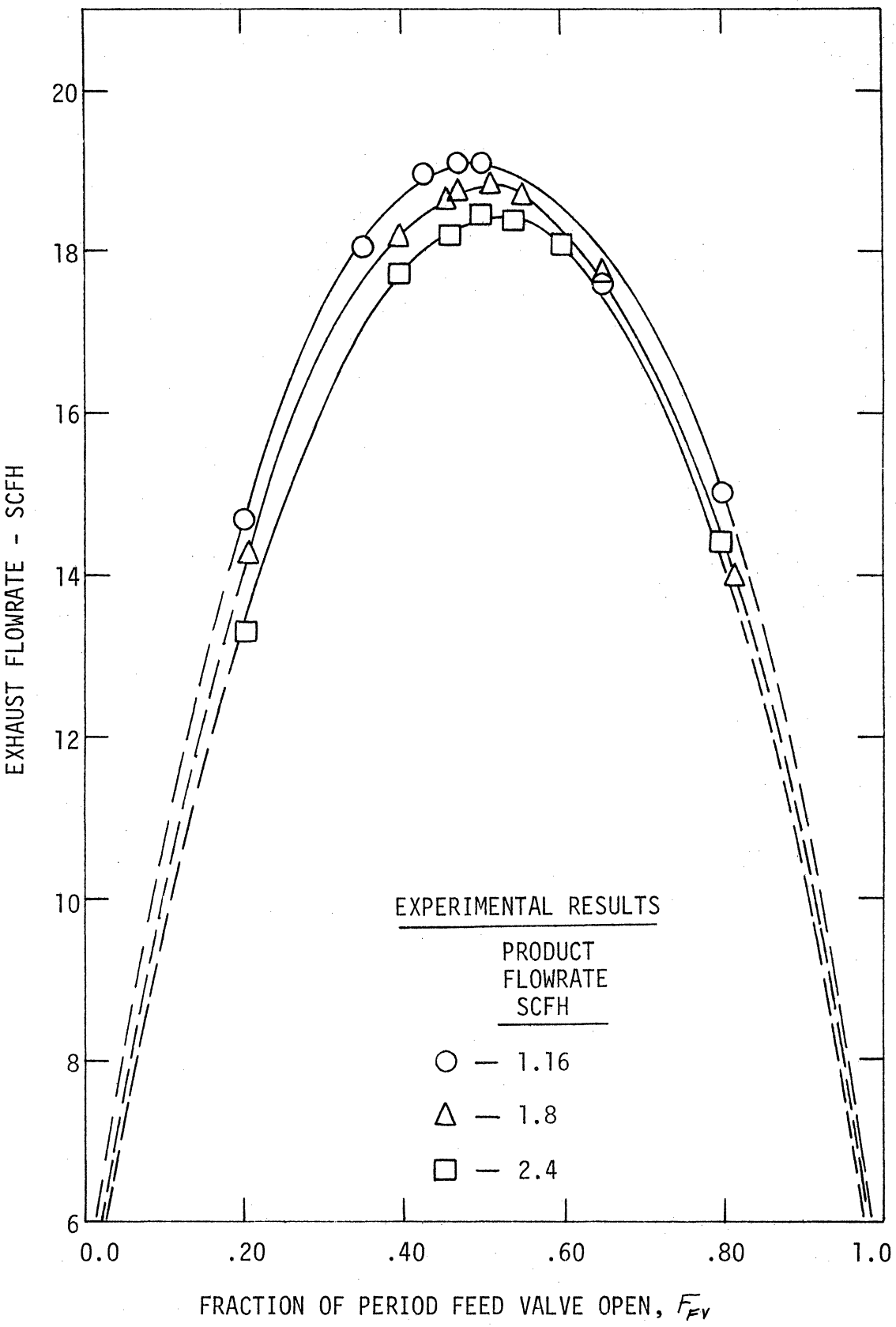

Figure 5.6. Effect of Fraction of Period Feed Valve Open on Exhaust Flowrate for 0.35 cyles/sec.

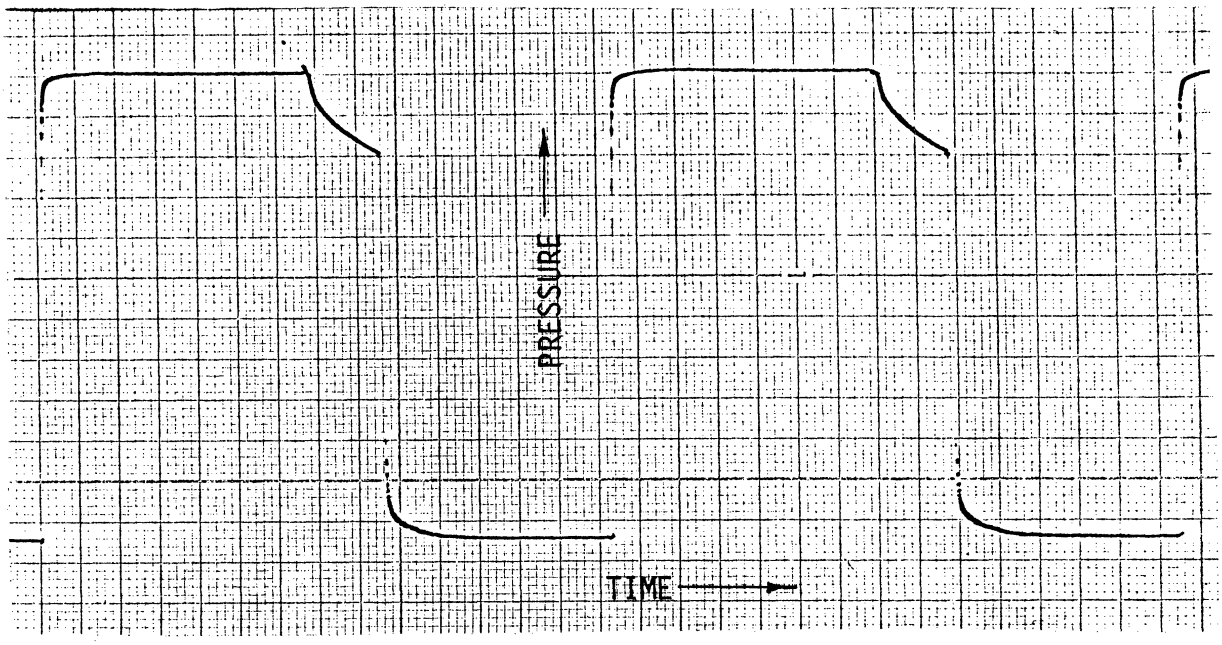

Figure 5.7. Feed Boundary Pressure Wave Form Resulting from Three Part Control Sequence.

upon making a control switch.

The system outputs for varying times of holding both valves closed simultaneously is shown in Figure 5.8. These runs were carried out at a frequency of 0.35 cycles/second with the feed valve open 47% of the period. The large deviations of the three data points from the curves for exhaust rates were probably caused by incorrect timing of the valve openings so that both feed and exhaust valves were open at the same time.

From the results in Table 4.2 it is clear that a change in bed resistance will not only alter the frequency and timing of the optimal control but will also change the system outputs. It was for this reason that Davison 5A molecular sieve had been chosen to insure constant bed resistance. In order to ascertain the effectiveness of this aspect of the round molecular sieve particles, the bed permeability was measured both before and after all the cyclic adsorption runs were made. The

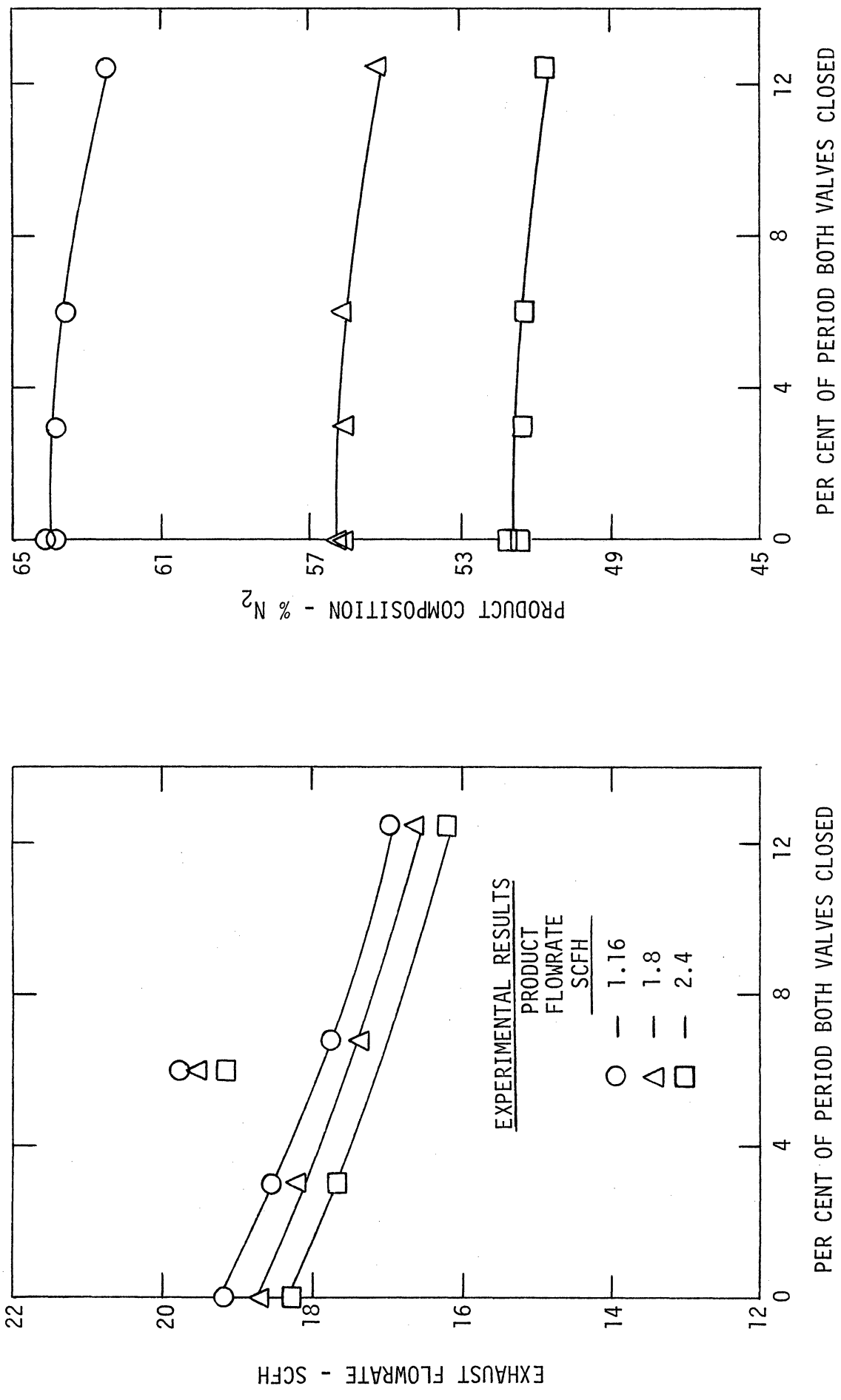

Figure 5.8. Effect of Closing Both Valves on Exhaust Flowrate and Product Composition for 0.35 cycles/sec., the Feed Valve Open 47% of the Period and a Feed Gas Composition of 32.2% N_2 - 67.8% CH_4.

resulting permeability of 101 Darcys was found to have remained constant over the course of the experimental exploration. These measurements, in the form of a graphical representation of Darcy's Law, as well as a complete tabulation of the experimental adsorption runs have been presented in Appendix IV.

6. INTERPRETATION OF RESULTS

6.1. Optimal Control Sequence for Maximization of Product Composition

The computational results presented in section 4.3 indicated that the optimal feed boundary control is the cyclic sequence [maximum pressure, zero flow, minimum pressure]. These results were based on models containing 6 cells or less. Before it can be concluded that this control sequence would be optimal for a model with any number of cells, n, the optimal trajectories shown in Figure 4.5 should be examined further.

For the 3, 4, 5 and 6 cell models with a product flowrate of 1.16 SCFH, the optimal trajectory for product composition maximization passes through the optimal control regions for u'_{max}, z_1 and u'_{min}. From Figure 4.6 it appears that the fraction of the period that the trajectory spends in each of the control regions for large n can be predicted by extrapolation. However, the path that the trajectory takes between these control regions may exhibit different behavior as the number of cells is increased.

As can be seen from Figure 4.5, as n is increased, the trajectory, in passing from the region of u'_{min} to u'_{max} (minimum pressure to maximum pressure), is approaching a path through the origin. This is expected for the path taken through the control regions of the distributed-parameter model previously presented in Figure 3.4. For this model the trajectory would be constrained to move through the origin because $\rho_2(0,t)=0$ for $u' < z_1$, and cannot instantaneously change to another value.

The direction of the trajectory moving away from the origin has special significance. If χ decreases as quickly as ψ increases, a singular control subarc would result. Although such a singular control component

can not be ruled out absolutely, it can be neglected practically. The rate of travel of the optimal trajectory from u'_{min} to u'_{max}, as indicated on the trajectory for $n=3$, is very rapid. Thus, if a singular control does exist here for large n, it would be applied for such a small fraction of the period that its effect would be insignificant.

The path taken by the optimal trajectory in moving from the region of u'_{max} to u'_{min} is also of interest. The control $u'=z_1$, from the interior of the admissible region of allowable controls, can be thought of as a singular control component which has a unique form; that which maintains the condition of zero flow at the feed boundary. From Figure 4.6 it is clear that the fraction of the period spent along this singular control line is decreasing to a very small value. Thus, it would be expected that application of this control component for a short interval following the maximal pressure control would have little noticeable effect on the product composition.

After the trajectory has moved onto the line for u'_{min} there is a reversal in direction for a short interval of time. This direction reversal has been attributed to numerical error because the time interval over which this reversal occurs decreases as the number of time increments used in the numerical computation increases.

Understanding that a very small singular control component, if it exists, is being ignored, it can be concluded that the cyclic sequence $[\ u'_{max}\ ,\ u'_{min}\ ]$ is the practical control that maximizes product composition. The optimal period, γ^*, for a maximum feed pressure of 10.0 PSIG and product flowrate of 1.16 SCFH was found by a straight line extrapolation in Figure 4.7 to be about 4 seconds. Although all the data shown on this figure are computed, there is uncertainty attached to the values

for $n = 10$ and $n = 12$. For these computations the adjoint system was not solved and τ^* was determined by comparing the product composition outputs for a fixed control form at different values of τ. This comparison is based on system values close to, but not exactly at steady state and thus the τ^* determined may be inaccurate.

Since it was found that the optimal fraction of period that the feed valve is to be open, F_{FV}, does not decrease significantly as n increases, the optimal control timing was also evolved for the product flowrates of 0.60, 1.80 and 2.40 SCFH using a 4 cell model. As shown in Table 4.2, the computed τ^* does not vary significantly with these different flowrates.

Experimental results, presented in Figure 5.3 have also shown that the optimal frequency of control cycling does not noticeably vary with product rate. At a constant frequency of 0.35 cycles/second, which corresponds to the maxima in product compositions in Figure 5.3, F_{FV} was varied for the flowrates of 1.16, 1.80 and 2.40 SCFH. From the resulting product compositions plotted in Figure 5.5, F_{FV}^* was determined and is compared with the computed results in Figure 6.1. Although the trend of an increase in F_{FV}^* with increasing product flowrate is evident with both sets of data, there is a larger difference between absolute values than can be explained by experimental uncertainty. In addition, the experimentally determined optimal frequency of 0.35 cycles/second is significantly different from the value of 0.25 cycles/second based upon computational results.

Of course, exact agreement of results could not have been expected because of the many simplifying assumptions made in the construction of the distributed-parameter model and because of the approximate numerical

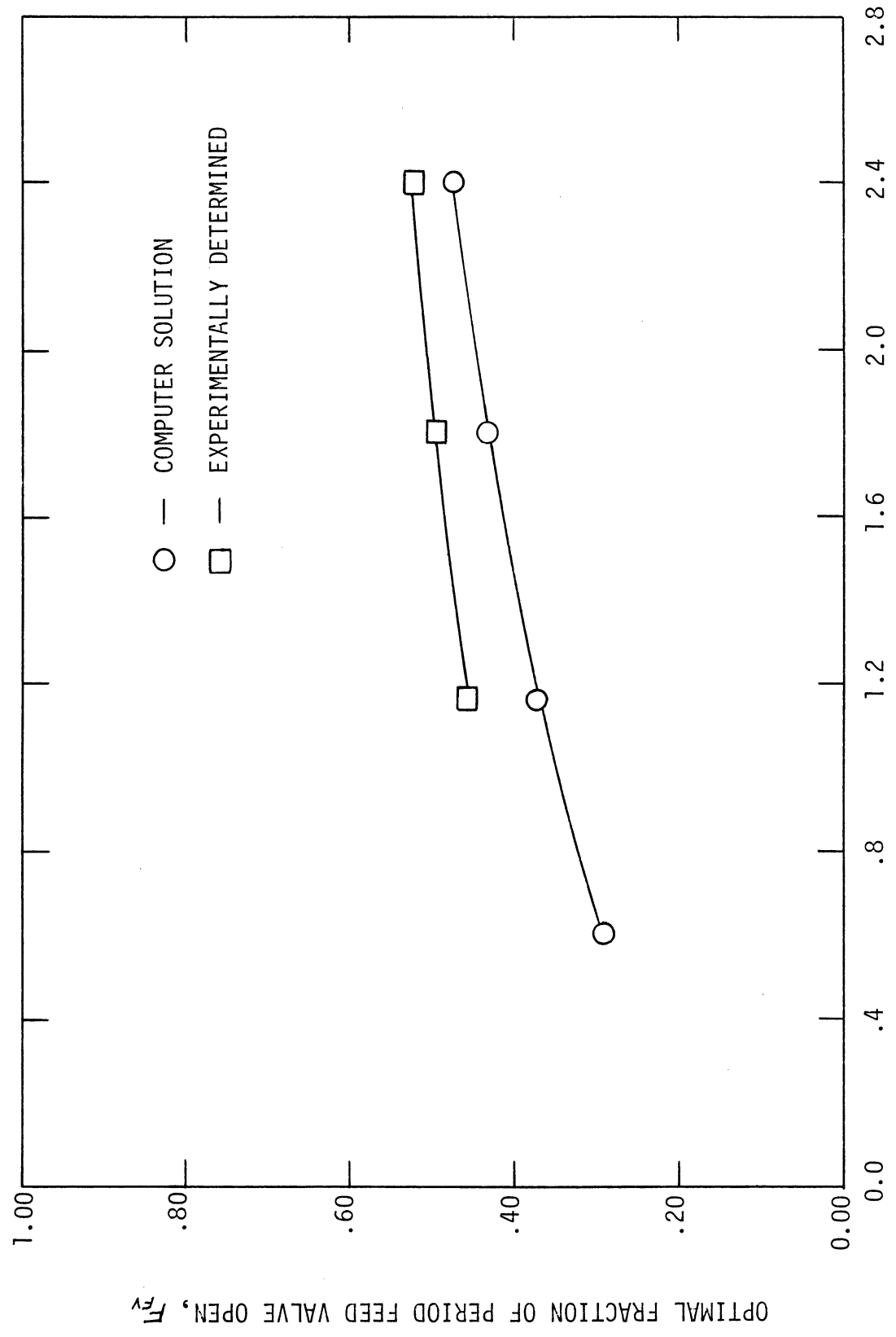

Figure 6.1. Variation of Optimal Fraction of Period Feed Valve Open as Product Flowrate Changes.

solution of it. In order to assess the factors within the model that may have contributed to the deviations between experimental and computational results, the effect on the computed optimal controls of variations in the values used for the system's properties must be examined.

Since the value for α was determined to be 2.35 with a standard deviation of .09, it is important to know the sensitivity of the numerical calculations to the value of α. As shown by the results in Table 4.2, wide variations in α (1.65-2.95) have almost no effect on the optimal control. Similarly, a variation was made in the value of ϵ, the porosity. The effect of changing this parameter, also presented in Table 4.2, is insignificant. However, variations in K and μ, the permeability and average viscosity, do have great effect on the computations.

A dimensional analysis of the state equations, presented in Appendix V, shows that if the dimensionless groups

$$\left(\frac{K\tau z_{max}^{1/2}}{\mu L^2}\right), \left(\frac{2RTLQ_p}{z_{max}(AK/\mu)}\right), \left(\frac{V_R}{AL}\right), \left(\frac{W}{AL}RTk\gamma z_{max}^{((\gamma-1)/2)}\right) \text{ and } \left(\frac{z_{min}}{z_{max}}\right).$$

are not changed, the solution to the dedimensionalized state equations will not change. This means that the optimal control which maximizes the product composition of the dimensionless state equations will not change form, other than the optimal period length, τ^*, if the above dimensionless groups are kept constant. Thus, if (K/μ) is changed to $(K/\mu)'$ the optimal solution will be maintained if the optimal time constant, τ^*, changes by a factor of $(K/\mu)/(K/\mu)'$. In addition, Q_p must be changed by the inverse of this factor. This is confirmed by the computed results in Table 4.2 where the values of K and μ were varied. Since Q_p was not changed, the τ^* computed in both cases was changed by the factor $(K/\mu)/(K/\mu)'$ but the F_{FV}^* corresponded to that of a product flowrate which was changed by the

same factor, $(K/\mu)/(K/\mu)'$. For any such solution of the dimensionless state equations where the above dimensionless groups are kept constant, the exhaust rate will change by the factor

$$\left(\frac{A L z_{max}^{1/2}}{2\tau RT}\right)$$

Thus, a variation in K or μ by changing the optimal period length, τ^*, will change the exhaust rate. Since τ^* is changed by the factor $(K/\mu)/(K/\mu)'$, the exhaust rate will change by the inverse factor $(K/\mu)'/(K/\mu)$ from the value corresponding to a product flowrate which was changed by $(K/\mu)/(K/\mu)'$.

The value of μ used in the computations, as shown in Table 4.1, was 0.0175cp., that of 100% N_2. Since an average viscosity was called for in the model, a value closer to 0.0108cp. for 100% CH_4 should have been used. For example, had μ =0.0127cp., the viscosity of the feed mixture, been used in the computations, the optimal frequency would have been

$$\left(\frac{1}{\tau^*}\right)' = \left(\frac{1}{\tau^*}\right) \frac{0.0175\text{cp.}}{0.0127\text{cp.}} \qquad (6.1)$$

Thus, the computed optimal frequency would have been 0.325 cycles/second which is in excellent agreement with the experimental value of 0.35 cycles/second. However, using this value of μ would have led to an increase in the difference between the experimental and computed values for F_{FV}^* as shown in Table 4.2.

A possible argument that could resolve the above problem is that the introduction of a composition invariant viscosity was expedient but not accurate. The average composition of N_2 over the feed portion of the cycle, when $z_\lambda(0,t) < 0$, is higher than the average composition

of N_2 over the exhaust portion of the cycle, when $z_\lambda(0,t)>0$. This is illustrated in Figure 6.2 for the computed pressure and composition profiles of the first 3 cells of the 10 cell model. In addition, when the control is switched so that $z_\lambda(0,t)<0$, the bed is pressurizing quickly. During this pressurization methane is being adsorbed in much greater quantity than nitrogen so that the concentration of the gas layer nearest the adsorbent would be more depleted of methane than the bulk of the gas flow. Conversely, when the control is switched so that $z_\lambda(0,t)>0$, the gas layer nearest the adsorbent particles would be richer in methane than the bulk of the fluid. Thus, because of these two factors, the viscosity when $z_\lambda(0,t)<0$ is closer to that of nitrogen than is the viscosity when $z_\lambda(0,t)>0$.

Had the viscosity differences been taken into account in the model, the computed exhaust portion of the cycle would have been of shorter duration. This results from the increased time derivatives caused by the lower viscosity value. Thus, the computed value of F_{FV}^* would increase and at the same time decrease the computed value of τ^* which would bring about a better agreement with experimental results.

The sensitivity of the optimal solution to the value of k, the adsorption constant, is not as simply defined as it is for K or μ. However, it is noted that the time derivatives of the system are inversely related to the value of k. Thus, it would be expected that the computed τ^* would be directly related to the value of k used. As shown in Table 4.2, an increase of 9% in the value of k leads to an increase of 6% in the computed τ^*. If a value of k corresponding more closely to that of the feed composition had been used, a smaller τ^*, closer to that determined experimentally, would have been computed.

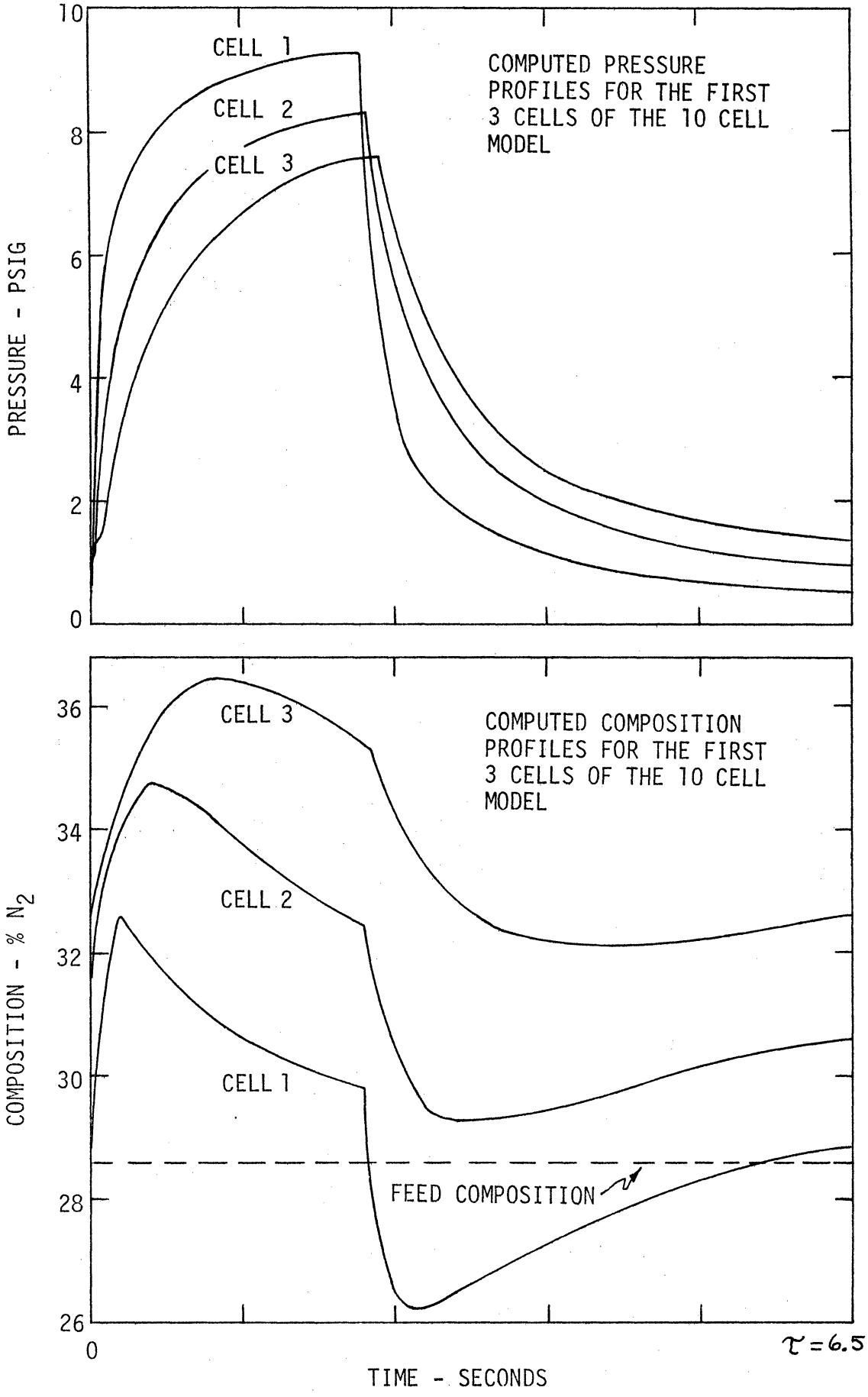

Figure 6.2. Computed Pressure and Composition Profiles for First 3 Cells of 10 Cell Model.

Since the feed composition in most of the experimental work was 32.2% N_2 and not 28.6% N_2 as used in the computations, the effect of changing y_F, the feed composition, was investigated. The change in the optimal solution for a change in y_F of 8.6% N_2, as shown in Table 4.2, was insignificant.

It is therefore evident that the optimal solution is not noticeably influenced by the parameters affecting only the composition, α and y_F. However, this solution is directly affected by the parameters relating to the flow and adsorption characteristics, K/μ and k. The relationship between flow and pressure drop, Darcy's Law (equation (3.5)), upon which the direct relation between the flow and K is based, includes a viscous term but assumes the inertial term is negligible. This assumption is essential to the construction of a model that is not too unwieldy to be treated numerically. Although the assumption is well founded over the major portion of the cycle, it is limited for the initial periods of rapid flow directly after a valve switch is made. Because of this limitation and the fact that both μ and k must be approximated by average values when in fact both vary with composition, it is not surprising that the solutions based upon this model will differ from experimental results. Although this precludes placing complete confidence in the model, there are still some very important conclusions that were drawn from the computed results that could not have been made otherwise.

From the computed optimal trajectories two significant conclusions were made. First, the possibility of singular control components was found to be of no practical importance. Second, because there was but one loop in the trajectory over a single cycle, it was concluded that the single cyclic sequence [u'_{max} , u'_{min}] maximized the product composition.

Without knowledge of this form of the trajectory, a control cycle with unequally timed switches between u'_{max} and u'_{min} may have been possible. An example of such a control cycle is shown in Figure 6.3. With such uneven control sequences possible, a thorough experimental exploration would then have been greatly complicated.

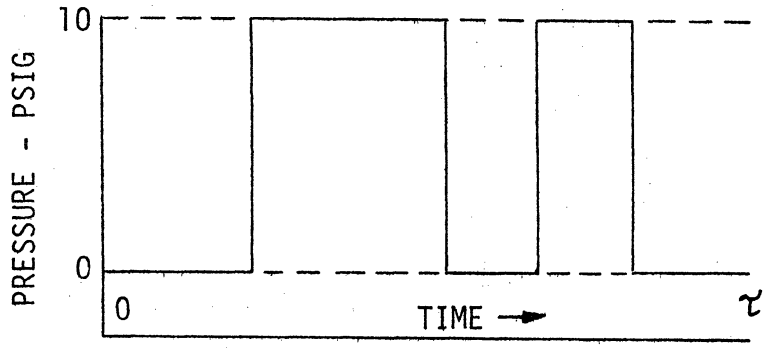

Figure 6.3. Control Cycle Form Ruled Out by Knowledge of the Form of the Optimal Trajectory.

In addition, although the computed results did not predict the exact location of the optimal solutions, they did locate the approximate area about which the experimental study should be based. Thus, the frequencies experimentally investigated were initiated in the range of the computed result of 0.25 cycles/second and quickly encompassed the true optimal frequency. Where the computations indicated that the control of $z_\lambda(0,t) = 0$ (zero flow) was not of significant value, the experimental exploration could then have ignored it as a possible control component. For completeness this control was studied and presented in Figure 5.8. Within the experimental uncertainty no increase of product composition was noted when $z_\lambda(0,t) = 0$ was applied although application of this control component for short intervals ($\sim$4% of the period) did not noticeably decrease the product composition. A discussion of the effect of this control on the exhaust rate will be held for the next section.

If a prior knowledge of the adsorption system's capabilities had been required, the numerical solution of the model would have given excellent approximations of the performance outputs. For example, for a feed composition of 28.6% N_2, a product composition of about 60% N_2 and an exhaust rate of about 13.4 SCFH would be the predicted outputs based on an extrapolation of the computer data in Figure 4.8. These results are in good agreement with the actual systems operation. For a 32.2% N_2 feed, a 4 second cycle with F_{FY}=0.35 resulted in a product composition of about 62.2% N_2 and an exhaust rate of 15.2 SCFH as read from Figures 5.3 and 5.4 respectively. Thus, if no experimental system were available, the model could be relied upon to predict the potential separations possible on this kind of separation system.

A point worth noting is that the use of a viscosity of 0.0175cp. was the factor that led to a computed exhaust flow smaller than that experienced with the experimental system. The use of this higher viscosity more than compensated for the higher flows that resulted from the absence of an inertial term in the equation relating flow and pressure drop.

6.2. Optimal Control Sequence for Product Composition Maximization with Exhaust Rate Minimization

Experience with the experimental system, as illustrated in Figures 5.3-5.6, clearly shows that increases in product composition are usually attained at the expense of increasing the exhaust rate. It is only natural, then, that a performance index was considered which included a term to minimize the exhaust rate.

This performance index was investigated for a product flowrate of 1.16 SCFH using the 4 cell model for a varying degree of importance placed on the waste minimization term. The optimal trajectory, presented

in Figure 4.10, passes through the regions of u'_{max}, z_1, and u'_{min}. Unlike the optimal solution for maximizing only the product composition, the fraction of the period spent in the region for $u' = z_1$(zero flow) is of major importance. The computed results in Figure 4.9 indicate that as the waste minimization term becomes more important, the optimal frequency decreases, F_{FV}^* decreases and the fraction of the period that both valves are to be kept closed increases.

Experimental results in Figures 5.4, 5.6 and 5.8 clearly illustrate the behavior of the exhaust rate as the times spent in the three control regions are varied. By employing the control sequence which includes the control component for zero flow, the exhaust rate can be reduced without significantly decreasing the product composition. A decrease in the frequency or a decrease in F_{FV} from the optimal values found for product composition maximization will also result in a decrease in the exhaust rate. However, from 5.6 it can be seen that increasing F_{FV} sufficiently from the previous optimal value will also decrease the exhaust rate. It would then be expected that two optimal solutions might exist. This was found not to be the case. For a product flowrate of 1.16 SCFH the F_{FV} for the maximum in exhaust rate does not correspond to the F_{FV} for the maximum in product composition. As F_{FV} is decreased from the value that maximizes composition, F_{FV}^*, the exhaust rate decreases. But as F_{FV} is increased from F_{FV}^* the exhaust first increases before it decreases. Thus, the optimal control for the performance index including exhaust minimization, for the values of C studied, has a unique solution for which the optimal F_{FV} is smaller than that for the optimal control which only maximizes product composition. Of course, the limiting case of $C = \infty$ has two optimal solutions: $F_{FV}^* = 0.0$ and $F_{FV}^* = 1.0$.

For the sake of completeness, the path of the trajectory in moving from the region of u'_{min} to u'_{max} should be discussed. Although the trajectory for the 4 cell system shown in Figure 4.10 jumps from the region for u'_{min} to u'_{max}, an analysis of the boundary adjoint variables of the distributed-parameter model as in Figure 3.5, leads to the conclusion that the trajectory must pass through the point where the singular control line meets the line for $u'^{*} = u'_{min}$ (or $u^{*} = u_{max}$). This arises because $\rho_2(0,t) = 0$ for $u' < z_1$ and being governed by the partial differential equation (3.44) it cannot instantaneously change to another value. The trajectory would then have to go along the singular control line until it enters the region for $u'^{*} = u'_{max}$. However, the time marks on the trajectory in Figure 4.10 indicate that the rate of travel along this singular control subarc would be so rapid that it would be of no practical significance.

From the preceding discussion it can be concluded that cyclic control sequence of major importance to the operation of the adsorption system is [maximum pressure, zero flow, minimum pressure]. The actual timing between control components would depend upon the importance of the exhaust minimization term relative to the product composition maximization.

6.3. Design Considerations

In the preceding experimental work a system of fixed dimensions was operated at different levels of product throughput for a fixed available feed pressure. The problem that should now be considered is how these operating variables and system dimensions affect the operation of the cyclic adsorption process.

From the experimental results in Figures 5.3 and 5.5 it is apparent that decreased product flowrate increases the separation accomplished.

However, accompanying this increase is a decrease in the fraction of feed gas that is recovered as product. Illustrated in Figure 6.4 is the change of the process outputs of separation accomplished and fraction of feed gas recovered, as the frequency of operation is varied or as the fraction of the period that the feed valve is open, is varied. These changes are shown for the three different product flowrates of 1.16, 1.8 and 2.4 SCFH. From this figure it is seen that decreased frequency results in an increase of the fraction of feed gas recovered while, as in Figure 5.3, the accomplished separation goes through a maximum. It is clear that variations of the frequency from the optimal value, $1/\tau^*$, do not decrease the separation accomplished with respect to the fraction of feed gas recovered, nearly as much as variations of F_{Fy} from its optimal value. Thus, if the system is to be run at different flowrates, the frequency of operation need not be set as carefully as the fraction of the period that the feed valve is to be open.

If the separation accomplished and the fraction of feed gas recovered as product were the only important factors in the operation of the system, it would appear from Figure 6.4 that operation at lower product flowrates would result in the best performance. However, a factor not yet discussed is the capacity of the system. For example, in obtaining a recovered fraction of 0.09, a 56.6% N_2 product would be achieved for a product flowrate of 1.16 SCFH whereas a product composition of only 55.8% N_2 would be achieved for a product flowrate of 1.8 SCFH. Although a smaller separation would be obtained for the latter operating condition, a 55% increase in capacity would result. Thus, in order to find the best operating conditions for the adsorption system, the capacity, as well as the fraction of feed gas recovered as product, needs to be considered.

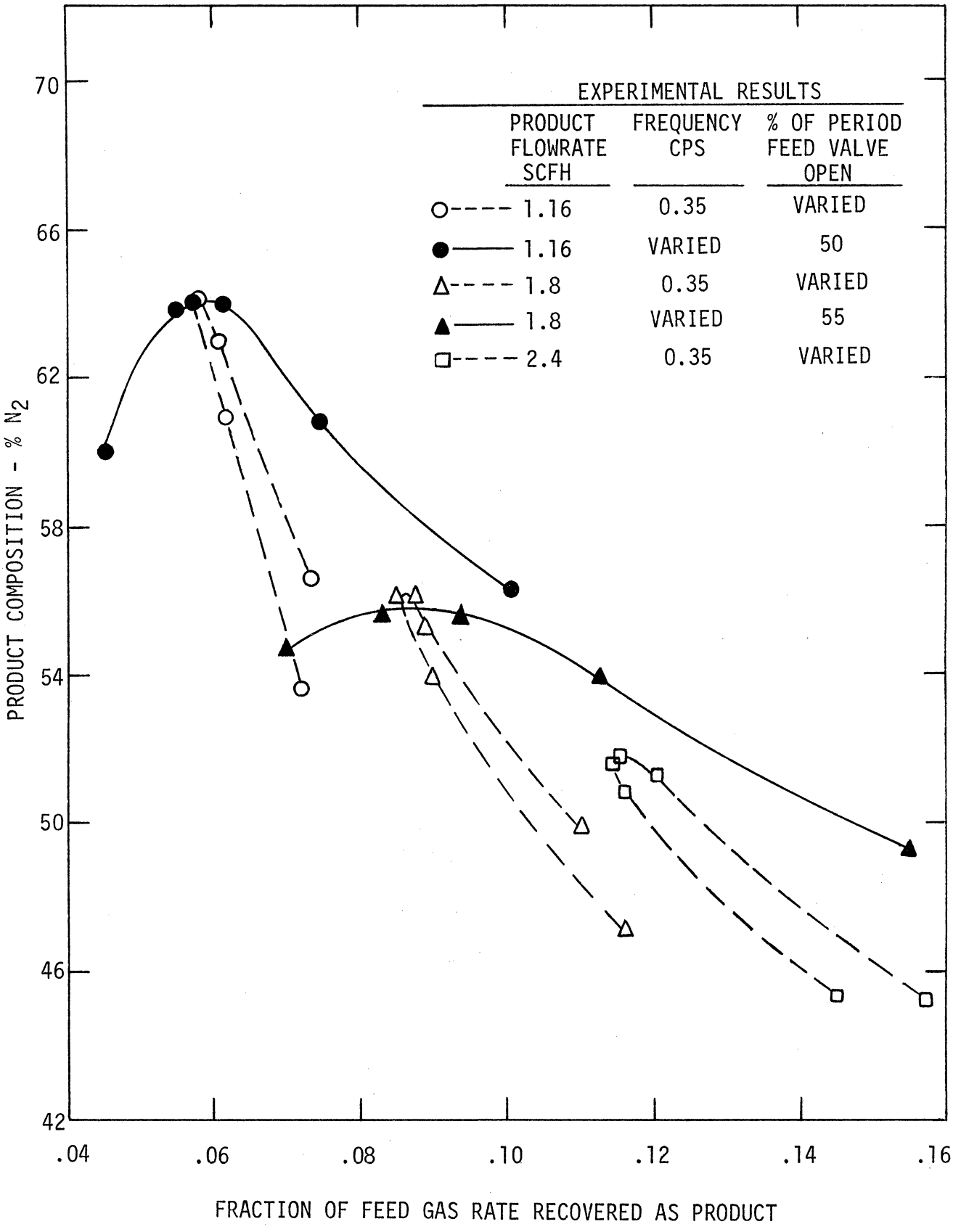

Figure 6.4. Comparison of Adsorption System Outputs with Individual Variations in Frequency of Control or in the Fraction of Period that the Feed Valve is Open, for a Feed Gas Composition of 32.2% N_2 - 67.8% CH_4.

Another factor of interest, for which no experimental exploration was made, is the level of the available feed pressure. From the computed results in Table 4.2 it can be seen that for an increased value of 20.0 PSIG for the constraint on feed pressure while maintaining the atmospheric exhaust pressure, the F_{FV} needed to maximize the product composition decreased to 0.21 for a product flowrate of 1.16 SCFH compared with 0.37 for a feed pressure of 10.0 PSIG. Although the separation for this increased pressure markedly increased, the amount of gas exhausted increased as well. In considering the pressure level for column operations, the increased separations for higher pressure levels must be balanced by the increase in the energy required for the pressurizing of the feed gas and the decreased fraction of feed gas recovered as product.

The system dimensions of A, L and V_R were constant during the course of the experimental work. In addition, the bed permeability, K, was a fixed quantity. In order to design a cyclic adsorption system, the effect on operations of these equipment specifications must be understood. The following discussion will be based on the model presented in Table 3.1 and the dimensional analysis presented in Appendix V.

As discussed in section 6.1, the optimal control will not change form, except for τ^* if the following dimensionless groups are held constant:

$$\left(\frac{K\tau z_{max}^{1/2}}{\mu L^2}\right), \left(\frac{2RTL\,Q_p}{z_{max}(AK/\mu)}\right), \left(\frac{V_R}{AL}\right), \left(\frac{W}{AL}RTk\gamma z_{max}^{((\gamma-1)/2)}\right) \text{ and } \left(\frac{z_{min}}{z_{max}}\right).$$

The corresponding exhaust rate is proportional to $(AL z_{max}^{1/2})/(2\tau RT)$.

Thus, if the area is changed from A to A', the optimal control will be unchanged if the product flowrate is changed by the factor (A'/A)

and V_R changed by the same factor. The resulting separation will be exactly the same as will be the fraction of the feed gas recovered as product since the exhaust rate also changes by the factor (A'/A) . Therefore, it can be concluded that the area affects only the capacity of the system.

As concluded in section 6.1, variation in permeability from K to K' will result in a change of τ^* by the factor (K/K'). If the product flowrate is also altered by this factor, the same separation will result and because the exhaust rate changes by the same factor, the fraction of the feed gas recovered as product will remain unchanged. It is then clear that the permeability directly affects the capacity of the system but not the relationship between the fraction of feed gas recovered and the separation achieved. This explains why Turnock was successful in correlating his results by plotting separation versus fraction of feed gas recovered (39), even though the permeability of the adsorbent used was variable. From the effect of the parameter K, it can be concluded that use of adsorbent particles more permeable to flow will increase the capacity of the system.

Caution must be used in extending the above result. Permeability changes are brought about by changes in the size of the molecular sieve particles. Because the permeability is increased by increasing particle size and because of the increased overall flowrates, the inertial term in the flow equation, neglected in the model of the system, becomes more important. In addition, the limitation of the rate of adsorption, previously neglected because the rate was considered to be extremely rapid, will be more significant as the particle size increases. The above two factors will result in greater deviations of predicted behavior from actual performance.

An increase in the length, L , of the adsorption column, unlike

the behavior of most chemical process equipment, will result in a decrease in the capacity of the system. A change in length from L to L' will change τ^* by a factor of $(L'/L)^2$ and the same optimal control form and separation will result if the product flowrate is changed by a factor of (L/L'). Since the exhaust rate is also altered by the factor (L/L'), the fraction of feed gas recovered as product does not change. Thus, the length of the column inversely affects the capacity of the system.

As before, caution must be used in extending the above result. It would appear that short lengths will favorably affect the performance of the system. However, since the frequency of the control is inversely proportional to L^2, the optimal frequency for shorter lengths may require faster operation than is attainable with available solenoid valves. In addition, the increased flowrates will increase the significance of the rate limiting factors.

The effect of changing the volume of the product line on the performance of the process is not obvious. However, results shown in Table 4.2 indicate that increasing V_R will not only increase the separation but also decrease the exhaust rate. Thus, a different boundary condition at $\lambda=L$ of z_R = constant, will result in improved equipment performance. Because the results in Table 4.2 are based only on the 4 cell model, further work would be required to completely define the importance of the design parameter V_R.

There has already been some consideration of the effect of increasing P_{max}. A further conclusion can be made by referring to the dimensionless equations. For $\gamma=1.0$, if P_{max} is increased and P_{min} increased by the same factor, the capacity of the system will be increased but not

the separation or the fraction of feed gas recovered. Since the work required in the compression of the feed gas is proportional to P_{max}/P_{min} no increase in work for compression is required for the increase in capacity. But again, the increase in optimal frequency and the resulting higher flowrates will limit the applicability of the model.

In the preceding experimental work, a nitrogen-methane mixture was used as the feed gas with Davison 5A molecular sieve. The relative volatility for this system was 2.35. For such a system only about 5% of the energy of compression is converted into energy of separation. To achieve significantly greater thermodynamic efficiencies, a system with a higher relative volatility would be required. Thus, although the purification of nitrogen-methane mixtures using a cyclically operated molecular sieve may not be commercially attractive, other gas pairs with an appropriate adsorbent may well have high enough relative volatilities so that the optimal design will be of practical value.

7. SUMMARY, CONCLUSIONS AND RECOMMENDATIONS

The primary purpose of this research was to investigate the optimal operation of a cyclically operated molecular sieve adsorber. This investigation was carried out both computationally and experimentally with a methane-nitrogen gas mixture and Davison 5A Molecular Sieve.

In order to study the adsorption system numerically, a mathematical model was required. The model that was presented to describe the behavior of the system was simplified by neglecting rate limitations and neglecting the variation of gas and adsorption properties with composition. With the resulting uncoupled partial differential equations describing the pressure and composition, the necessary conditions for optimality were derived for product composition maximization and exhaust rate minimization, using the variational technique proposed by Denn (12). With the use of a maximum principle, it was concluded that for nonsingular controls the optimal boundary control components are maximum pressure, zero flow and minimum pressure. Without computational work, the optimal timing and sequence for the control components are unknown.

Because of the complexity of the distributed state and adjoint system, a cell approximation of the adsorption system was formulated. This new model, made up of ordinary differential equations, was used in conjunction with Pontryagin's Maximum Principle to locate the optimal feed boundary pressure controls. The algorithm used for the numerical computations was based on the work of Horn and Lin (20) which dealt with a periodic lumped-parameter process. Since the cell model is, in a sense, a discretization of a distributed system, the successful use of the method of Horn and Lin in this work suggests that this method may

be useful in treating other periodic distributed systems. Certainly, the solution of the homogeneous part of the adjoint system was invaluable in locating the periodic steady state composition profiles.

From the numerical computations it was seen that the cyclic sequence [maximum pressure, minimum pressure] will maximize the product composition. For a product flowrate of 1.16 SCFH, the effect on the optimal control function of the number of cells used in the model was studied. Although it was found that the number of cells used greatly influences the optimal frequency, the timing of the optimal switching sequence within a dedimensionalized period length does not change significantly for cell models larger than the 4 cell model. For the above product flowrate, it was found that the optimal frequency approaches 0.250 cycles/second as the size of the cell model increases.

A numerical investigation of a 4 cell model for the two other product flowrates of 1.8 SCFH and 2.4 SCFH showed that the optimal frequency does not vary significantly for this operating variable. However, greater product flowrates require application of the maximum pressure for larger fractions of the cycle. Operations on the experimental adsorption system substantiated the above behavior.

The experimental results verified the fact that the control component of zero flow was not needed in the control sequence to maximize product composition. Although the optimal frequency of 0.35 cycles/second was not in exact agreement with the computed results, there was no noticeable effect of changing product flowrate on this frequency. In addition, it was verified that the optimal fraction of the period spent applying maximum pressure increased with increasing product flowrate.

By including a separate term for exhaust minimization in the

performance index, as well as product composition maximization, the control component of zero flow becomes important. This component is applied after the maximum pressure component has been applied but before the minimum pressure component is applied. As the importance of minimizing exhaust rate increases, the computed optimal frequency decreases, the optimal fraction of the period spent applying maximal pressure decreases and the fraction of the period spent applying the control component of zero flow increases. This behavior was confirmed by experimental results. In fact, it appears that applying the zero flow control for a short interval ($< 6\%$ of the period) does not noticeably decrease the product composition although it does significantly reduce the exhaust rate and, thus, improves the performance of the adsorption system. To construct this control component, two valves are needed at the feed boundary of the adsorption column. The timing of the optimal sequence [feed valve open (exhaust valve closed), both valves closed, exhaust valve open (feed valve closed)] will depend upon the relative importance of the exhaust minimization term compared to the term for maximization of product composition.

In the thermal parametric pumping separation process developed by Wilhelm, et al. (40), the derivative for composition depends upon the direction of the flow of the solvent. It is this kind of behavior in the cyclic adsorber that gives rise to the possibility of the optimal control component of zero flow. Thus, it is anticipated that this control component may also play a role in the optimal control of the thermal parametric pumping process. A full theoretical and numerical investigation would be necessary to define the actual optimal sequence.

In an analysis of the dimensionless state equations of the cyclic adsorber, it was found that the area of the adsorber affects only the capacity. In addition, it was found that the permeability of the packed bed will also affect the capacity if the frequency of operation is adjusted. The higher the permeability, the greater the capacity of the system provided that the appropriate higher frequencies are used. Consideration of this behavior for design purposes requires two notes of caution. First, if larger adsorbent particles are used to achieve higher permeability, the optimal operation will be at higher frequencies and higher flowrates, for which the rate limitations previously neglected may become significant enough to invalidate the predictions of the model. Second, unless the permeability is constant, the optimal timing of the control sequence will vary and unless corrections for this are made in the control, suboptimal operation will result. To avoid this problem, adsorbent particles that resist abrasion and maintain a constant flow resistance should be used. The round particles of the Davison 5A Molecular Sieve used in this research were found to be satisfactory.

Another factor that affects the operation of the adsorber is the length of the column. Unlike most chemical process equipment, decreased length increases the capacity of the system. To achieve the same maximum product composition for shorter lengths, higher frequencies are required. Since the optimal frequency increases as the inverse of the square of the length, shorter lengths would require faster operation. Again, this result is valid for flowrates for which the rate limitations can be neglected in the model. In fact, since the optimal frequency increases so quickly as length decreases, the performance of the controlling solenoid valves may limit the achievement of the optimal frequency for shorter lengths.

Despite these limitations, it is clear that attempts should be made to use shorter lengths of column to increase capacity and decrease equipment costs at the same time.

From numerical computations with the 4 cell model, it was found that the effect of increasing the volume of the product line preceding the pressure regulator is beneficial to the process. Product composition increased while exhaust rate decreased. This means that the cyclic adsorption process will operate best with the boundary condition of constant pressure at the end of the adsorption column rather than at the outlet of the pressure regulator. Further experimental work would be required to determine the extent of the process improvement with this new boundary condition.

Before the operations of the cyclic adsorber can be fully specified, the maximum available feed pressure must be set. Although it is known that higher feed pressures decrease the optimal fraction of the period for applying maximum pressure, the resulting increase in product composition is not simply defined. Since higher feed pressures require more energy of compression, a careful study, either numerical or experimental, would be required to find the optimal feed pressure.

Having found the optimal feed boundary cyclic control of [maximum pressure, zero flow, minimum pressure] and having gained a better understanding of the design parameters, a cyclic adsorption system can now be more properly designed. For the separation of gas pairs for which there exists an adsorbent with a high relative volatility, the cyclic adsorption process may well be of commercial value.

APPENDIX I

INVESTIGATION OF METHANE-NITROGEN ADSORPTION ON DAVISON 5A MOLECULAR SIEVE

Because of its high abrasion resistance, Davison 5A Molecular Sieve was chosen over Linde 5A Molecular Sieve as the adsorbent in this research. Although Lederman (26) had examined the characteristics of methane-nitrogen adsorption on the Linde Sieve, his study was not applicable for this new system. Therefore, for the operating conditions of 1 to 2 atm. pressure and 295°K, the methane-nitrogen adsorption on the Davison 5A Molecular Sieve has been investigated.

I.1. Experimental Apparatus

In order to insure that the properties of the investigated molecular sieve were exactly the same as the molecular sieve used for the cyclic adsorption system, the 440g of 20-50 mesh sieve used in the adsorption system was used as the sample. With the adsorption column as an integral component, the equipment for this study was set up as in the schematic shown in Figure I.1.

The column, isolated by needle valves at each end, was placed in a loop with a large surge volume and a Manostat tube roller pump. This loop can, in total or part, be connected to either a vacuum system or to the supply of the gas being studied. A continuous flow thermal conductivity cell, for composition measurement, is fed by a nitrogen reference stream and either the sample stream from the surge volume or a calibration stream. The flowrates of these streams are controlled by needle valves at the entrance to the rotameters that precede the thermal conductivity cell.

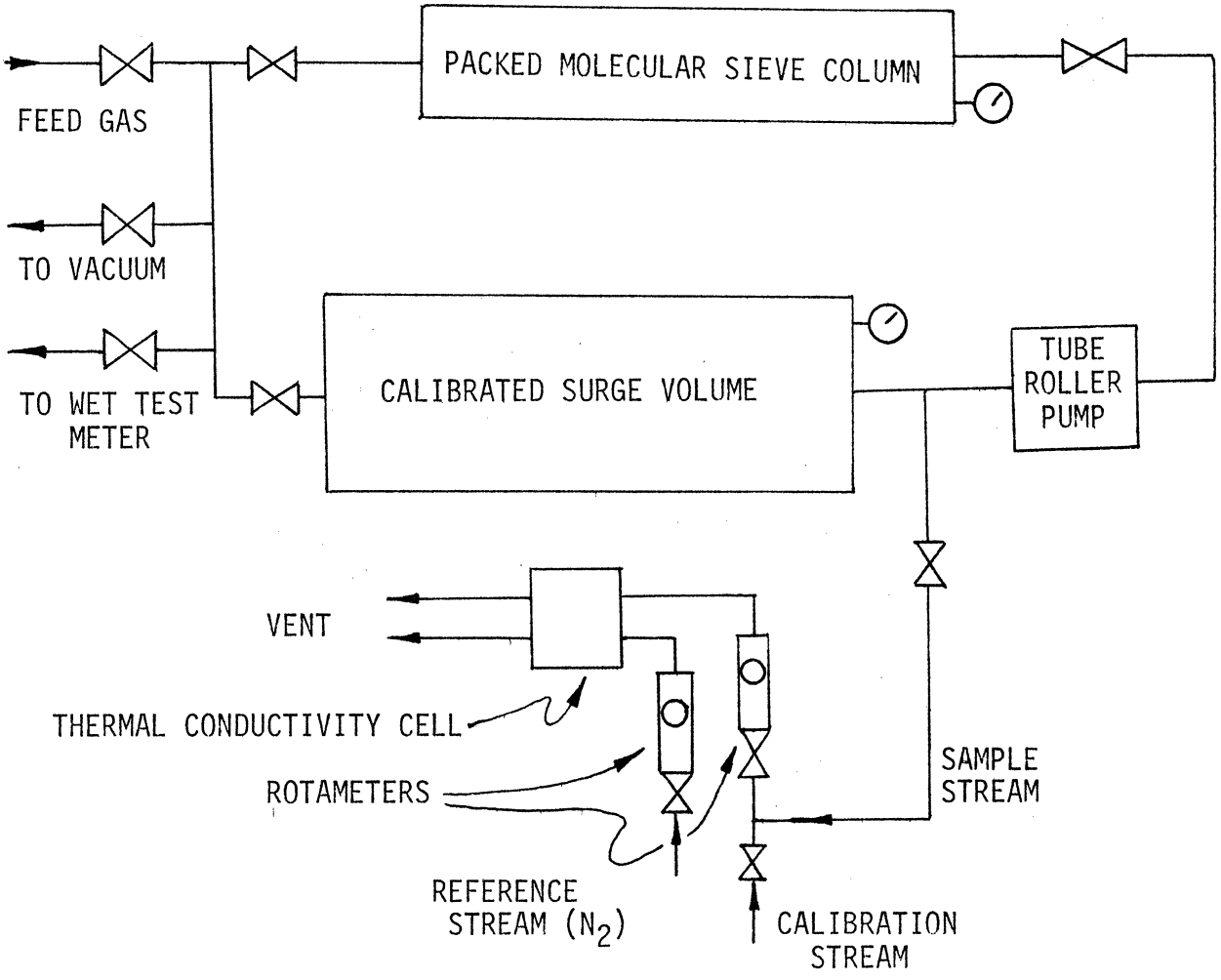

Figure I.1. Schematic Diagram of Adsorption Measurement Apparatus.

I.2. Experimental Procedure

Before the adsorption isotherms can be determined, the void volumes of the packed molecular sieve column and the surge system must be calibrated accurately. As helium is not adsorbed by the molecular sieve, yet is small enough to fill the 5A pores, the void volume of the packed bed is determined using helium. First the column is pressurized to a known pressure and then the flow is measured when the column is vented through a wet test meter to a lower known pressure. Application of Dalton's Law yields the void volume of that portion of the system. The

same procedure was used for calibrating the surge volume although nitrogen was used instead of helium.

Because the adsorption of methane and nitrogen on the molecular sieve can be affected by the adsorption of water vapor, the bed was regenerated after it was packed. This was accomplished by alternately purging with nitrogen and evacuating while the temperature of the column was maintained at 300°F with the steam jacket.

For pure component adsorption isotherms, the bed is completely evacuated while the surge system is pressurized to a known pressure. The two systems are then connected. The new equilibrium pressure and knowledge of the volumes of the systems involved coupled with Dalton's Law makes the amount adsorbed readily calculable. Repeating this procedure for various pressure levels in the surge system yields the adsorption isotherms at the ambient temperature of 295°K.

For mixed methane-nitrogen adsorption, the bed is again evacuated while the surge system is pressurized with a known mixture. The two systems are then connected and allowed to equilibrate. The Manostate tube roller pump is used at a low flowrate to allow ample circulation to speed attainment of composition equilibrium. After a period of 30 minutes the surge system is isolated from the bed. The composition of the gas is then measured by using the pressurized mixture in the surge system to supply the sample flow for the thermal conductivity cell. Knowledge of the original gas mixture composition and the pressure levels involved allows calculation of the composition and of the amount of the adsorbed phase.

For adsorption of arbitrary methane-nitrogen mixtures, the bed and the surge system are first pressurized with one pure component. The surge system alone is then further pressurized with the other component. The two

systems are then allowed to equilibrate and are measured as outlined above.

I.3. Experimental Results

Having determined the void fraction of the 525 $cm.^3$ packed column (0.623) and the volume of the surge system (2535 $cm.^3$), the adsorption of 100% CH_4, 28.6% N_2 - 71.4% CH_4 and 100% N_2 were studied and presented in Figure I.2. The data are well represented by the Freundlich Adsorption Isotherm.

$$N = kWP^{\gamma}$$

Thus, the data are plotted on a log-log scale and straight lines drawn. The Freundlich constants, which are the intercepts and slopes of these three isotherms, are shown in Table I.1. It should be noted that these constants are based on data for the pressure range of 1-2 atm.

TABLE I.1

FREUNDLICH ADSORPTION ISOTHERMS (295°K)

$$N = kWP^{\gamma}$$

Gas	kW mg. moles	γ
100% CH_4	97.8	0.83
71.4% CH_4 - 28.6% N_2	77.2	0.87
100% N_2	36.5	0.88

To relate the equilibrium compositions in the gas and adsorbed phases, the relative volatility is used.

$$\alpha = \frac{y/x}{(1-y)/(1-x)}$$

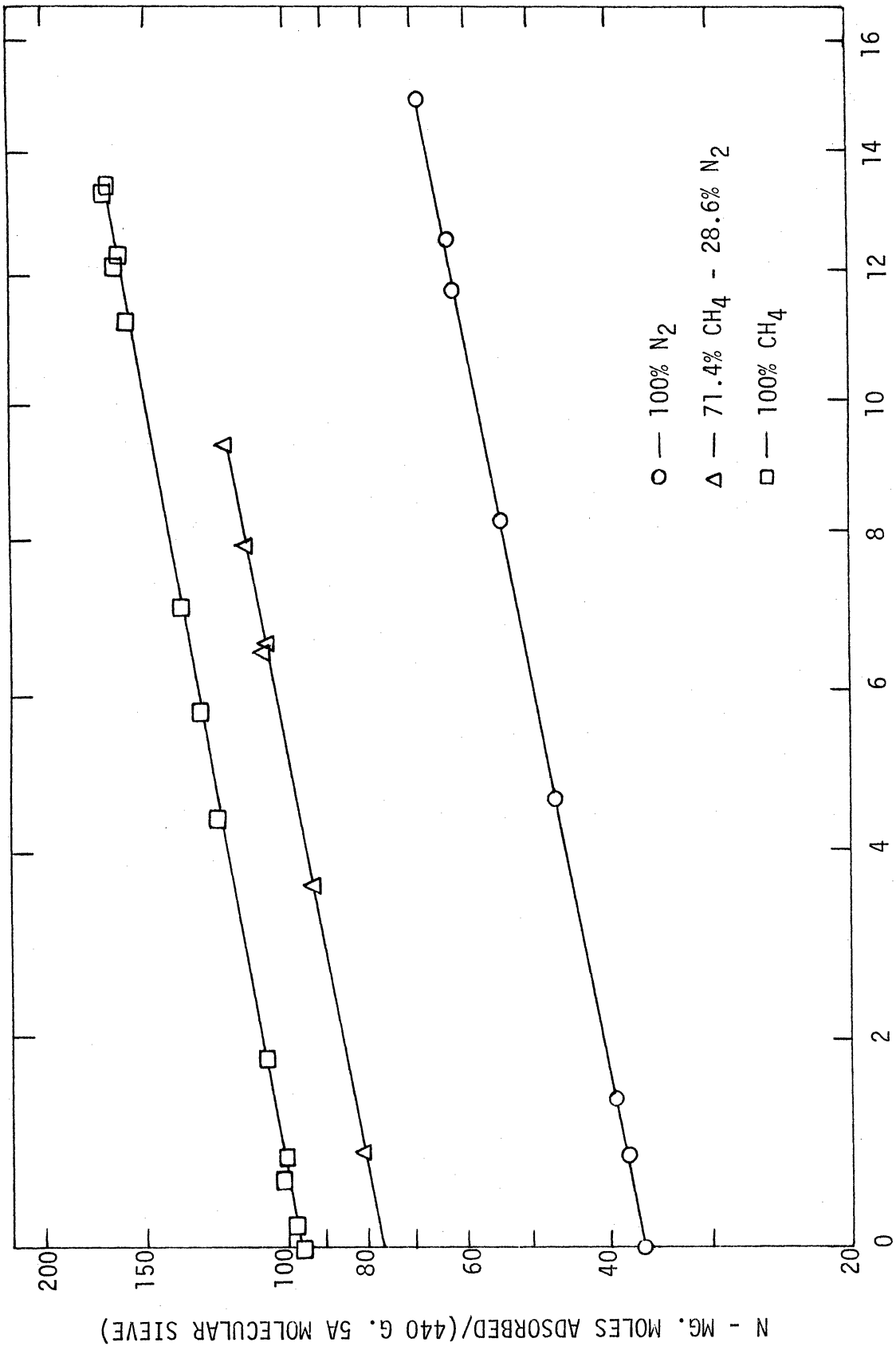

Figure I.2. Methane - Nitrogen Adsorption Isotherms (295°K).

This relative volatility was investigated over the range of pressures and compositions expected in the experimental adsorption system. The results are shown in Table I.2. Although there is some variation, these results are sufficiently accurate because the optimal control calculation, for which the value of α is needed, is not very sensitive to variations in α.

TABLE I.2

RELATIVE VOLATILITY FOR METHANE-NITROGEN ADSORPTION (295°K)

$$\alpha = \frac{y/x}{(1-y)/(1-x)}$$

Equilibrium Pressure PSIG	x %	y %	α
1.55	18.7	34.8	2.32
1.56	18.8	34.7	2.29
3.66	18.2	35.0	2.43
6.58	18.1	34.9	2.43
7.91	18.0	34.9	2.44
8.72	29.2	48.6	2.29
9.35	19.1	34.2	2.20
10.80	35.4	56.8	2.39

Average α = 2.35

Standard Deviation = 0.09

APPENDIX II

DERIVATION OF THE DISTRIBUTED-PARAMETER NECESSARY CONDITIONS

In order to eliminate the unwanted terms involving $\delta\omega_i$, $\delta\omega_{i_\lambda}$ and δr_i from the variational equation (3.42) on page 21, the following relations must hold:

$0 < \lambda < L$,

$$\left[\dot{\rho}_i + \rho_j \frac{\partial F_j}{\partial \omega_i} - \left(\rho_j \frac{\partial F_j}{\partial \omega_{i_\lambda}}\right)_\lambda + \left(\rho_j \frac{\partial F_j}{\partial \omega_{i_{\lambda\lambda}}}\right)_{\lambda\lambda}\right]\delta\omega_i = 0 \qquad \text{(II.1)}$$

$\lambda = 0$,

$$\left[-B\left(\rho_j \frac{\partial F_j}{\partial \omega_{i_\lambda}} - \left(\rho_j \frac{\partial F_j}{\partial \omega_{i_{\lambda\lambda}}}\right)_\lambda\right)\right]\delta\omega_i = 0 \qquad \text{(II.2)}$$

$\lambda = L$,

$$\left[B\rho_j \frac{\partial F_j}{\partial \omega_{i_{\lambda\lambda}}} + \eta_j \frac{\partial G_j}{\partial \omega_{i_\lambda}}\right]\delta\omega_{i_\lambda} = 0 \qquad \text{(II.3)}$$

$$\left[B\left(\rho_j \frac{\partial F_j}{\partial \omega_{i_\lambda}} - \left(\rho_j \frac{\partial F_j}{\partial \omega_{i_{\lambda\lambda}}}\right)_\lambda\right) + \eta_j \frac{\partial G_j}{\partial \omega_i}\right]\delta\omega_i + \left[\dot{\eta}_i + \eta_j \frac{\partial G_j}{\partial r_i} + \frac{\partial m_3}{\partial r_i}\right]\delta r_i = 0 \qquad \text{(II.4)}$$

$0 < \lambda < L$,

$$\rho_i(t_o)\,\delta\omega_i(t_o) = \rho_i(t_o+\tau)\,\delta\omega_i(t_o+\tau) \qquad \text{(II.5)}$$

$\lambda = L$,

$$\eta_i(t_o)\,\delta r_i(t_o) = \eta_i(t_o+\tau)\,\delta r_i(t_o+\tau) \qquad \text{(II.6)}$$

To further simplify the above relations, attention is directed to the state equations, time conditions and boundary conditions.

Writing out the components of the state equations (3.33),

$$
\begin{aligned}
\dot{\omega}_1 &= F_1(\omega_1, \omega_{1\lambda\lambda}) \\
\dot{\omega}_2 &= F_2(\omega_1, \omega_2, \omega_{1\lambda}, \omega_{2\lambda}, \omega_{1\lambda\lambda}) \\
\dot{r}_1 &= G_1(r_1, [\omega_{1\lambda}]_{\lambda=L}) \\
z_\lambda(L,t) < 0, \quad \dot{r}_2 &= G_2(r_1, r_2, [\omega_{1\lambda}, \omega_2]_{\lambda=L}) \\
z_\lambda(L,t) > 0, \quad \dot{r}_2 &= 0
\end{aligned}
\tag{II.7}
$$

From the above,

$$
\begin{aligned}
&\frac{\partial F_1}{\partial \omega_{1\lambda}} = \frac{\partial F_1}{\partial \omega_2} = \frac{\partial F_1}{\partial \omega_{2\lambda}} = \frac{\partial F_1}{\partial \omega_{2\lambda\lambda}} = 0 \\
&\qquad\qquad\qquad\qquad\qquad\qquad \frac{\partial F_2}{\partial \omega_{2\lambda\lambda}} = 0 \\
&\frac{\partial G_1}{\partial r_2} = \frac{\partial G_1}{\partial \omega_1} = \frac{\partial G_1}{\partial \omega_2} = \frac{\partial G_2}{\partial \omega_{2\lambda}} = 0 \\
&\qquad\qquad\qquad\qquad\qquad\qquad \frac{\partial G_2}{\partial \omega_1} = \frac{\partial G_2}{\partial \omega_{2\lambda}} = 0 \\
&\omega_{1\lambda}(L,t) > 0 \\
&\qquad \frac{\partial G_2}{\partial r_1} = \frac{\partial G_2}{\partial r_2} = \frac{\partial G_2}{\partial \omega_2} = \frac{\partial G_2}{\partial \omega_{1\lambda}} = 0
\end{aligned}
\tag{II.8}
$$

From the periodic time conditions (3.11), (3.24), (3.17) and (3.29),

$$
\begin{aligned}
\vec{\omega}(t_0) &= \vec{\omega}(t_0 + \tau) \\
\vec{r}(t_0) &= \vec{r}(t_0 + \tau)
\end{aligned}
\tag{II.9}
$$

Thus,

$$
\begin{aligned}
\delta\vec{\omega}(t_0) &= \delta\vec{\omega}(t_0 + \tau) \\
\delta\vec{r}(t_0) &= \delta\vec{r}(t_0 + \tau)
\end{aligned}
\tag{II.10}
$$

Boundary conditions (3.25), (3.12) and (3.26) can be rewritten as

$$\begin{aligned} &\lambda = 0, && \omega_2 = y_F && \text{for} \quad \omega_{1\lambda} = u < 0 \\ &\lambda = L, && \omega_1 = r_1 \\ & && \omega_2 = r_2 && \text{for} \quad \omega_{1\lambda} > 0 \end{aligned} \tag{II.11}$$

These relations lead to

$$\begin{aligned} &\lambda = 0 && \delta\omega_2 = 0 && \text{for} \quad \omega_{1\lambda} = u < 0 \\ &\lambda = L && \delta\omega_1 = \delta r_1 \\ & && \delta\omega_2 = \delta r_2 && \text{for} \quad \omega_{1\lambda} > 0 \end{aligned} \tag{II.12}$$

Equipped with relations (II.8), (II.10) and (II.12), equations (II.1)-(II.6) can now be fully examined.

From equation (II.1) since $\delta\omega_i$ are arbitrary nonzero variations

$$\begin{aligned} \dot{\rho}_1 = &- \left(\rho_1 \frac{\partial F_1}{\partial \omega_1} + \rho_2 \frac{\partial F_2}{\partial \omega_1} \right) + \left(\rho_2 \frac{\partial F_2}{\partial \omega_{1\lambda}} \right)_\lambda \\ &- \left(\rho_1 \frac{\partial F_1}{\partial \omega_{1\lambda\lambda}} + \rho_2 \frac{\partial F_2}{\partial \omega_{1\lambda\lambda}} \right)_{\lambda\lambda} \end{aligned}$$

$$\dot{\rho}_2 = -\left(\rho_2 \frac{\partial F_2}{\partial \omega_2} \right) + \left(\rho_2 \frac{\partial F_2}{\partial \omega_{2\lambda}} \right)_\lambda \tag{II.13}$$

The partial differential equation describing ρ_1 is parabolic and will require two boundary conditions and a time condition. The partial differential equation describing ρ_2 is hyperbolic and will require a time condition as well as boundary conditions at $\lambda = 0$ or $\lambda = L$ when gas flow is leaving the adsorber.

At $\lambda = o$, equation (II.2) yields boundary conditions for the above partial differential equations.

$$\lambda = o, \quad \left(\rho_2 \frac{\partial F_2}{\partial \omega_{1\lambda}} - \left(\rho_1 \frac{\partial F_1}{\partial \omega_{1\lambda\lambda}} + \rho_2 \frac{\partial F_2}{\partial \omega_{1\lambda\lambda}} \right)_\lambda \right) = 0 \qquad \text{(II.14)}$$

$$\omega_{1\lambda} > 0, \qquad B \rho_2 \frac{\partial F_2}{\partial \omega_{2\lambda}} = 0 \qquad \text{(II.15)}$$

Since $\dfrac{\partial F_2}{\partial \omega_{2\lambda}} \neq 0$ for $\omega_{1\lambda} > 0$, $\qquad \rho_2 = 0 \qquad$ (II.16)

At $\lambda = L$, equation (II.3) produces one boundary condition

$$\omega_{1\lambda} < 0, \quad B\left(\rho_1 \frac{\partial F_1}{\partial \omega_{1\lambda\lambda}} + \rho_2 \frac{\partial F_2}{\partial \omega_{1\lambda\lambda}} \right) + \left(\eta_1 \frac{\partial G_1}{\partial \omega_{1\lambda}} + \eta_2 \frac{\partial G_2}{\partial \omega_{1\lambda}} \right) = 0$$

$$\omega_{1\lambda} > 0, \quad B\left(\rho_1 \frac{\partial F_1}{\partial \omega_{1\lambda\lambda}} + \rho_2 \frac{\partial F_2}{\partial \omega_{1\lambda\lambda}} \right) + \eta_1 \frac{\partial G_1}{\partial \omega_{1\lambda}} = 0 \qquad \text{(II.17)}$$

From equation (3.35), $m_3(\vec{r}) = m_3(r_2)$.

$$\frac{\partial m_3}{\partial r_1} = 0 \qquad \text{(II.18)}$$

With the above, relations (II.8) and (II.12), equation (II.4) then yields the differential equations describing $\vec{\eta}$ and another boundary condition.

$$\omega_{1\lambda} < o, \quad \dot{\eta}_1^o = -\left(\eta_1 \frac{\partial G_1}{\partial r_1} + \eta_2 \frac{\partial G_2}{\partial r_1} \right) - B\left(\rho_2 \frac{\partial F_2}{\partial \omega_{1\lambda}} - \left(\rho_1 \frac{\partial F_1}{\partial \omega_{1\lambda\lambda}} + \rho_2 \frac{\partial F_2}{\partial \omega_{1\lambda\lambda}} \right)_\lambda \right)$$

$$\dot{\eta}_2^o = -\left(\eta_2 \frac{\partial G_2}{\partial r_2} + \frac{\partial m_3}{\partial r_2} \right)$$

$$\omega_{1\lambda} > o, \quad \dot{\eta}_1^o = -\left(\eta_1 \frac{\partial G_1}{\partial r_1} \right) - B\left(\rho_2 \frac{\partial F_1}{\partial \omega_{1\lambda}} - \left(\rho_1 \frac{\partial F_1}{\partial \omega_{1\lambda\lambda}} + \rho_2 \frac{\partial F_2}{\partial \omega_{1\lambda\lambda}} \right)_\lambda \right)$$

$$\dot{\eta}_2^o = -\left(B \rho_2 \frac{\partial F_2}{\partial \omega_{2\lambda}} + \frac{\partial m_3}{\partial r_2} \right) \qquad \text{(II.19)}$$

And for $\omega_{1_\lambda} < 0$ $$B\rho_2 \frac{\partial F_2}{\partial \omega_{2_\lambda}} + \eta_2 \frac{\partial G_2}{\partial \omega_2} = 0 \qquad \text{(II.20)}$$

The time conditions are derived from (II.5) and (II.6) and use relation (II.10) to yield

$$\vec{\rho}(t_0) = \vec{\rho}(t_0 + \tau)$$
$$\vec{\eta}(t_0) = \vec{\eta}(t_0 + \tau) \qquad \text{(II.21)}$$

With equations (II.13)-(II.21) governing the behavior of the adjoint variables, equation (3.42) reduces to

$$\delta I = \frac{1}{\tau} \int_{t_0}^{t_0+\tau} \left(-B\rho_j \frac{\partial F_j}{\partial \omega_{i_{\lambda\lambda}}} + \frac{\partial m_1}{\partial u} \right)_{\lambda=0} \delta u \, dt \qquad \text{(II.22)}$$

With relation (II.8) the above becomes

$$\delta I = \frac{1}{\tau} \int_{t_0}^{t_0+\tau} \left(\frac{\partial m_1}{\partial u} - B\left(\rho_1 \frac{\partial F_1}{\partial \omega_{1_{\lambda\lambda}}} + \rho_2 \frac{\partial F_2}{\partial \omega_{1_{\lambda\lambda}}} \right) \right) \delta u \, dt \qquad \text{(II.23)}$$

In the preceding development the mathematical description of the adjoint variables and the remainder of the variational equation was written in terms of functions F_1, F_2, G_1, and G_2. At this point, conversion to terms involving ω_1, ω_2, r_1 and r_2 or z, y, z_R and y_R is required.

From the state equations in Table 3.1 the following relations are derived for $\gamma = 1.0$.

In the following let $$D = \left(a_1 + \frac{\alpha a_3}{(y + \alpha(1-y))^2} \right). \qquad \text{(II.24)}$$

$$\frac{\partial F_1}{\partial \omega_1} = \frac{\partial F_1}{\partial z} = \frac{a_2 z^{-1/2} z_{\lambda\lambda}}{2(a_1 + a_3)} = \frac{\dot{z}}{2z}$$

$$\frac{\partial F_1}{\partial \omega_{1_{\lambda\lambda}}} = \frac{\partial F_1}{\partial z_{\lambda\lambda}} = \frac{a_2 z^{1/2}}{(a_1 + a_3)} \qquad \text{(II.25)}$$

$$\frac{\partial F_2}{\partial w_1} = \frac{\partial F_2}{\partial z} = -\frac{a_2 z_\lambda y_\lambda + \dfrac{a_2 a_3 z_{\lambda\lambda} y(1-y)(1-\alpha)}{(a_1+a_3)(y+\alpha(1-y))}}{4z^{3/2} D} = -\frac{\dot{y}}{2z}$$

$$\frac{\partial F_2}{\partial w_{1\lambda}} = \frac{\partial F_2}{\partial z_\lambda} = \frac{a_2 y_\lambda}{2z^{1/2} D}$$

$$\frac{\partial F_2}{\partial w_{1\lambda\lambda}} = \frac{\partial F_2}{\partial z_{\lambda\lambda}} = \frac{-a_2 a_3 y(1-y)(1-\alpha)}{2z^{1/2}(a_1+a_3)(y+\alpha(1-y)) D} \qquad \text{(II.26)}$$

$$\frac{\partial F_2}{\partial w_2} = \frac{\partial F_2}{\partial y} = \left\{ \begin{array}{l} \dfrac{-a_3 \dot{z}(1-\alpha)\left[a_1(\alpha(y-1)^2 - y^2) - \dfrac{\alpha a_3 (y(3y(1-\alpha) - 2(2\alpha-1)) - \alpha)}{(y+\alpha(1-y))^2}\right]}{2z D^2 (y+\alpha(1-y))^2} \\ + \dfrac{a_2 z_\lambda y_\lambda a_3 \alpha(1-\alpha)}{2z^{1/2} D^2 (y+\alpha(1-y))^3} \end{array} \right\}$$

$$\frac{\partial F_2}{\partial w_{2\lambda}} = \frac{\partial F_2}{\partial y_\lambda} = \frac{a_2 z_\lambda}{2z^{1/2} D}$$

$$\frac{\partial G_1}{\partial w_{1\lambda}} = \frac{\partial G_1}{\partial z_\lambda} = \frac{-a_2 z_R^{1/2}}{V_R}$$

$$\frac{\partial G_1}{\partial r_1} = \frac{\partial G_1}{\partial z_R} = \frac{-(a_2 z_\lambda + a_4 Q_p)}{2z_R^{1/2} V_R} = \frac{\dot{z}_R}{2z_R} \qquad \text{(II.27)}$$

$$\frac{\partial G_2}{\partial w_{1\lambda}} = \frac{\partial G_2}{\partial z_\lambda} = \frac{-a_2 (y - y_R)}{2z_R^{1/2} V_R}$$

$$\frac{\partial G_2}{\partial w_2} = \frac{\partial G_2}{\partial y} = \frac{-a_2 z_\lambda}{2z_R^{1/2} V_R} \qquad \text{(II.28)}$$

$$\frac{\partial G_2}{\partial r_1} = \frac{\partial G_2}{\partial z_R} = \frac{a_2 z_\lambda (y - y_R)}{4z_R^{3/2} V_R} = -\frac{\dot{y}_R}{2z_R}$$

$$\frac{\partial G_2}{\partial r_2} = \frac{\partial G_2}{\partial y} = \frac{a_2 z_\lambda}{2z_R^{1/2} V_R}$$

Relations (II.25)-(II.28) are then substituted into equations (II.13)-(II.20) and (II.23) to give the final form of the adjoint equations and variational equation.

$$\dot{\rho}_1 = \left\{ \begin{array}{l} -\left(\frac{\rho_1 \dot{z}}{2z} - \frac{\rho_2 \dot{y}}{2z}\right) + \left(\frac{\rho_2 a_2 y_\lambda}{2z^{1/2} D}\right)_\lambda \\ -\left(\frac{\rho_1 a_2 z^{1/2}}{(a_1+a_3)} - \frac{\rho_2 a_2 a_3 y(1-y)(1-\alpha)}{2z^{1/2}(a_1+a_3)(y+\alpha(1-y))D}\right)_{\lambda\lambda} \end{array} \right\} \tag{II.29}$$

$$\dot{\rho}_2 = \left\{ \begin{array}{l} \frac{\rho_2 a_3 \dot{z}(1-\alpha)[a_1(\alpha(y-1)^2 - y^2) - \frac{\alpha a_3 (y(3y(1-\alpha)-2(2\alpha-1))-\alpha)}{(y+\alpha(1-y))^2}]}{2z(y+\alpha(1-y))^2 D^2} \\ + \left(\frac{\rho_2 a_2 z_\lambda}{2z^{1/2} D}\right)_\lambda - \frac{\rho_2 a_2 a_3 (1-\alpha)\alpha y_\lambda z_\lambda}{2z^{1/2}(y+\alpha(1-y))^3 D^2} \end{array} \right\}$$

At $\lambda = 0$,

$$-\frac{\rho_2 a_2 y_\lambda}{2z^{1/2} D} + \left(\frac{\rho_1 a_2 z^{1/2}}{(a_1+a_3)} - \frac{\rho_2 a_2 a_3 y(1-y)(1-\alpha)}{2z^{1/2}(a_1+a_3)(y+\alpha(1-y))D}\right)_\lambda = 0 \tag{II.30}$$

for $u > 0$, $\rho_2 = 0$

At $\lambda = L$,

$$\dot{\eta}_1 = \left(-\frac{\eta_1 \dot{z}_R}{2z_R} + \frac{\eta_2 \dot{y}_R}{2z_R}\right) \tag{II.31}$$

$$-B\left(\frac{\rho_2 a_2 y_\lambda}{2z^{1/2} D} - \left(\frac{\rho_1 a_2 z^{1/2}}{(a_1+a_3)} - \frac{\rho_2 a_2 a_3 y(1-y)(1-\alpha)}{2z^{1/2}(a_1+a_3)(y+\alpha(1-y))D}\right)_\lambda\right)$$

for $z_\lambda(L,t) < 0$,

$$\left\{ \begin{array}{l} B\left(\frac{\rho_1 a_2 z^{1/2}}{(a_1+a_3)} - \frac{\rho_2 a_2 a_3 y(1-y)(1-\alpha)}{2z^{1/2}(a_1+a_3)(y+\alpha(1-y))D}\right) \\ -\frac{\eta_1 a_2 z_R^{1/2}}{V_R} - \frac{\eta_2 a_2 (y-y_R)}{2z_R^{1/2} V_R} \end{array} \right\} = 0 \tag{II.32}$$

$$\dot{\eta}_2 = \frac{-\eta_2 a_2 z_\lambda}{2 z_R^{1/2} V_R} - \frac{\partial m_3}{\partial y_R} \tag{II.33}$$

For $z_\lambda(L,t) > 0$,

$$B\left(\frac{\rho_1 a_2 z^{1/2}}{(a_1+a_3)} - \frac{\rho_2 a_2 a_3 y(1-y)(1-\alpha)}{2z^{1/2}(a_1+a_3)(y+\alpha(1-y))D}\right) - \frac{\eta_1 a_2 z_R^{1/2}}{V_R} = 0 \tag{II.34}$$

$$\dot{\eta}_2 = \frac{-B\rho_2 a_2 z_\lambda}{2 z^{1/2} D} - \frac{\partial m_3}{\partial y_R} \tag{II.35}$$

At $\lambda = 0$,

$$\delta I = \frac{1}{\tau}\int_{t_0}^{t_0+\tau}\left(\frac{\partial m_1}{\partial u} - \frac{B a_2}{(a_1+a_3)}\left(\rho_1 z_1^{1/2} - \frac{\rho_2 a_3 y(1-y)(1-\alpha)}{2z^{1/2}(y+\alpha(1-y))D}\right)\right)\delta u\, dt$$

(II.36)

APPENDIX III

DERIVATION OF THE CELL MODEL ADJOINT EQUATIONS

This section will deal with the specification of the adjoint equations for the cell model and will establish the relation between these equations and those derived for the distributed-parameter model.

The adjoint equations for this system, using z_i and y_i as the state variables, take the form

$$\dot{p}_i = -\left(p_j \frac{\partial f_j}{\partial z_i} + q_j \frac{\partial g_j}{\partial z_i}\right) - \frac{\partial m_5}{\partial z_i}$$
$$\dot{q}_i = -\left(q_j \frac{\partial g_j}{\partial y_i}\right) - \frac{\partial m_5}{\partial y_i} \qquad (3.92)$$

Using the relations for f_i and g_i given in Table 3.3 and letting

$$D_i = \left(a_1 + \frac{\alpha a_3}{(y_i + \alpha(1-y_i))^2}\right) \qquad (III.1)$$

For $i = 2, n-1$,

$$\frac{\partial g_i}{\partial y_{i-1}} = \frac{a_2 (z_{i-1} - z_i) \frac{\partial y_i}{\partial y_{i-1}}}{2 z_i^{1/2} D_i (L/n)^2} \qquad (III.2)$$

For $i = 1, n-1$,

$$\frac{\partial g_i}{\partial y_i} = \frac{a_2}{2 z_i^{1/2} D_i^2 (L/n)^2} \left\{ \begin{array}{l} (z_{i-1} - z_i)\left[\left(\frac{\partial \bar{y}_i}{\partial y_i} - 1\right) D_i + \frac{2\alpha a_3 (1-\alpha)(\bar{y}_i - y_i)}{(y_i + \alpha(1-y_i))^3}\right] \\ -(z_i - z_{i+1})\left[\left(\frac{\partial \bar{y}_{i+1}}{\partial y_i} - 1\right) D_i + \frac{2\alpha a_3 (1-\alpha)(\bar{y}_{i+1} - y_i)}{(y_i + \alpha(1-y_i))^3}\right] \end{array} \right\}$$
$$+ \frac{a_3 \dot{z}_i (1-\alpha)}{2 z_i D_i^2 (L/n)} \left[\frac{\alpha a_4 (y_i (3y_i(1-\alpha) + 2(2\alpha - 1)) - \alpha^2)}{(y_i + \alpha(1-y_i))^4} - \frac{a_1 (\alpha(y_i - 1)^2 - y_i^2)}{(y_i + \alpha(1-y_i))^2}\right]$$

$$\frac{\partial g_i}{\partial y_{i+1}} = \frac{-a_2 (z_i - z_{i+1}) \frac{\partial \bar{y}_{i+1}}{\partial y_{i+1}}}{2 z_i^{1/2} D_i (L/n)^2} \qquad (III.3)$$

For $i = n$,

$$\frac{\partial g_n}{\partial y_{n-1}} = \frac{a_2 (z_{n-1} - z_n) \frac{\partial \bar{y}_n}{\partial y_{n-1}} \left(\frac{1}{L/n}\right)}{2 z_n^{1/2} \left[D_n (L/n) + V_R\right]} \qquad (III.4)$$

$$\frac{\partial g_n}{\partial y_n} = \frac{\left\{ \begin{array}{l} a_2\left(\frac{1}{L/n}\right)(z_{n-1}-z_n)\left[\left(\frac{\partial \bar{y}_n}{\partial y_n}-1\right)\left(D_n(L/n)+V_R\right)+\frac{2\alpha a_3 (L/n)(1-\alpha)(\bar{y}_n-y_n)}{(y_n+\alpha(1-y_n))^3}\right] \\ +a_3\,\dot{z}_n(1-\alpha)(L/n)\left\{ \begin{array}{l} \frac{\alpha a_3 (L/n)(y_n(3y_n(1-\alpha)+2(2\alpha-1))-\alpha)}{(y_n+\alpha(1-y_n))^2} \\ -(a_1(L/n)+V_R)(\alpha(y_n-1)^2-y_n^2) \end{array}\right\} \end{array}\right\}}{2z_n^{1/2}\left[D_n(L/n)+V_R\right]^2}$$

For $i=1$, $u'=z_0$,

$$\frac{\partial g_1}{\partial z_1} = \frac{-a_2 z_1^{1/2}\left[((\bar{y}_1-y_1)+(\bar{y}_2-y_1)) - \frac{2a_3 y_1(1-y_1)(1-\alpha)}{(a_1+a_3)(y_1+\alpha(1-y_1))}\right]}{2z_1 D_1 (L/n)^2} - \frac{\dot{y}_1}{2z_1}$$

$$\frac{\partial f_1}{\partial z_1} = \frac{a_2(u'-6z_1+z_2)}{2(a_1+a_3)(L/n)^2 z_1^{1/2}} = \frac{\dot{z}_1}{2z_1} - \frac{2a_2 z_1^{1/2}}{(a_1+a_3)(L/n)^2} \qquad \text{(III.5)}$$

For $i=1$, $u=(z_1-z_0)/(L/n)$,

$$\frac{\partial g_1}{\partial z_1} = \frac{-a_2 z_1^{1/2}\left[(\bar{y}_2-y_1) - \frac{a_3 y_1(1-y_1)(1-\alpha)}{(a_1+a_3)(y_1+\alpha(1-y_1))}\right]}{2z_1 D_1 (L/n)^2} - \frac{\dot{y}_1}{2z_1}$$

$$\frac{\partial f_1}{\partial z_1} = \frac{a_2(u(L/n)-3z_1+z_2)}{2(a_1+a_3)(L/n)^2 z_1^{1/2}} = \frac{\dot{z}_1}{2z_1} - \frac{a_2 z_1^{1/2}}{(a_1+a_3)(L/n)^2} \qquad \text{(III.6)}$$

For $i=2, n-1$,

$$\frac{\partial g_i}{\partial z_{i-1}} = \frac{a_2 z_{i-1}^{1/2}\left[(\bar{y}_i-y_i) - \frac{a_3 y_i(1-y_i)(1-\alpha)}{(a_1+a_3)(y_i+\alpha(1-y_i))}\right]}{2z_i D_i (L/n)^2}$$

$$\frac{\partial f_i}{\partial z_{i-1}} = \frac{a_2 z_i^{1/2}}{(a_1+a_3)(L/n)^2} \qquad \text{(III.7)}$$

$$\frac{\partial g_i}{\partial z_i} = \frac{-a_2 z_1^{1/2}\left[(\bar{y}_i-y_i)+(\bar{y}_{i+1}-y_i) - \frac{2a_3 y_i(1-y_i)(1-\alpha)}{(a_1+a_3)(y_i+\alpha(1-y_i))}\right]}{2z_i D_i (L/n)^2} - \frac{\dot{y}_i}{2z_i}$$

$$\frac{\partial f_i}{\partial z_i} = \frac{a_2(z_{i-1}-6z_i+z_{i+1})}{2(a_1+a_3)z_i^{1/2}} = \frac{\dot{z}_i}{2z_i} - \frac{2a_2 z_i^{1/2}}{(a_1+a_3)(L/n)^2}$$

For $i = 1, n-1$,

$$\frac{\partial g_i}{\partial z_{i+1}} = \frac{a_2 z_{i+1}^{1/2}\left[(\bar{y}_{i+1} - y_i) - \dfrac{a_3 y_i (1-y_i)(1-\alpha)}{(a_1+a_3)(y_i+\alpha(1-y_i))}\right]}{2 z_i D_i (L/n)^2}$$

$$\frac{\partial f_i}{\partial z_{i+1}} = \frac{a_2 z_i^{1/2}}{(a_1+a_3)(L/n)^2} \qquad \text{(III.8)}$$

For $i = n$,

$$\frac{\partial g_n}{\partial z_{n-1}} = \frac{a_2 z_{n-1}^{1/2}\left[(\bar{y}_n - y_n) - \dfrac{a_3 (L/n) y_n (1-y_n)(1-\alpha)}{((a_1+a_3)(L/n)+V_R)(y_n+\alpha(1-y_n))}\right]}{2 z_n \left[D_n (L/n) + V_R\right](L/n)}$$

$$\frac{\partial f_n}{\partial z_{n-1}} = \frac{a_2 z_n^{1/2}}{\left[(a_1+a_3)(L/n)+V_R\right](L/n)} \qquad \text{(III.9)}$$

$$\frac{\partial g_n}{\partial z_n} = \frac{-a_2 z_n^{1/2}\left[(\bar{y}_n - y_n) - \dfrac{a_3 (L/n) y_n (1-y_n)(1-\alpha)}{((a_1+a_3)(L/n)+V_R)(y_n+\alpha(1-y_n))}\right]}{2 z_n \left[D_n (L/n) + V_R\right](L/n)} - \frac{\dot{y}_n}{2 z_n}$$

$$\frac{\partial f_n}{\partial z_n} = \frac{a_2 (z_{n-1} - 3 z_n - a_4 Q_P)}{2\left[(a_1+a_3)(L/n)+V_R\right](L/n) z_n^{1/2}} = \frac{\dot{z}_n}{2 z_n} - \frac{a_2 z_1^{1/2}}{2(L/n)\left[(a_1+a_3)(L/n)+V_R\right]}$$

Substituting equations (III.1)-(III.4) into equation (3.92) for $i = 2, n-2$:

$$\dot{q}_i = \left\{ \begin{array}{l} \dfrac{a_2 (z_i - z_{i-1})}{(L/n)^2}\left[\dfrac{q_i \left(\dfrac{\partial \bar{y}_i}{\partial y_i} - 1\right)}{2 z_i^{1/2} D_i} - \dfrac{q_{i-1}\left(\dfrac{\partial \bar{y}_i}{\partial y_i}\right)}{2 z_{i-1}^{1/2} D_{i-1}}\right] \\ + \dfrac{a_2 (z_{i+1} - z_i)}{(L/n)^2}\left[\dfrac{q_{i+1}\left(\dfrac{\partial \bar{y}_{i+1}}{\partial y_i}\right)}{2 z_{i+1}^{1/2} D_{i+1}} - \dfrac{q_i \left(\dfrac{\partial \bar{y}_{i+1}}{\partial y_i} - 1\right)}{2 z_i^{1/2} D_i}\right] \\ - \dfrac{a_2 q_i \alpha a_3 (1-\alpha)\left[(\bar{y}_{i+1} - y_i)(z_{i+1} - z_i) - (\bar{y}_i - y_i)(z_i - z_{i-1})\right]}{z_i^{1/2} D_i^2 (y_i + \alpha(1-y_i))^3 (L/n)^2} \\ - \dfrac{a_3 q_i \dot{z}_i (1-\alpha)}{(y_i+\alpha(1-y_i))^2}\left[\dfrac{\alpha a_3 (y_i (3 y_i (1-\alpha) + 2(2\alpha-1)) - \alpha)}{(y_i+\alpha(1-y_i))^2} - a_1 (\alpha (y_i - 1)^2 - y_i^2)\right] \\ \hline 2 z_i D_i^2 \end{array} \right\} \qquad \text{(III.10)}$$

Note that when $z_{i+1} < z_i < z_{i-1}$,

$$\frac{\partial \bar{y}_i}{\partial y_i} = 0 \quad \text{and} \quad \frac{\partial \bar{y}_{i+1}}{\partial y_i} = 1 \tag{III.11A}$$

And when $z_{i+1} > z_i > z_{i-1}$,

$$\frac{\partial \bar{y}_i}{\partial y_i} = 1 \quad \text{and} \quad \frac{\partial \bar{y}_{i+1}}{\partial y_i} = 0 \tag{III.11B}$$

Then a close examination of equation (III.10), recognizing the finite difference forms, shows that in the limit as $n \longrightarrow \infty$, for $i = 2$, $n-2$,

$$\dot{q} = \left\{ \begin{array}{l} a_2 \dfrac{\partial \left(q \dfrac{\partial z}{\partial \lambda} \Big/ 2z^{1/2} D \right)}{\partial \lambda} - \dfrac{a_2 a_3 q \alpha (1-\alpha) \left(\dfrac{\partial y}{\partial \lambda}\right)\left(\dfrac{\partial z}{\partial \lambda}\right)}{2 z^{1/2} D^2 (y + \alpha(1-y))^3} \\ + a_3 q \dot{z} (1-\alpha) \left[a_1 (\alpha (y-1)^2 - y^2) - \dfrac{\alpha a_3 (y(3y(1-\alpha) + 2(2\alpha - 1)) - \alpha)}{(y + \alpha(1-y))^2} \right] \\ \hline 2z D^2 (y + \alpha(1-y))^2 \end{array} \right\} \tag{III.12}$$

Comparison with equation (3.44) in Table 3.2 shows that p_2 and q are identical. Thus, the adjoint equations associated with composition for the cell model will converge, as $n \longrightarrow \infty$, to the partial differential adjoint equation for the distributed-parameter model.

However, at $i = 1$, equation (III.10) does not hold. Since $i=1$ is within the adsorption column, it should also converge to equation (3.44). In order to make equation (II.10) valid for this first cell, the following term must be added:

$$\frac{-q_0 \left(a_2 (z_1 - z_0) \dfrac{\partial \bar{y}_1}{\partial y_1} \right)}{2 z_0^{1/2} D_0 (L/n)^2}$$

If this term is equated to zero then it can be introduced into the equation for $\dot{q}_1$, and in effect make equation (III.10) valid.

Thus, a new condition, i.e. boundary condition, must be satisfied.

At $\lambda = 0$,

$$q \frac{a_2 z_\lambda \frac{\partial \bar{y}_1}{\partial y_1}}{2z^{1/2} D(L/n)} = 0 \qquad \text{(III.13)}$$

When $z_\lambda < 0$, $\bar{y}_1 \neq y_1$, and the above relationship is satisfied as $\frac{\partial \bar{y}_1}{\partial y_1} = 0$.

When $z_\lambda > 0$, $\frac{\partial \bar{y}_1}{\partial y_1} = 1$, and thus it is required that

For $z_\lambda(0,t) > 0$, $\quad q = 0 \qquad \text{(III.14)}$

Using equations (III.1)-(III.4) for $i=n$, equation (3.92) becomes

$$\dot{q}_n = \left\{ \begin{array}{l} -q_n \left[\begin{array}{l} -\frac{a_2(z_n - z_{n-1})}{(L/n)} \left\{ \left(\frac{\partial \bar{y}_n}{\partial y_n} - 1 \right) \left[D_n(L/n) + V_R \right] + \frac{2\alpha a_3 (1-\alpha)(\bar{y}_n - y_n)(L/n)}{(y_n + \alpha(1-y_n))^3} \right\} \\ + \frac{a_3 \dot{z}_n (1-\alpha)(L/n)^2}{z_n^{1/2} (y_n + \alpha(1-y_n))^2} \left\{ \begin{array}{l} \frac{\alpha a_3 (L/n)(y_n(3y_n(1-\alpha) + 2(2\alpha-1)) - \alpha)}{(y_n + \alpha(1-y_n))^2} \\ - (a_1(L/n) + V_R)(\alpha(y_n-1)^2 - y_n^2) \end{array} \right\} \end{array} \right] \\ \hline 2 z_n^{1/2} \left[D_n(L/n) + V_R \right]^2 \\ + q_{n-1} \left[\frac{a_2 (z_{n-1} - z_n) \frac{\partial \bar{y}_n}{\partial y_n}}{2 z_{n-1}^{1/2} D_{n-1} (L/n)^2} \right] - \frac{\partial m_5}{\partial y_n} \end{array} \right\} \qquad \text{(III.15)}$$

In the limit as $n \longrightarrow \infty$, q_n becomes associated with the composition in the pressure regulator, Replacing q_n with q_R, and noting that $i = n-1$ approaches the end of the column, equation (III.15) converges to

$$\dot{q}_R = \frac{q_R a_2 z_\lambda \left(\frac{\partial \bar{y}_n}{\partial y_n} - 1 \right)}{2 V_R z_R^{1/2}} - \frac{q a_2 z_\lambda \left(\frac{\partial \bar{y}_n}{\partial y_n} \right)}{2 z^{1/2} D(L/n)} - \frac{\partial m_5}{\partial y_R} \qquad \text{(III.16)}$$

Where z, z_λ and q are evaluated at $\lambda = L$. Then for $z_\lambda(L,t) < 0$,

$$\dot{q}_R = \frac{-q_R a_2 z_\lambda}{2 V_R z_R^{1/2}} - \frac{\partial m_5}{\partial y_R} \qquad \text{(III.17A)}$$

and for $z_\lambda(L,t) > 0$,

$$\dot{q}_R = \frac{-q\, a_2 z_\lambda}{2 z^{1/2} D(L/n)} - \frac{\partial m_5}{\partial y_R} \qquad \text{(III.17B)}$$

Comparison of equations (II.17) with (3.48) and (3.50) shows the equivalence of q_R and η_2 provided the arbitrary constant B is taken to be $1/(L/n)$. A discussion of the convergence of this factor is presented in Section 3.6 of the text.

Equation (III.10) was presented for $i = 2, n-2$. At $i = n-1$, the factor $(L/n)D_{i+1}$ is replaced by $[D_n(L/n)+V_R]$. Since $i = n-1$ is within the adsorption column, the adjoint variable for composition at this point should, in the limit as $n \longrightarrow \infty$, be described by the partial differential equation (III.12). With q_n converging to q_R (or η_2), a new variable, q_n', is introduced to be associated with the $\lambda = L$ end of the column. Then equation (III.12) becomes valid at $i = n-1$ if

$$-q_R\left[\frac{a_2(z_{n-1}-z_n)\,\frac{\partial \bar{y}_n}{\partial y_{n-1}}}{2(L/n)z_R^{1/2}(D_n(L/n)+V_R)}\right] - q_n'\left[\frac{a_2(z_{n-1}-z_n)\,\frac{\partial \bar{y}_n}{\partial y_{n-1}}}{2(L/n)^2 z_n^{1/2} D_n}\right] = 0 \qquad \text{(III.18)}$$

When $z_\lambda(L,t) > 0$, $\frac{\partial \bar{y}_n}{\partial y_{n-1}} = 0$ and the above relationship is automatically satisfied. When $z_\lambda(L,t) < 0$, as $n \longrightarrow \infty$

$$\frac{q_n' a_2 z_\lambda}{2 z^{1/2} D(L/n)} - \frac{q_R a_2 z_\lambda}{2 V_R z_R^{1/2}} = 0 \qquad \text{(III.19)}$$

Then for B chosen as before, the above relation becomes equivalent to the boundary condition (3.47) given in Table 3.2. Now attention is turned to the adjoint variables associated with pressure. Using equation (3.92) and (III.6)-(III.9),

For $i = 2, n-2,$

$$\dot{p}_i = \left\{ \begin{array}{l} \dfrac{-a_2}{(a_1+a_3)(L/n)^2}\left[p_{i-1} z_{i-1}^{1/2} - 2 p_i z_i^{1/2} + p_{i+1} z_{i+1}^{1/2}\right] \\ \\ \dfrac{-q_{i-1} a_2}{2 z_{i-1}^{1/2} D_{i-1} (L/n)^2}\left[(\bar{y}_i - y_{i-1}) - \dfrac{a_3 (y_{i-1})(1-y_{i-1})(1-\alpha)}{(a_1+a_3)(y_{i-1}+\alpha(1-y_i))}\right] \\ \\ + \dfrac{q_i a_2}{2 z_i^{1/2} D_i (L/n)^2}\left[(\bar{y}_i - y_i) - (\bar{y}_{i+1} - y_i) - \dfrac{2a_3 y_i (1-y_i)(1-\alpha)}{(a_1+a_3)(y_i+\alpha(1-y_i))}\right] \\ \\ - \dfrac{q_{i+1} a_2}{2 z_{i+1}^{1/2} D_{i+1} (L/n)^2}\left[(\bar{y}_{i+1} - y_i) - \dfrac{a_3 (y_{i+1})(1-y_{i+1})(1-\alpha)}{(a_1+a_3)(y_{i+1}+\alpha(1-y_{i+1}))}\right] \\ \\ + \dfrac{q_i \dot{y}_i}{2 z_i} - \dfrac{p_i \dot{z}_i}{2 z_i} \end{array} \right\} \qquad \text{(III.20)}$$

Examination of the above equation, recognizing the finite difference forms, leads to the following equation in the limit as $n \longrightarrow \infty$.

$$\dot{p} = \left\{ \begin{array}{l} \dfrac{-a_2}{(a_1+a_3)} \dfrac{\partial^2 (p z^{1/2})}{\partial \lambda^2} - \dfrac{p \dot{z}}{2z} + \dfrac{q \dot{y}}{2z} \\ \\ + \left[\dfrac{\partial \left(\dfrac{q a_2 y_\lambda}{2 z^{1/2} D} \right)}{\partial \lambda} + \dfrac{\partial^2 \left(\dfrac{a_2 a_3 q y (1-y)(1-\alpha)}{2 z^{1/2} (a_1+a_3) D (y+\alpha(1-y))} \right)}{\partial \lambda^2} \right] \end{array} \right\} \qquad \text{(III.21)}$$

Comparison with equation (3.44) shows that ρ_1 and p are identical. Proceding, as before, to make the adjoint equation (III.20) valid at $i = 1$, the following condition must hold when $u = \dfrac{(z_1 - z_0)}{(L/n)}$:

$$\left\{ \begin{array}{l} \dfrac{-a_2 (p_0 z_0^{1/2} - p_1 z_1^{1/2})}{(a_1+a_3)(L/n)^2} - \dfrac{q_0 a_2}{2 z_0^{1/2} D_0 (L/n)^2}\left[(\bar{y}_1 - y_0) - \dfrac{a_3 y_0 (1-y_0)(1-\alpha)}{(a_1+a_3)(y_0+\alpha(1-y_0))}\right] \\ \\ + \dfrac{q_1 a_2}{2 z_1^{1/2} D_1 (L/n)^2}\left[(\bar{y}_1 - y_1) - \dfrac{a_3 y_1 (1-y_1)(1-\alpha)}{(a_1+a_3)(y_1+\alpha(1-y_1))}\right] \end{array} \right\} = 0$$

(III.22)

Then as $n \to \infty$, this becomes

$$-\frac{q a_2 y_\lambda}{2 z^{1/2} D} + \frac{\partial\left(\frac{p a_2 z^{1/2}}{(a_1+a_3)}\right)}{\partial \lambda} - \frac{\partial\left(\frac{q a_2 a_3 y(1-y)(1-\alpha)}{(a_1+a_3) 2 z^{1/2} D (y+\alpha(1-y))}\right)}{\partial \lambda} = 0 \qquad \text{(III.23)}$$

which is equivalent to the boundary condition at $\lambda = 0$ given in equation (3.45). Again, to make equation (III.20) valid at $i = n-1$, the following requirement results:

$$\left\{ \begin{array}{l} \dfrac{-p_R a_2 z_R^{1/2}}{(L/n)((a_1+a_3)(L/n)+V_R)} - \dfrac{q_R a_2 \left[(\bar{y}_R - y_R) - \dfrac{a_3 (L/n) y_R (1-y_R)(1-\alpha)}{((a_1+a_3)(L/n)+V_R)(y_R+\alpha(1-y_R))}\right]}{2(L/n) z_R^{1/2} (D_n (L/n)+V_R)} \\ \\ + \dfrac{p_n' a_2 z_n^{1/2}}{(L/n)^2 (a_1+a_3)} + q_n' \dfrac{a_2 \left[(\bar{y}_n - y_n) - \dfrac{a_3 y_n (1-y_n)(1-\alpha)}{(a_1+a_3)(y_n+\alpha(1-y_n))}\right]}{2(L/n)^2 z_n^{1/2} D_n} \end{array} \right\} = 0 \qquad \text{(III.24)}$$

As $n \to \infty$, this converges to the boundary condition

$$\frac{p a_2 z^{1/2}}{(a_1+a_3)(L/n)} - \frac{q a_2 a_3 y(1-y)(1-\alpha)}{2 z^{1/2} D (a_1+a_3)(y+\alpha(1-y))(L/n)} - \frac{p_R a_2 z_R^{1/2}}{V_R} - \frac{q_R a_2 (y-y_R)}{2 V_R z_R^{1/2}} = 0 \qquad \text{(III.25)}$$

which is equivalent to (3.46A) for $B = \frac{1}{(L/n)}$. The differential equation for $\overset{\circ}{p}_n$, taken from the n^{th} cell, gives rise to the last equation for comparison.

At $i = n$,

$$\overset{\circ}{p}_n = \left\{ \begin{array}{l} \dfrac{q_n a_2}{2(L/n) z_n^{1/2}} \dfrac{\left[(\bar{y}_n - y_n) - \dfrac{a_3 y_n (1-y_n)(1-\alpha)}{((a_1+a_3)(L/n)+V_R)(y_n+\alpha(1-y_n))}\right]}{(D_n (L/n)+V_R)} \\ \\ \dfrac{+q_n \overset{\circ}{y}_n}{2 z_n} - \dfrac{p_n \overset{\circ}{z}_n}{2 z_n} - \dfrac{p_{n-1} a_2 z_{n-1}^{1/2}}{(a_1+a_3)(L/n)^2} + \dfrac{p_n a_2 z_n^{1/2}}{((a_1+a_3)(L/n)+V_R)(L/n)} \\ \\ \dfrac{-q_{n-1} a_2}{2(L/n)^2 z_{n-1} D_{n-1}} \left[(\bar{y}_n - y_{n-1}) - \dfrac{a_3 y_{n-1}(1-y_{n-1})(1-\alpha)}{(a_1+a_3)(y_{n-1}+\alpha(1-y_{n-1}))}\right] \end{array} \right\} \qquad \text{(III.26)}$$

As $n \longrightarrow \infty$, $q_n \longrightarrow q_R$ and $p_n \longrightarrow p_R$. Equation (III.24) when substituted into (III.26) then converges to

$$\dot{p}_R = \left\{ \begin{array}{l} -\dfrac{p_R \dot{z}_R}{2z_R} + \dfrac{q_R \dot{y}_R}{2z_R} - \dfrac{q a_2 y_\lambda}{2z^{1/2} D(L/n)} \\ \left[\left(\dfrac{p a_2 z^{1/2}}{(a_1+a_3)} - \dfrac{q a_2 a_3 y(1-y)(1-\alpha)}{2z^{1/2}(a_1+a_3)(y+\alpha(1-y))D} \right)_\lambda \right] \left(\dfrac{1}{L/n} \right) \end{array} \right\}_{\lambda=L} \qquad \text{(III.27)}$$

which, for the value of B used previously, shows that p_R and η_1 are equivalent.

To complete the derivation of the necessary conditions for optimality, the Hamiltonian should be presented. Since the Hamiltonian is to be maximized with respect to the control, only the portion of this function that depends directly upon the control is shown.

For $u = \dfrac{(z_1 - z_0)}{(L/n)}$, $\quad m_5 = m_5(u, y_n)$

$$H_0 = m_5(u) - \frac{a_2 u}{(a_1+a_3)(L/n)} \left[p_1 z_1^{1/2} + \frac{q_1 \left((a_1+a_3)(\bar{y}_1 - y_1) - \dfrac{a_3 y_1 (1-y_1)(1-\alpha)}{(y_1 + \alpha(1-y_1))} \right)}{2z_1^{1/2} D_1} \right] \qquad \text{(III.28A)}$$

For $u' = z_0$, $\quad m_5' = m_5'(z_1, u, y_n)$

$$H_0 = m_5'(z_1, u) + \frac{a_2 (u - z_1)}{(a_1+a_3)(L/n)^2} \left[p_1 z_1^{1/2} + \frac{q_1 \left((a_1+a_3)(\bar{y}_1 - y_1) - \dfrac{a_3 y_1 (1-y_1)(1-\alpha)}{(y_1 + \alpha(1-y_1))} \right)}{2z_1^{1/2} D_1} \right] \qquad \text{(III.28B)}$$

Examining the behavior of this function, it is noted that

$$\begin{array}{lll} \text{For } z_1 > z_0, & (z_\lambda(0,t) > 0) & \bar{y}_1 = y_1 \\ \text{For } z_1 < z_0, & (z_\lambda(0,t) < 0) & \bar{y}_1 = y_F \end{array} \qquad \text{(III.29)}$$

which makes H_0 exhibit a discontinuous behavior, as in the distributed system, when the control is switched. Because when $z_1 < z_0$,

$$\lim_{n \to \infty} y_1 = y_F \quad \text{and} \quad \lim_{n \to \infty} q_1 = q(0,t) \qquad \text{(III.30)}$$

The above Hamiltonian will approach the form given in equation (3.53) for the distributed system as the number of cells taken in the model increases.

In the preceding development the forms of the adjoint equations for the cell model have been derived. It has been shown that as the number of cells in the model increases these equations will become equivalent in all aspects to the necessary conditions derived for the distributed-parameter model.

APPENDIX IV

COMPILATION OF EXPERIMENTAL RESULTS

Flow measurements made to determine the flow resistance of the adsorbent bed were made directly after packing the bed and after all the experimental cyclic runs were completed. As can be seen by the graphical representation of Darcy's Law in Figure IV.1, the resistance did not change over the course of the experimental studies.

The complete set of experimental data for the cyclic adsorption runs are tabulated in Table IV.1. As noted in the table, runs 1-17 were carried out using a 28.6% N_2 feed gas whereas the feed gas for runs 18-74 contained 32.2% N_2.

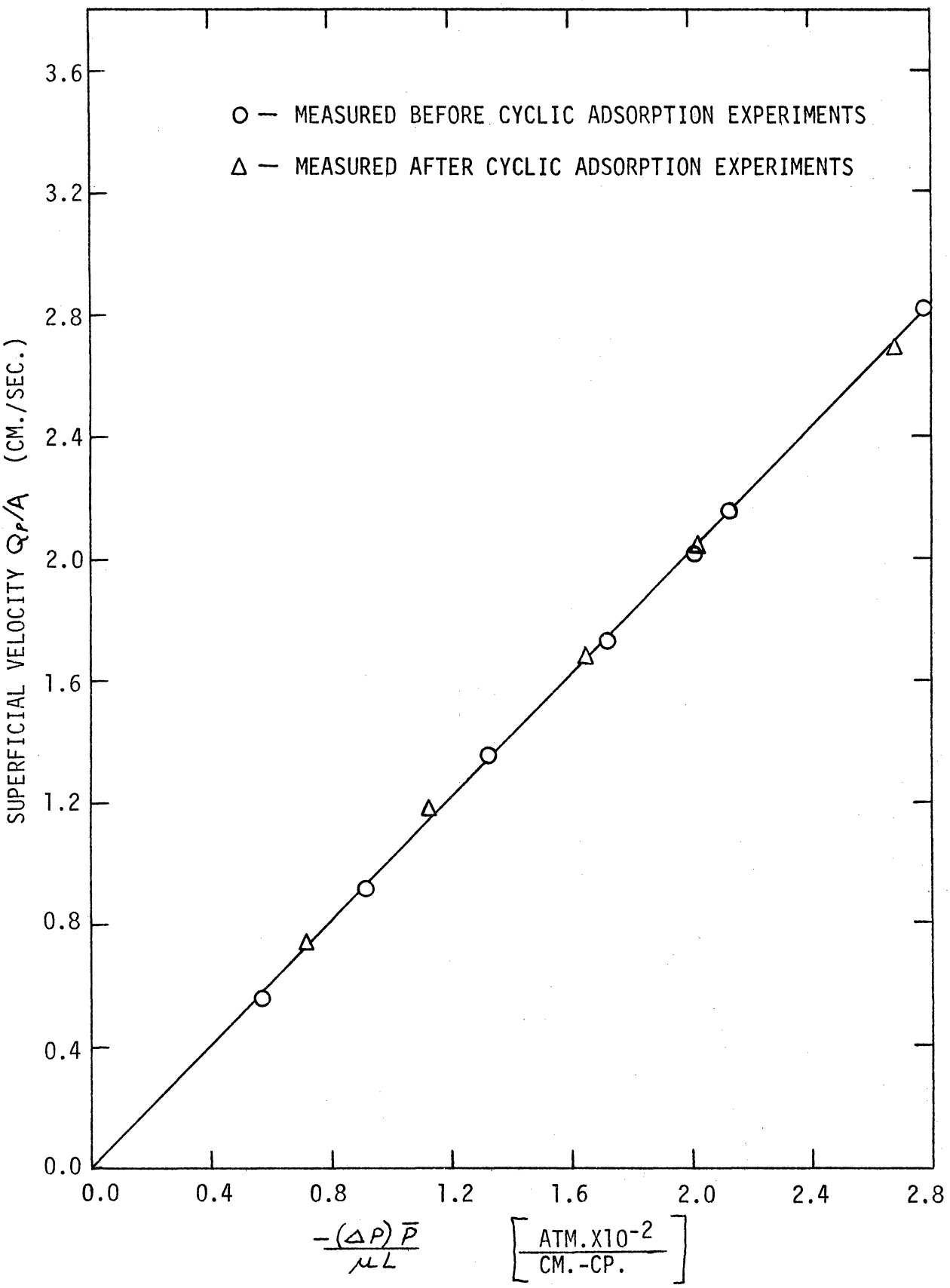

Figure IV.1. Measurement of Darcy's Law Permeability Through the Packed Adsorption Column.

TABLE IV.1

TABULATION OF EXPERIMENTAL RESULTS

Experiment Number	Fixed Parameters: Cycling Frequency (cps)	Fixed Parameters: Part of Period Feed Valve Open *	Fixed Parameters: Product Rate (SCFH)	System Outputs: Exhaust Rate (SCFH)	System Outputs: Product Composition % N_2
Feed Composition of 28.6% N_2 - 71.4% CH_4 for Experiments 1-17					
1	0.100	0.493	1.20	10.0	53.0
2	0.100	0.492	0.54	10.4	68.4
3	0.100	0.492	1.85	9.6	46.1
4	0.133	0.493	1.83	11.2	48.4
5	0.133	0.493	1.19	11.4	55.7
6	0.133	0.493	0.53	12.0	71.5
7	0.200	0.496	0.52	14.5	75.2
8	0.200	0.496	1.17	13.9	58.7
9	0.200	0.496	1.83	13.6	51.0
10	0.285	0.495	1.17	16.5	60.4
11	0.285	0.500	1.82	16.0	52.7
12	0.285	0.500	1.17	16.7	60.0
13	0.400	0.500	1.82	19.9	53.1
14	0.400	0.500	1.185	20.6	59.4
15	0.547	0.498	1.19	21.6	58.0
16	0.547	0.498	1.83	21.5	51.9
17	0.790	0.500	1.84	25.0	50.1
Feed Composition of 32.2% N_2 - 67.7% CH_4 for Experiments 18-74					
18	0.200	0.350	1.16	13.3	61.0

* Unless otherwise indicated, the following runs alternate opening the feed and exhaust valves.

TABLE IV.1 (continued)

Experiment Number	Fixed Parameters			System Outputs	
	Cycling Frequency (cps)	Part of Period Feed Valve Open	Product Rate (SCFH)	Exhaust Rate (SCFH)	Product Composition % N_2
19	0.300	0.350	1.16	16.7	62.7
20	0.400	0.350	1.16	19.3	62.7
21	0.600	0.350	1.16	23.6	60.8
22	0.100	0.350	1.16	9.4	55.9
23	1.000	0.350	1.16	32.5	58.1
24	0.350	0.350	1.16	18.0	62.8
25	0.100	0.500	1.16	10.2	56.3
26	0.200	0.500	1.16	14.4	61.8
27	0.300	0.500	1.16	17.8	64.0
28	0.400	0.500	1.16	19.9	63.8
29	0.600	0.500	1.16	24.6	62.0
30	0.350	0.500	1.16	19.2	64.0
31	0.350	0.800	1.16	15.0	53.6
32	0.350	0.650	1.16	17.6	60.9
33	0.350	0.500	1.16	19.2	64.0
34	0.350	0.350	1.16	18.1	63.0
35	0.350	0.200	1.16	14.7	56.6
36	0.350	0.425	1.16	18.9	64.0
37	0.350	0.470	1.16	19.2	64.1
38	0.100	0.550	1.81	9.9	49.2
39	0.200	0.550	1.79	14.2	53.9
40	0.300	0.550	1.78	17.3	55.5
41	0.400	0.550	1.79	19.9	55.6

TABLE IV.1 (continued)

Experiment Number	Fixed Parameters: Cycling Frequency (cps)	Part of Period Feed Valve Open	Part of Period Both Valves Closed *	Product Rate (SCFH)	System Outputs: Exhaust Rate (SCFH)	Product Composition % N_2
42	0.600	0.550		1.82	24.3	54.7
43	0.350	0.550		1.78	18.7	55.9
44	0.350	0.815		1.83	13.9	47.1
45	0.350	0.650		1.75	17.7	53.9
46	0.350	0.396		1.76	18.2	55.2
47	0.350	0.207		1.77	14.3	49.8
48	0.350	0.483		1.74	18.8	56.1
49	0.350	0.510		1.79	18.8	56.1
50	0.350	0.455		1.72	18.6	56.0
51	0.350	0.798		2.47	14.4	45.2
52	0.350	0.604		2.42	18.1	51.3
53	0.350	0.398		2.38	17.7	50.8
54	0.350	0.202		2.44	13.3	45.3
55	0.350	0.500		2.41	18.5	51.8
56	0.350	0.540		2.38	18.4	51.8
57	0.350	0.459		2.37	18.2	51.6
58	0.350	0.470	0.06	1.16	19.8	63.6
59	0.350	0.470	----	1.16	19.2	64.1
60	0.350	0.470	0.06	1.78	19.6	56.2

* For the following runs, there is a delay between closing the feed valve and opening the exhaust valve.

TABLE IV.1 (continued)

Experiment Number	Fixed Parameters				System Outputs	
	Cycling Frequency (cps)	Part of Period		Product Rate (SCFH)	Exhaust Rate (SCFH)	Product Composition % N_2
		Feed Valve Open	Both Valves Closed			
61	0.350	0.470	---	1.78	18.7	56.3
62	0.350	0.470	0.06	2.43	19.1	51.3
63	0.350	0.470	---	2.40	18.3	51.5
64	0.350	0.470	0.125	2.43	16.1	50.7
65	0.350	0.470	0.125	1.78	16.6	55.2
66	0.350	0.470	0.125	1.16	17.0	62.5
67	0.350	0.478	0.031	1.16	18.6	63.9
68	0.350	0.478	---	1.16	19.2	63.9
69	0.350	0.478	0.031	1.75	18.2	56.1
70	0.350	0.478	---	1.79	18.7	56.3
71	0.350	0.478	0.031	2.43	17.7	51.4
72	0.350	0.478	---	2.41	18.2	51.4
73	0.350	0.480	0.068	1.16	17.7	----
74	0.350	0.480	0.068	1.77	17.4	----

APPENDIX V

DIMENSIONAL ANALYSIS OF THE STATE EQUATIONS

In order to assess the significance of the design parameters A, K and L, in the state equations a dimensional analysis of these equations is needed. From Table 3.1 the state equations for pressure and composition can be rewritten in dimensionless form.

Letting $\theta = \frac{t}{\tau}$, $\ell = \frac{\lambda}{L}$, $Z_i = \frac{z}{z_{max}}$ and $Z_R = \frac{z_R}{z_{max}}$

$$\frac{\partial Z}{\partial \theta} = \left(\frac{K\tau z_{max}^{1/2}}{\mu L^2}\right) \frac{Z^{1/2} \frac{\partial^2 Z_i}{\partial \ell^2}}{\left(\epsilon + \frac{WRTk\gamma z_{max}^{((\gamma-1)/2)}}{AL} Z^{((\gamma-1)/2)}\right)} \tag{V.1}$$

$$\frac{\partial y}{\partial \theta} = \left(\frac{K\tau z_{max}^{1/2}}{\mu L^2}\right) \left[\frac{\frac{\partial Z_i}{\partial \ell}\frac{\partial y}{\partial \ell} - \frac{\frac{\partial^2 Z_i}{\partial \ell^2}\left[\frac{WRTk\gamma z_{max}^{((\gamma-1)/2)}}{AL} Z^{((\gamma-1)/2)} y(1-y)(1-\alpha)\right]}{\left(\epsilon + \frac{WRTk\gamma z_{max}^{((\gamma-1)/2)}}{AL} Z^{((\gamma-1)/2)}\right)\left(y+\alpha(1-y)\right)}}{2Z^{1/2}\left(\epsilon + \frac{\alpha WRTk z_{max}^{((\gamma-1)/2)}}{AL(y+\alpha(1-y))^2} Z^{((\gamma-1)/2)}\right)} \right] \tag{V.2}$$

Factoring out the dimensionless term

$$\left(\frac{K\tau z_{max}^{1/2}}{\mu L^2}\right)$$

the boundary conditions become

At $\ell = 1$,

$$\frac{\partial Z_R}{\partial \theta} = \left(\frac{K\tau z_{max}^{1/2}}{\mu L^2}\right) \left[\frac{-Z_R^{1/2}\left(\frac{\partial Z_i}{\partial \ell} + \left[\frac{2RTL Q_p}{(z_{max} AK/\mu)}\right]\right)}{\left(\frac{V_R}{AL}\right)} \right] \tag{V.3}$$

For $\frac{\partial Z_i}{\partial \ell}(1,\theta) < 0$,

$$\frac{\partial y_R}{\partial \theta} = -\left(\frac{K\tau z_{max}^{1/2}}{\mu L^2}\right) \frac{\frac{\partial Z_i}{\partial \ell}(y - y_R)}{2\left(\frac{V_R}{AL}\right) Z_R^{1/2}} \tag{V.4A}$$

For $\frac{\partial z_i}{\partial \ell}(1,\theta) > 0$

$$\frac{\partial y_R}{\partial \theta} = 0 \tag{V.4B}$$

With the pressure constraint at the control boundary (3.37) written with a controllable exhaust pressure

$$z_{min} \leq z \leq z_{max} \tag{V.5}$$

the dimensionless constraint becomes

$$\left(\frac{z_{min}}{z_{max}}\right) \leq Z_i \leq 1 \tag{V.6}$$

Because the system output of exhaust rate is also of interest, the expression for this rate is also dedimensionalized.

$$\text{when } z_\lambda(0,t) > 0 \qquad \text{exhaust rate} = \frac{1}{\tau}\int_0^\tau \frac{AK}{2\mu RT}\frac{\partial z}{\partial \lambda}\,dt \tag{V.7}$$

In terms of dimensionless variables,

$$\text{when } \frac{\partial Z_i}{\partial \ell}(0,\theta) > 0 \qquad \text{exhaust rate} = \left(\frac{AL z_{max}^{1/2}}{2\gamma RT}\right)\left(\frac{K\gamma z_{max}^{1/2}}{\mu L^2}\right)\int_0^1 \frac{\partial Z_i}{\partial \ell}\,d\theta \tag{V.8}$$

Thus, if the dimensionless terms involving equipment specifications

$$\left(\frac{K\gamma z_{max}^{1/2}}{\mu L^2}\right), \quad \left(\frac{2RTL\,Q_P}{z_{max}(AK/\mu)}\right) \text{ and } \left(\frac{V_R}{AL}\right),$$

the dimensionless terms involving adsorbent properties

$$\epsilon, \quad \alpha, \quad \gamma \text{ and } \left(\frac{W}{AL}RTk\gamma z_{max}^{((\gamma-1)/2)}\right),$$

and the dimensionless terms involving operating conditions $\left(\frac{z_{min}}{z_{max}}\right)$ and F_{FV} are not changed, the solution to the dimensionless equations (V.1)-(V.4) will not change.

BIBLIOGRAPHY

1. Alexis, R. W. "Upgrading Hydrogen via Heatless Adsorption." Chem. Eng. Progr. Symp. Ser. 63, 74, 51 (1967)

2. Aris, R. "Studies in Optimization." Chem. Eng. Sci. 13, 1, 18 (1960).

3. Athans, M. and Falb, P. L. Optimal Control, McGraw-Hill Book Co., New York, 1966.

4. Bilous, O. and Amundson, N. R. "Optimum Temperature Gradients in Tubular Reactors." Chem. Eng. Sci. 5, 81 and 5, 115 (1956).

5. Butkovskii, A. G. and Lerner, A. Y. "The Optimal Control of Systems with Distributed Parameters." Automat. Remote Control. 21, 6, 682 (1960).

6. Butkovskii, A.G. "Optimum Processes in Systems with Distributed Parameters." Automat. Remote Control. 22, 1, 17 (1961).

7. Butkovskii, A.G. "The Maximum Principle for Optimal Systems with Distributed Parameters." Automat. Remote Control. 22, 10, 1288 (1961).

8. Butkovskii, A.G. "Some Approximate Methods for Solving Problems of Optimal Control of Distributed-Parameter Systems." Automat. Remote Control. 22, 12, 1565 (1961).

9. Cannon, M.R. "Controlled Cycling Improves Various Processes." Ind. Eng. Chem. 53, 629 (1961).

10. Chang, K.S. and Bankoff, S.G. "Oscillatory Operation of Jacketed Tubular Reactors." Ind. Eng. Chem. Fundam. 7, 4, 633 (1968).

11. Chang, K.S. and Bankoff, S.G. "Optimal Control of Tubular Reactors-Parts I and II." A.I. Ch. E. Journal. 15, 3, 410 (1969).

12. Denn, M.M. "Optimal Boundary Control for a Non-Linear Distributed System." Int. J. Control. 4, 2, 167 (1966).

13. Denn, M.M., Gray, R.D., Jr. and Ferron, J.R. "Optimization in a Class of Distributed-Parameter Systems." Ind. Eng. Chem. Fundam. 5, 1, 59 (1966).

14. Douglas, J.M. "Periodic Reactor Operation." Ind. Eng. Chem. Process Des. Develop. 6, 1, 43 (1967)

15. Egorov, A. I. "Optimal Control of Processes in Certain Systems with Distributed Parameters." Automat. Remote Control. 25, 5, 613 (1964).

16. Egorov, A. I. "Optimal Processes in Systems Containing Distributed-Parameter Plants." Automat. Remote Control. 26, 6, 977 (1965).

17. Egorov, A. I. "Optimal Processes in Distributed-Parameter Systems and Certain Problems in Invariance Theory." Jour. SIAM Control. 4, 4,601 (1966)

18. Esso Research Laboratories. "Nonsteady State (Pulsed) Gas Separations." File 732-1 (1964) and File 403-1 (1965).

19. Hersh, C. K. Molecular Sieves. Reinhold Publishing Corp., New York, 1961

20. Horn, F.J.M. and Lin, R.C. "Periodic Processes: A Variational Approach." Ind. Eng. Chem. Process Des. Develop. 6, 1, 21 (1967).

21. Jackson, R. "Optimum Startup Procedure for an Autothermic Reaction." Chem. Eng. Sci. 21, 3, 241 (1966).

22. Javinsky, M.A. "Optimal Control of a Continuous Flow Stirred Tank Chemical Reactor." Ph.D. Thesis. The University of Michigan (1967).

23. Katz, S. "A General Minimum Principle for End-Point Control Problems." J. Elect. Control. 16, 189 (1964).

24. Koppel, L.B. and Shih, Y.-P. "Optimal Control of a Class of Distributed-Parameter Systems with Distributed Controls." Ind. Eng. Chem. Fundam. 7, 3, 414 (1968).

25. Laurence, R.L. and Vasudevan, G. "Performance of a Polymerization Reactor in Periodic Operation." Ind. Eng. Chem. Process Des. Develop. 7, 3, 427 (1968).

26. Lederman, P.B. "Adsorption of Nitrogen-Methane on Linde Molecular Sieve Type 5A." Ph.D. Thesis. The University of Michigan (1961).

27. McAndrew, M.A. "Parametric Pumping Separation with Special Attention to Gaseous Mixtures." Ph.D. Thesis. Princeton University (1967).

28. Mantel, C.L. Adsorption. McGraw-Hill Book Co., New York, 1951

29. Newberger, M.R. "Optimal Operation of a Tubular Chemical Reactor." Ph.D.Thesis. The University of Michigan (1968).

30. Pigford,R.L., Baker, B. and Blum, P.E. "An Equilibrium Theory of the Parametric Pump." Ind. Eng. Chem. Fundam. 8, 1, 144 (1969).

31. Pontryagin, L.S. et al. Mathematical Theory of Optimal Processes. John Wiley, New York, 1962.

32. Ray, W.H. "Periodic Operation of Polymerization Reactors." Ind. Eng. Chem. Process Des. Develop. 7, 3, 422 (1968).

33. Rolke, R.W. and Wilhelm, R.H. "Recuperative Parametric Pumping, Model Development and Experimental Evaluation." Ind. Eng. Chem. Fundam. 8,2, 235 (1969).

34. Rozonoer, L.I. "L.S. Pontryagin's Maximum Principle in the Theory of Optimal Systems." Automat. Remote Control. 20, 10, 1320 and 20, 11, 1441 (1959).

35. Schrodt, V.N. et al. "Plant Scale Study of Controlled Cyclic Distillation." Chem. Eng. Sci., 22, 759 (1967).

36. Seinfeld, J.H. "Optimal Control of Distributed-Parameter Systems." Ph.D. Thesis, Princeton University (1967).

37. Skarstrom, C.W. "Use of Adsorption Phenomena in Automatic Plant-Type Gas Analyzers." Ann. N.Y. Acad. Sci., 72, 751 (1959).

38. Sweed, N.H. and Wilhelm, R.H. "Parametric Pumping: Separations via Direct Thermal Mode." Ind. Eng. Chem. Fundam. 8, 2, 221 (1969).

39. Turnock, P.H. "The Separation of Nitrogen and Methane by Pulsating Flow Through a Fixed, Molecular Sieve Bed." Ph.D. Thesis, The University of Michigan (1968).

40. Wilhelm, R.H., Rice, A.W., and Bendelius, A.R. "Parametric Pumping: Dynamic Principle for Separating Fluid Mixtures." Ind. Eng. Chem. Fundam. 5, 1, 141 (1966).

41. Wilhelm, R.H., Rice, A.W., Rolke, R.W. and Sweed, N.H. "Parametric Pumping: Dynamic Principle for Separating Fluid Mixtures." Ind. Eng. Chem. Fundam. 7,3,337 (1968).